UNIVERSITY OF SOUTHAMPTON

FACULTY OF ENGINEERING AND APPLIED SCIENCE

INSTITUTE OF SOUND AND VIBRATION RESEARCH

THE EFFECTS OF HIGH STRAIN AND TEMPERATURES ON THE FATIGUE OF METALS AND THE RELATIONSHIP WITH A DISCONTINUITY IN THE S/N CURVE

Thesis submitted for the degree of

Master of Philosophy

by

CHRISTOPHER JOHN TAYLER

APRIL 1968

CONTENTS

SUMMARY

The mechanism of fatigue and some factors which affect the fatigue properties of metals and alloys are reviewed and discussed. A discontinuity found in the S/N curve of metals is also discussed and it is shown that this is probably the most important parameter in the fatigue of a metal. Criteria based on the discontinuity are proposed to predict crack propagation in a material.

The effect of cold rolling on the fatigue characteristics of 18/8 stainless steel was investigated and the benefit obtained was limited to plain specimens. Cold stretching 70/30 brass was found to raise the level of the discontinuity in both the notched and plain fatigue tests.

Preliminary investigations were made to determine the effect of cold rolling prior to the fatigue testing of an 18/8 stainless steel with a raised nitrogen content. The results indicate promising possibilities and the role of nitrogen as an austenite stabilizer is also discussed.

Fatigue testing of 18/8 stainless steel was performed at -80°C to find the effect on the discontinuity. The endurance shift remained, as found at room temperature, but the stress level at which the discontinuity appeared was considerably raised.

High temperature fatigue tests undertaken on mild and 18/8 stainless steels at 250°C and 350°C revealed slight improvements in fatigue strength.

Fluctuating tension tests performed on 18/8 and mild steels

were found to be considerably beneficial compared with reversed stress cycling. Little benefit was found from L73 aluminium. Fluctuating compression stress cycling of L73 aluminium alloy resulted in fatigue.

The results of random stress loading on L73 aluminium alloy are discussed and compared with the equivalent sinusoidal loading. An increase in scatter found is related to the S/N curve, along with a theory for crack propagation.

Preliminary investigations were made to assess the use of infra-red thermography for fatigue detection.

ACKNOWLEDGEMENTS

I wish to thank my supervisor, T.R.G. Williams, for his invaluable help and discussions in connection with this thesis.

Discussions held with C. Shurmer and M. Bily and the assistance of Richard Thomas and Baldwins are duly recognised.

INTRODUCTION

For more than a century engineers have been confronted with the failure of metals by fatigue, but it is without doubt the advent and the development of the aeroplane that has highlighted this phenomenon. The problem of aircraft design entails keeping weight at a minimum with the consequence of high stress levels throughout the structure. As a result the designs are usually such that there is a maximum finite flying time after which parts will have to be replaced.

However it is insufficient to concentrate on the material aspect alone as careful design to eliminate fatigue is also of paramount importance. Examination of the crashed Comet aeroplane in 1954 revealed that the fuselage had exploded through the catastrophic propagation of fatigue cracks which had formed at hatch corners - regions of high, localised stress. A different hatch shape could have resulted in a more even stress distribution with the delay or prevention of fatigue cracks.

Recent investigations into the understanding of metal fatigue have highlighted on a discontinuity found in the S/N curve but it is to be observed that this occurs in a position in the curve with fairly high stress and correspondingly low endurance. The importance of this discontinuity in metal fatigue is open to discussion and one of the aims of this thesis is to show its importance and to correlate it with other fatigue parameters.

The effect of prestrain on annealed metals is known to raise

the yield stress and can change considerably many of the mechanical properties of a material but its importance in connection with fatigue is doubtful. Frost has investigated the effect of prestrain on the fatigue of mild steel and has shown that over and above a certain amount of prestrain the benefit obtained is negligible and this will be discussed in the review. Therefore another aim of this thesis is directed at investigating the effect of prior strain hardening on the fatigue of both 18/8 stainless steel and 70/30 brass and to compare the results with those obtained by Frost and other researchers. Since, as has been mentioned, the role of stress concentrations plays a significant part in metal fatigue it was decided that notched and plain fatigue tests be carried out wherever possible so that a comparison can be made between the results and a determination of the notch effect would become more apparent. Wherever notched fatigue results are presented they may be shown either as the nominally applied stress with stress concentration effects ignored or as the nominal stress multiplied by the elastic stress concentration factor. For each of these cases the terms 'unfactored stress' and 'factored stress' respectively have been used.

The occurrence of high stresses may be in forms other than prestraining and they frequently occur during stress cycling in a random manner. To understand the effects more clearly would be to obtain results from a material subjected to occasional high stresses during sinusoidal fatigue cycling but since this was not a practical

possibility it was decided that the results of tests subjected to a random stress pattern of the form of a Rayleigh distribution would be a suitable alternative for investigation.

When concerned with static properties the importance of nitrogen in steels is considerable but the role nitrogen plays during fatigue is not so well defined. It was therefore decided to investigate the importance of prestrain upon the fatigue strength of an 18/8 stainless steel with a raised nitrogen content and to obtain information which would be complementary to that with the conventional low nitrogen 18/8 stainless steel. A further important study when concerned with the fatigue of 18/8 steel is the role of martensitic transformation.

Relationships exist between the Ms temperatures and the alloy content but the instability of anstenite in 18/8 steel when under deformation is without doubt a phenomenon which may be of benefit for improved fatigue strengths. The role of temperature may be expected to have a significant effect, and so tests were carried out at both high and low temperatures. Comparative tests were also carried out on mild steel where the effect of temperature may be simply to change the rate at which strain ageing occurs.

In comparing the static strength of a material with the fatigue strength it is difficult to know what effect the reversed cycling can have and the optimum way to compare these two types of tests would be to cycle in plain tension only (or plain compression). At the same time the information obtained would provide some indication of the effect of mean

loads.

The production of large amounts of heat in steels during stress cycling has been shown to cause a considerable increase in fatigue resistance, probably due to strain ageing. This phenomenon of heat generation could be used as a means for the detection of fatigue and the revelation of the discontinuity. Preliminary studies to investigate this field were made using an infra red camera.

REVIEW OF METAL FATIGUE

When a stress of sufficient magnitude is repeatedly applied to a material, cracks may form and propagate resulting in complete fracture of the material. This process is one known as fatigue and is an everyday occurrence in engineering practice. The repeated stress applied need not be as great as that of the ultimate tensile strength of the material, and in many instances repeated stresses at levels less than the yield point of the material are sufficient to cause fatigue failure.

The earliest known fatigue tests were those conducted by Alberts (ref.1) in 1829, but no classification of results was attempted until 1859 when Wöhler (ref.2) plotted, in a graphical form, stress against the logarithm of the number of cycles to failure. This resulting graph is known as the S/N curve.

The main types of fatigue testing utilized in the laboratory today can be divided into three categories. Firstly there is the type which applies direct stress to the specimen in the form of tension or compression. Secondly reversed bending can be used, which renders part of the specimen in tension while the other part is in compression. Reversed torsion is another widely used method.

Each of these fundamental testing conditions can be subdivided into two parts - those which subject the material to the same stress throughout the duration of the test (constant loading, K_L), and those

which subject the material to the same strain (constant straining, K_S).

Results of rotating cantilever fatigue tests of an 18/8/Ti stainless steel reported by Williams and Stevens (ref.3) were found to be appreciably different in the constant strain and constant load conditions. Whereas the S/N curve obtained from K_S conditions resulted in a fairly linear relationship between stress and log (cycles) at endurances from 10^3 cycles to 10^5 cycles, the K_L curve was found to be more complex; a fairly distinct change of endurance and an increase in scatter was found at stress levels in the region of 32 Tons/in^2. Below this stress level and above the fatigue limit the difference in endurances obtained from K_S and K_L testing was found to be nearly an order of magnitude, constant strain being higher, but at stress levels greater than 32 Tons/in^2 the endurances were found to be coincident under both conditions of testing. Williams and Stevens attribute this difference in fatigue lives to three differences between the K_S and K_L conditions:-

(1) In K_S the area of crack propagation is greater because the fatigue crack traverses the full cross section without becoming a fast tensile failure.

(2) During the crack growth stage in K_L the stress level in the test piece rises substantially as the cross sectional area of the specimen is reduced.

(3) Strain hardening effects which raise the yield point can reduce the deflection under load in the K_L test, whereas the combined elastic and plastic strain remains constant in K_S tests.

It is estimated that the propagation of fatigue cracks occurs at a fairly high rate (ref. 4) taking probably less than 5% of the total life to failure in 'small' test pieces, thus it may be expected that (1) would cause only a slight increase in the endurance of K_S compared with K_L testing. The effect of (2) therefore, can only be very small, and the combination of (1) and (2) may be expected to cause maximum changes in endurance of about 5%. (3) must therefore, account for the remaining difference between the endurances. From the explanation it may be expected that K_L endurances would be more than those obtained from K_S conditions, but it should be noted that the constraint imposed by K_S testing causes yet further strain hardening than would otherwise occur in the K_L testing.

The cancellation of difference in endurances of K_S and K_L tests at the stress level of 32 Tons/in^2 in this 18/8Ti steel implies an exhaustion of strain hardening, and a change of the fatigue mechanism to a general yielding and plasticity. In the range of stress between the fatigue limit and this discontinuity, persistent slip lines observed in the surface indicate that a condition of plasticity is achieved in the weakly supported surface grains, before it is reached in the core grains.

Benham and Ford (ref. 5) have found from fatigue tests performed on a hot rolled mild steel that above a certain stress level the fracture surface changes and becomes similar to that of monotonic tension. They term this type of fracture as 'cyclic creep'. Immediately below the

stress level at which this occurs they report the fracture surface to be similar to that found at stress levels near that of the fatigue limit. Furthermore, from tests performed on L65 aluminium alloy in a Rolls Royce rotating cantilever fatigue machine, Williams, Hayden and Hallwood (ref. 6) report that the fracture surface changes from eccentric crack propagation at stress levels below the discontinuity to concentric propagation at stress levels above it.

Forsyth (ref. 7) has shown that slip bands in the surface are responsible for the production of initiation cracks which provide the necessary trigger points for propagation cracks. The initiation cracks are classified as stage I cracks and propagation cracks as stage II. Forsyth points out that stage I cracks extend the whole width of grains in the surface, and follow the slip bands in the plane of maximum shear stress, i.e. at 45° to the direction of the principal stress. The process of forming these cracks may take a large proportion of the life to failure when at stress levels just above that of the fatigue limit.

Stage II cracks usually occur at the base of a stage I crack and propagate in a direction perpendicular to the principal stress. The stage II crack is responsible for the striations which are characteristic of fatigue fracture surfaces. Forsyth has shown that the size of striations produced by alternate tension-compression fatigue is proportional to the magnitude of the applied stress and that each complete cycle produces one striation, which is composed of a ductile tear and a brittle fracture. The effect of a mean tensile static load is to

cause the crack to tunnel, but this condition of loading also favours the direct growth of a stage II crack, thus eliminating the need for stage I. Localised stress, as in the case of stress concentrations, are also believed to lead to the direct propagation of stage II cracks, but this seems to be a field where little is known. Frost (ref. 8) has shown that stage I cracks can be formed at the base of a notch; he tested round specimens in a rotating cantilever fatigue machine, and as notches he used "vee-grooves", the sides of which were inclined to each other at 55°, but the root radii varied from 0.006 inches to a radius very much smaller. He shows that with the large root radius (0.006 inch) the stage I cracks are formed, but with smaller root radii stage II cracks are directly formed. It seems, therefore, that tri-axiality resulting from the presence of a notch, and the root radius of the notch are two important factors necessary for the direct growth of a stage II crack, and that if the root radius is more than a certain quantity, stage I cracks must initiate the fatigue process.

In describing the significance of the discontinuity Frost (ref. 9) suggests that the mechanism of fatigue damage changes from slip band cracking below the discontinuity to cracking at sub-grain boundaries at stress levels above it. From investigations in copper, Porter and Levy (ref. 10) confirm that the crack path follows the slip bands at stress levels below the discontinuity, but that the crack path at stress levels above the discontinuity seems to be completely independent of structure defects, e.g. grain boundaries, slip bands, etc.

It seems, therefore, that the weakly supported surface grains reach a condition of collapse or exhaustion of strain hardening before the core grains of the material, and the cracks formed provide the necessary conditions for stage II cracks.

Abdilla (ref. 11) has shown that by strengthening the surface of both an 18/8 stainless and annealed mild steels the fatigue limits can be raised to the stress levels of their respective discontinuities. The strengthening of the surface was obtained by cyanide carbo-nitriding and Abdilla shows that the surface is the final part of the specimen to fracture. The evidence indicates fairly convincingly that the increase in strength is entirely owing to the prevention of stage I cracks, although there is some doubt as to how this is achieved, and this will be discussed later. The work of Abdilla also indicates that having reached a certain stress level (namely that of the discontinuity) fatigue will occur whether or not stage I cracks are formed.

In his investigations of frequency effects, Finney (ref. 12) fatigue tested 2024-T4 extruded aluminium alloy at the three frequencies 100, 1000, and 12,000 cycles per minute. The results show clearly that the effect of different testing speeds is most marked in the region immediately below the discontinuity. Finney shows some of the fracture surfaces throughout the complete stress range at each of the testing frequencies. It can be seen that at the stress level of the discontinuity

the mechanism involved changes from smooth fractures below to 'tensile' type fractures above. At 12,000 cycles per minute the fractures at stress levels above the discontinuity are cup and cone, a type of fracture associated with a large quantity of plastic deformation as in the tensile test. The phenomenon occurring in this alloy is similar to that described by Benham and Ford as cyclic creep. The evidence, therefore, suggests that the discontinuity represents the limiting stress level for strain hardening, and above this stress level a collapse of work hardening occurs resulting in macro plastic deformation. Therefore the discontinuity is the true fatigue limit of the material, but at stress levels below that of the discontinuity the weak surface collapses ahead of the substrate thus initiating the fatigue process.

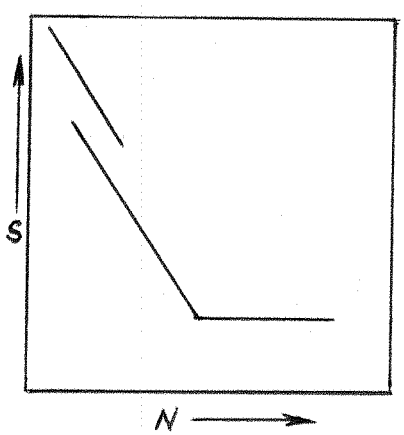

S/N curve for mild steel

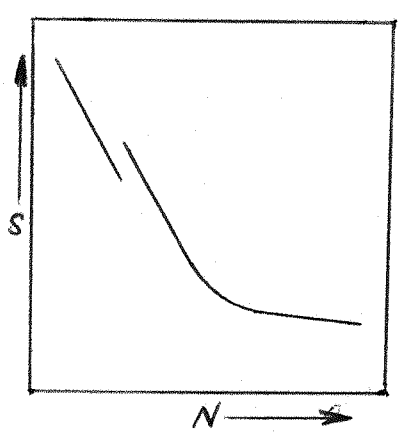

S/N curve for aluminium alloy

Diagram 1

If the S/N curves for mild steel and an age-hardening aluminium alloy be compared (see diagram 1) it can be seen that in the case of the aluminium alloy an endurance limit is found, whereas the mild steel exhibits a 'knee' resulting in a clearly defined fatigue limit. Now Levy (ref. 13) has shown that the coaxing* of mild steel can raise the fatigue limit by approximately 2 Tons/inch^2 and at the same time the 'knee' disappears resulting in a gentle curve and an endurance limit, with fractures at lives greater than 10^7 cycles. Levy shows that coaxing causes the maximum amount of strain ageing to occur in the mild steel before the fatigue mechanism comes into operation, and therefore further strain ageing during fatigue is unlikely. It may be concluded therefore that the knee is caused by strain ageing and were this phenomenon not to occur then an endurance limit would result. Adair and Lipsitt (ref. 14) have put forward the suggestion that the fatigue limit behaviour is due to the body-centered-cubic structures but since it is this particular structure which exhibits the most benefit from strain ageing, it seems more likely that the knee is still caused by the phenomenon of strain ageing.

Further comparison from the S/N curves in diagram 1, reveals that the discontinuities are dissimilar. Whereas in the mild steel curve the discontinuity causes an increase in life at stress levels above

*Coaxing:- The application of a large number of cycles (say 10^6) at a stress level just below the fatigue limit (say 5 Tons/in^2 less) followed by another 10^6 cycles at a slightly higher stress and so on at increasing stress levels until failure occurs.

it, a corresponding decrease in endurance is found from the aluminium alloy. Since the 'knee' occurs only in materials capable of strain ageing, and since the strain ageing occurs during the fatigue process, it may be deduced that the phenomenon of increase in endurance at stress levels above the discontinuity is also brought about by strain ageing.

At a temperature of -80°C it can be shown that the diffusion process necessary for the strain ageing mechanism to proceed is negligible. Shurmer (ref. 15) fatigue tested mild steel and showed that the shift of life found at the discontinuity at room temperature was reversed when the process was carried out at -80°C (see Figure 1).

From the information presented it may be deduced that the increase in life found at the stress level of the discontinuity is owing to a temperature dependent strengthening process resulting from the plastic deformation which occurs during the fatigue mechanism, and that this strengthening is due, therefore, to strain ageing.

Strengthening affects can be brought about in many ways, but so far nothing has been mentioned about the dependence of fatigue strength on surface finish. If notched specimens are fatigue tested it may be that the surface plays a negligible part, but in plain specimens the surface is of vital importance as shown by case carburising.

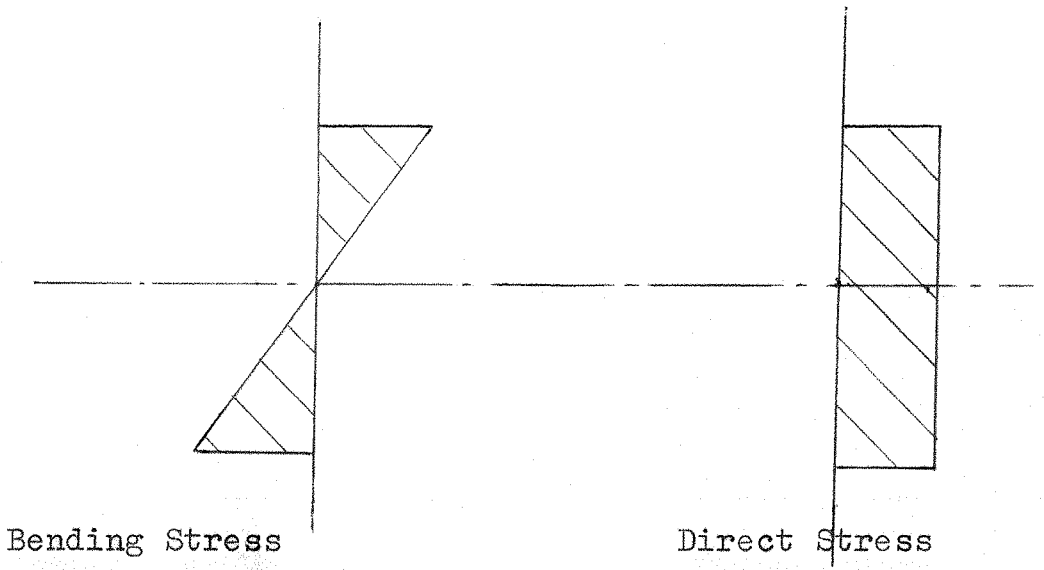

Diagram 2

If the stress distributions which occur in bending and direct stress be compared (see diagram 2) it may be deduced by inspection that the surface finish is very much more important in rotating cantilever or reversed bending than it is in the case of direct stress. Because the maximum stress in the bending specimens occurs only at the surface it may be expected that an increase in the fatigue limit will occur proportionally with an increase of surface strength.

Cina (ref. 16) has investigated the effects of surface preparation of test pieces utilizing several varieties of chromium-nickel steels. From tests on an 18/8 chromium-nickel steel he shows that mechanical polishing of the specimens introduced a structural change in the surface grains from parent austenite to ferrite. The austenite in this steel is unstable and when cold worked readily undergoes a change to martensite or ferrite (see App. C). Cina, therefore, concludes that mechanical polishing causes a substantial quantity of cold work and

supports this deduction by showing a fully austenitic structure in the surface of electropolished specimens. Further investigations by Cina into the changes of fatigue strength between mechanically polished and electropolished specimens revealed that work hardening of and residual stresses in the surface, caused by mechanical polishing, were responsible for an increase in the fatigue limit. These tests, performed in a rotating cantilever machine, resulted in a maximum change of 5 Tons/in^2. In direct stress fatigue little difference in the fatigue limit was found between the electropolished and the mechanically polished specimens, but when electropolished specimens were tested in both types of machine a difference of 2 Tons/in^2 was found in the fatigue limits. In each type of testing the specimens used were round, but in the case of direct stressing the diameter was larger. Cina comments on this size difference stating that the bigger specimens would be likely to have more imperfections resulting in a lower fatigue limit, but it may be more realistic to say that the surface of rotating bending specimens is so important that an increase in fatigue strength may be expected in small specimens as predicted by Frost (ref. 17).

The effect of the surface layer on fatigue has also been investigated by Frost (ref. 17) for both direct stress and rotating cantilever testing. He shows that an increase in the fatigue limit is produced with an increase of surface hardness, but the effect is much less pronounced in direct stress.

The above investigators into surface effects were concerned only with the degree of work hardening introduced by the machining process. However, Coomb et al (ref. 18) have investigated the effect of shot peening upon the fatigue strength of a hardened and tempered spring steel. The peening process would result in residual surface stresses of a compressive nature and also cause work hardening in the surface grains. Fatigue tests were carried out on a rotating cantilever fatigue machine and it was found that, if the specimens were mechanically polished, an increase in the fatigue limit of 10 Tons/in^2 resulted. The optimum increase obtained from shot peening was also about 10 Tons/in^2, but if the specimens were peened and polished the maximum increase was of the order of 18 Tons/in^2. Coombs shows a sub-surface fatigue crack in one of the specimens which had been both peened and polished. The crack had initiated immediately below the work hardened layer and it would appear that the condition reached in this material is similar to that obtained by Abdilla in case-carburised mild steel; i.e. the peening and polishing operations prevent stage I crack growth.

So far mention has only been made of constant load or constant strain fatigue, but the engineer is frequently confronted with failure caused by a random stress pattern and this presents additional complexities. In 1945 Miner (ref. 19) first published a cumulative fatigue damage theory which is still in use today. The theory states that, irrespective of sequence effects, the amount of damage produced in a fatigued specimen,

at any one stress level, is proportional to the number of cycles applied at that stress level divided by the number of cycles required for failure at the same stress. If, therefore, failure is caused by a random stress series and if n_1 cycles are applied at a stress S_1, n_2 cycles are applied at a stress S_2 ..... and n_i cycles are applied at a stress S_i, then:-

$$\frac{n_1}{N_1} + \frac{n_2}{N_2} \quad \ldots\ldots + \frac{n_i}{N_i} = 1$$

i.e.

$$\sum \frac{n}{N} = 1$$

where N_1 is the total number of cycles necessary for failure at a stress level S_1, etc.

This theory also discounts rest periods and stresses which are below the conventional fatigue or endurance limits. Marsh (ref. 20) has modified a rotating-bending fatigue machine to obtain a symmetrical saw-tooth programme as shown in diagram 3 below.

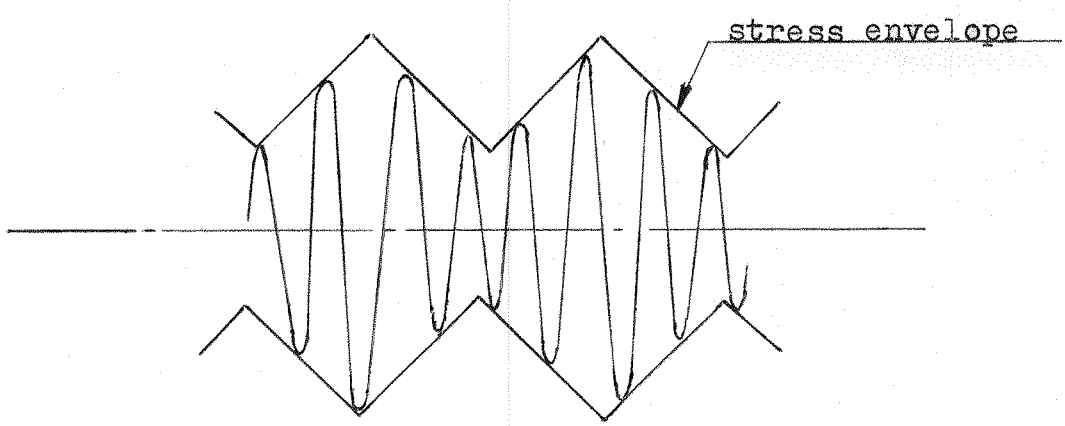

Diagram 3

The machine, which ran at a constant frequency, yielded results which caused an overestimation of life when predicted by Miner's rule, but Marsh shows that an accurate prediction can be made if the low amplitude cycles at stress levels down to 80% of the fatigue limit are assumed to contribute to the fatigue damage.

It may be deduced from Miner's rule that if a specimen is run for half of its life at one stress, then on application of a different stress the specimen should fail after half the corresponding number of cycles to failure.

$$\frac{n_1}{N_1} = \tfrac{1}{2}$$

$$\frac{n_2}{N_2} = 1 - \frac{n_1}{N_1} = \tfrac{1}{2}$$

$$\therefore \quad n_2 = \tfrac{1}{2} N_2$$

Several people have investigated the effect of applying two discrete stress levels and the results can be separated into two categories. (This type of test is known as a sequence test). Pope Foster and Bloomer (ref. 21) have investigated sequence effects arising in mild steel and discovered that when the high stress levels are applied first values of $\sum \frac{n}{N}$ less than one were obtained and vice-versa.

Williams and Lowcock (ref. 22) have reported a reverse effect in an age hardening aluminium alloy and a theory is proposed to account for the mild steel phenomenon. They suggest that the development of

stage I cracks in the surface grain would be hindered by the strain ageing process when low stress cycling is applied first. In the case of the aluminium alloy, however, strain ageing does not occur and the material has but little capability to work harden. Therefore initial application of low stress cycling would allow the stage I cracks to develop uninterruptedly whereas initial high stress cycling causes a dispersal in slip and a delay in the crack initiation process.

Sequence tests carried out on 70/30 brass and copper by Wood and Reimann (ref. 23) show that the 'high-low' sequence of testing produces the highest rate of damage, thus agreeing with the results obtained from the aluminium alloy. Wood and Reimann applied torsion fatigue to plain specimens. They suggest that the 'low-high' sequence involves the application of large strains to a structure containing slip zone micro-cracks which have divided the grain into loosely attached blocks. The cracks are opened up by the application of high stress and a rapid rate of fatigue damage occurs. In the 'high-low' sequence a dispersal of slip is caused by the high stress which hinders the crack initiation process.

It can be seen from the above evidence that sequence effects can play a vital role in cumulative fatigue damage. It may be expected that rest periods would only have effect on materials which in some way improve or reduce their strength with time. Thus for ferritic materials strain ageing may occur during a rest period resulting in an improved

fatigue strength.

Mitchell (ref. 24) has investigated the effect of cumulative fatigue damage under sinusoidal and random loading conditions. He compares the results obtained on L73 aluminium alloy and they indicate that the scatter produced in the random loading is less than that produced from sinusoidal loading at similar stress levels. He uses Miner's rule to predict the S/N curve obtained in random loading and it compares very favourably with the results.

A discontinuity is shown in both curves, but whereas shorter endurances are obtained at stress levels above the discontinuity in sinusoidal loading, a corresponding increase in lives is found in the random loading curve. Mitchell attributes this change in the random loading conditions to blunting of the crack front arising from general plastic yielding when a significant proportion of cycles exceeds the stress level of the discontinuity in the sinusoidal fatigue curve.

With the exception of surface hardening treatments, mention so far has only been made about fundamental aspects which occur in fatigue, resulting directly from testing and specimen preparation. However, Frost (ref. 25) has investigated the effect of prior strain hardening on the fatigue behaviour of normalised mild steel. He compressed the mild steel various amounts and tested specimens from the prestrained material in a Rolls Royce rotating cantilever machine. Beneficial effects were obtained until a collapse occurred, after 60% prestrain, causing the

fatigue limit to fall to the same level as found in the normalised condition. (The results are given below.)

% Nominal Compressive Strain	Fatigue Limit (Tons/in^2) (Plain Specimens)
0	$\pm$ 16.3
30	$\pm$ 20.5
50	$\pm$ 22.7
65	$\pm$ 17.0
90	+ 17.0

FATIGUE TESTING APPARATUS

(Descriptions, Principles, Calibration Techniques and Operation)

Fatigue tests were carried out on three different fatigue machines:

(A) Rolls Royce rotating cantilever - bending stress sytem

(B) Resonant Beam - direct stress

(C) Avery Midget Pulsator - direct stress

(A) Rolls Royce Rotating Cantilever - see plate I

The machine was run at a constant speed of 80 cycles per second. Although other speeds were available up to 120 cycles per second, the shafts were found to vibrate at most of the available range. Both notched and plain test pieces were used in this machine, and a drawing for each type is shown in figure 26. A calibration curve for the plain specimens is shown in figure 27.

Trouble free running was experienced with this machine and it can be recommended for accurate fatigue testing.

(B) Resonant Beam System - see plates II and III
(Resonant frequency = 120 cycles per second).

Basically this apparatus consisted of a horizontal beam, which, securely fixed at each end, was vibrated at its resonant frequency by an electro-magnetic vibrator. One end of the beam was coupled directly to the super-structure by means of a spring steel plate, and the other end of the beam was coupled by another spring steel plate to a vertical shaft which had specimen grips at the lower end. Specimen grips were

also mounted on the base of the superstructure below the shaft, and the specimen formed the final fixture for the beam. Surrounding the vertical shaft was an air bearing which served to prevent any form of buckling which may result in bending of the specimens during the compressive part of the stress cycle (see appendix I).

Mounted above and attached to the same end of the beam as the shaft was a spring which served to remove the weight of the beam from the specimen. This spring was also used to apply a static mean load to the specimen either in the form of tension or compression. Calibration of this spring was obtained in an Avery tensile machine and a calibration graph appears in Figure 28.

This machine could be used to provide constant amplitude or random amplitude stress patterns.

(a) Constant Amplitude.

To obtain constant amplitude stress in the form of a sine wave a signal generator was used. The output from this was coupled via an attenuator to the power amplifier which was connected to the electromagnetic vibrator.

(b) Random Amplitude.

Because the beam was vibrated at its resonant frequency a narrow band excitation of similar frequency was required. Initially the output from a white noise generator was passed through a Cawkell band-pass filter, and this resulting narrow band signal was then passed

through the pre-amplifier, the attenuator and into the main amplifier.

Monitoring of the stress level was obtained by semi-conductor strain gauges arranged in 'wheatstone-bridge' form and these were mounted on the vertical shaft interposed between the beam and the specimen. The applied voltage to the strain gauges was six volts (direct current), and the output signal was fed to an a.c. millivoltmeter. For constant amplitude signals the millivoltmeter indicated a constant value which could be related to the applied stress level by the calibration graph shown in figure 29.

However, for random amplitude the millivoltmeter was insufficient, therefore the output from its a.c. amplifier was recorded into a magnetic tape and compared on a correlator with a sine wave of known amplitude. This enabled the root mean square value of the waveform to be obtained along with the maximum peak stress obtained.

This control unit of the fatigue machine was fitted with a 'cut-out' device which could be made to switch off the power when a specimen failed. The endurance of the specimen was recorded by an electric clock and this was also switched off by the 'cut-out'. Essentially the 'cut-out' consisted of a relay capacitor circuit and an amplifier. The output signal from the strain gauges was amplified and used to charge the capacitor thus causing the relay to be closed. Failure of the test piece caused the strain gauge output to fall to zero, the capacitor became uncharged and the relay opened, isolating the control cabinet and

stopping the clock. An oscilloscope mounted in the control cabinet was used to monitor the output signal from the strain gauges. If the waveform was not a true sine-wave then conditions in the air bearing were unsatisfactory, e.g. the air pressure may have been low or the air bearing was misaligned. (If other faults in the appratus developed e.g. if there were a lack of rigidity in the bolted units, or if the specimen grips were slack, then these also were indicated by a faulty sine-wave.) Two filters were placed in the air supply line, but it was found necessary to dismantle and clean the air bearing at regular intervals of about one month's continuous running.

Calibration of this appratus was performed as follows:-

A mild steel plate was mounted in the specimen grips and attached to both sides of the plate were thin foil strain gauges. The spring, which was used for applying a static mean load to specimens, was extended to produce a known tensile load on the plate, and the changes in the outputs from both sets of strain gauges were measured on a dual beam oscilloscope. Several readings were obtained for different static loads and the results for the permanent gauges are shown in figure 29.

The spring was then released to produce zero mean stress on the plate and the beam was vibrated at its resonant frequency. The amplitudes of the sine-waves produced by each set of strain gauges were compared and it was found that the ratio of the amplitudes was the same as that obtained in the case of static loading. This indicated that the

frictional effect of the air bearing was negligible.

Flat test pieces were used in this machine and in the case of mild steel and L73 aluminium alloy the specimens were punched from the sheet material in a flypress. In the case of stainless steel, however, the specimens had to be machined individually. Drawings of the test pieces are shown in figure 30. Owing to the power limitations of the machine the test pieces had a centrally drilled hole resulting in a stress concentration and for high strength materials the smaller sized specimens were introduced. These modifications enabled the high stress - low endurance testing of materials.

Another machine similar to the one just described was also used for experiments and calibration curves for the spring and strain gauges are shown in figures 31 and 25 respectively. This second machine had a resonant frequency of 90 cycles per second.

The ease of access to the specimen grips of the resonant beam fatigue rig whose resonant frequency was 120 cycles per second enabled the placing of either an "electric furnace" or an "ice box" round the test piece under test.

Electric Furnace - see plate IV.

This was constructed from 'syndanio' tubes, and consisted of two halves, each containing a separate winding. This enabled the furnace to be easily applied to the specimen without dismantling any of the apparatus. Control of the temperature was obtained with a 'Transitrol'

control unit and with the use of a variac the temperature could be maintained within $\pm$ 5°C of any setting. Temperature measurement was obtained with a thermocouple which projected through the walls of the furnace so that the junction was within 0.1 inches from the stressed section of the test piece. The maximum temperature obtainable from the furnace was 750°C which was the limitation of the syndanio. A period of 15 minutes at temperature was given to each specimen to enable the conditions to become stable before fatigue testing commenced.

Ice-Box - see plate V

This consisted of a wooden, topless box which enclosed the specimen. It was constructed in two halves, hinged together so that it could be positioned after the specimen to be tested had been mounted in the grips. The box was filled with small pieces of solid carbon dioxide and acetone was added to obtain a temperature of -80°C. The temperature was measured by a thermocouple and to ensure complete cooling of the test piece the solid carbon-dioxide and acetone mixture was added 15 minutes before fatigue testing began.

(C) Avery Midget Pulsator - see plate VI

Specimens used in this machine were the same as those used in the resonant beam fatigue machine.

Calibration of the machine was found necessary and this was achieved with the use of a proof ring. The resulting calibration curve is shown in figure 24.

Principles and Operation of the Infra-Red Camera - see plates VII and VIII)

The principles of this machine involved focussing infra-red radiation onto a sensitive semi-conductor, amplifying the output and using it to produce thermographs.

The radiation was reflected by a system of special mirrors through a filter to remove all other forms of radiation, e.g. light radiation, and then focussed by a lens onto the semi-conductor. The radiation signal to the semi-conductor was passed through a revolving slotted disc to 'chop' the signal and produce a series of pulses from the semi-conductor. This changed the 'would-be' direct current signal to an alternating current which could then be amplified more easily than the direct current. The amount of radiation produced by a surface is proportional to the fourth power of the temperature of the surface, so the output signal from the semi-conductor was passed through a correcting attenuator to make the final output of the machine proportional to the temperature of the radiating surface.

The final output voltage was then discharged throuch chemically impregnated paper which, as a result, changed from white, through shades of grey, to black - the intensity of the change being proportional to the signal and hence the temperature of the radiating surface. A contrast switch was incorporated to enable the high temperatures to be represented either as black against a white (cool) background or as white against a black (cool) background.

The aforementioned mirrors were designed to scan an area and the output signal was coupled to another scanning mechanism which enabled a thermograph to be produced representing the scanned area. However, when used during the fatigue experiments, the ability of the machine to scan an area was disregarded and thermographs were produced from continuous scanning of a narrow band along the axis of the specimen as shown in diagram 7 below.

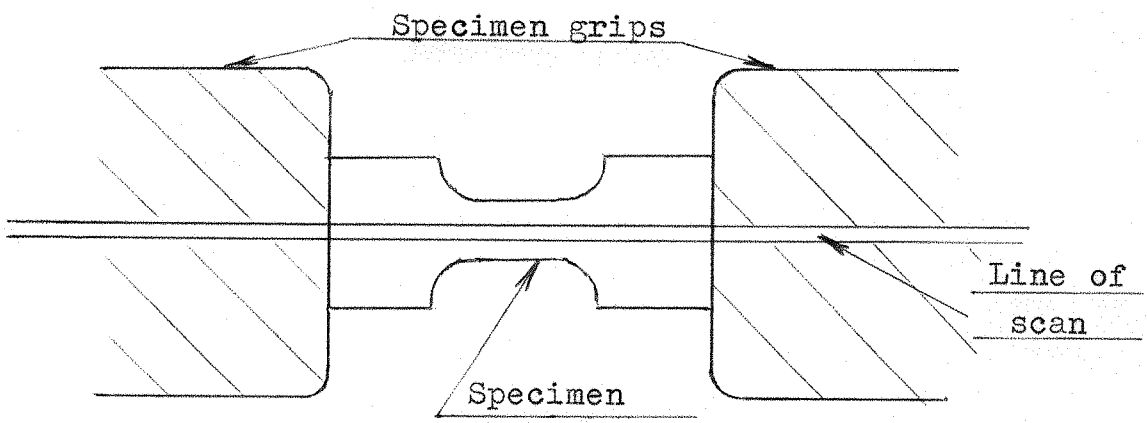

Diagram 7

Because the focussing of the camera could not be adjusted, to produce optimum results it was necessary to position the camera at the fixed distance of eighteen inches from the fatigue specimen. The radiation sensitive semi-conductor was placed in the bottom of a small dewar flask into which liquid nitrogen had to be poured at intervals of fifteen minutes. This was to prevent overheating of the semi-conductor.

Impact Testing

A Hounsfield balanced impact testing machine was used for all impact tests. Specimen dimensions are shown in figure 23.

Tests were conducted in the temperature range -196°C to +100°C and the temperatures were obtained as follows:- +20°C - +100°C: the specimen was immersed in a glycerine bath which was heated above, and allowed to cool to the required temperature; the specimen was then quickly transferred to the impact machine and tested.

-80°C - +20°C: this temperature range was obtained by cooling acetone with solid carbon dioxide. The specimen was immersed in the acetone, which was cooled below, and allowed to rise to the required temperature; the specimen was then transferred to the machine and tested.

-196°C: the specimen was immersed in liquid nitrogen before testing in the impact machine.

All temperatures were measured by a thermocouple discriminating to within $\pm \frac{1}{2}$°C throughout the range -196°C to +100°C.

EXPERIMENTAL PROGRAMME

Annealed 18/8 stainless steel rod, specification S110, was cold rolled from a diameter of 0.628 inch to the shape as illustrated in figure 2. The required reduction of 65% was obtained by five passes through the rolling mill, the steel being water cooled between each successive pass. Plain and notched fatigue specimens as shown in figure 26(a) and (b) were made from the rolled bar and S/N curves obtained on a Rolls Royce machine - figures 3 and 4.

A further quantity of the annealed stainless steel was cold rolled to a similar shape as that shown in figure 2 and the material was again cooled between each of the seven passes required to obtain a reduction in area of more than 70%; the original diameter was 0.765 inch and the final area after rolling was 0.115in.^{2} S/N curves were obtained with this steel, with a 75% reduction in area, utilizing plain and notched fatigue specimens (see figure 26(a) and (b)) tested in a Rolls Royce machine - figures 5 and 6; impact tests were also performed on this rolled steel in the range of temperatures from -196°C to +100°C - a Hounsfield impact machine was used.

Twelve tensile specimens were machined from the cold rolled steel with a reduction in area of 75% and each was stretched in an Avery tensile machine to produce an extension of 5% which resulted in localised necking. Notched fatigue test pieces were produced from these tensile specimens such that the position of maximum stress would coincide with the

position of necking - see figure 7. The fatigue specimens were of the variety shown in figure 26(b) and the Rolls Royce rotating cantilever test results are shown in figure 8. A tensile test was undertaken on this steel with a 75% rolling reduction in an Instron tensile machine, and the results obtained are shown on page 102.

A melt of nominal 18/8 stainless steel, titanium free, and with a raised nitrogen content was produced by Richard, Thomas and Baldwins. The analysis is given on page 92 . This material was produced in sheet form and finally cold rolled from the annealed condition to produce a reduction in area of 60%. Notched fatigue specimens of the type shown in figure 30(b) were made from this material and tested in the resonant beam machine - figure 9. Three plain fatigue specimens (without the centrally drilled hole) were strained until failure occurred. An Instron tensile machine was used and the results are given on page 112 . Each test piece was strained at the constant rate of 0.1 millimetre per minute.

A fatigue S/N curve was obtained for annealed 70/30 brass utilizing plain specimens tested in a Rolls Royce rotating cantilever fatigue machine - figure 10. Annealed rods of 70/30 brass were stretched in an Avery tensile machine to produce an extension of 25%, plain fatigue samples were prepared and tested in a Rolls Royce machine - figure 11. A statistical plot of probability against log (cycles) was made in order to determine the level of the discontinuity for the stretched brass -

figure 12. An S/N curve was obtained for the stretched brass utilizing notched fatigue specimens of the type shown in figure 26(c). The results undertaken in a Rolls Royce machine are shown in figure 13.

Notched specimens of annealed 18/8 steel (as shown in figure 30(b)) were fatigue tested in an Avery midget pulsator. S/N curves were obtained with alternating tension-compression stresses and with pure tensile stresses, the mean stress being equal to half the maximum applied stress, (i.e. the minimum stress = 0 Tons/inch^2) - figure 14. Similar fatigue tests were also performed on mild steel utilizing notched specimens of the type shown in figure 30(a) (see figures 15 and 16), and on L73 aluminium alloy for which the additional fatigue tests in pure compression were obtained with the mean stress equal to half the peak compressive stress - figure 17.

Low temperature fatigue testing at -80°C was carried out on 18/8 stainless steel utilizing notched specimens of the type shown in figure 30(b) - see figure 18.

High temperature fatigue tests at 250 and 350°C were carried out on 18/8 stainless steel utilizing notched specimens of the type shown in figure 30(b). The results are shown in figures 19 and 20. Direct stress notched fatigue tests of mild steel at 350°C were carried out (the specimen dimensions are shown in figure 30(a)) and the results are shown in figure 21.

Random stress fatigue testing was performed with L73 aluminium

alloy, utilizing notched specimens as shown in figure 30(a). The testing was undertaken with an unfactored static mean load of 6 Tons/inch^2 and the results are shown in figure 22.

An infra red camera was used to indicate the temperature rise which occurs in both 18/8 stainless steel and mild steel when under cyclic stress. Plain specimens were used. Initially thermographs were obtained at various stress levels utilizing plain specimens and the heat signals were recorded.A high-low sequence loading test was carried out on 18/8 steel with stress levels of 36 and 28 Tons/inch^2 respectively and the thermograph recorded is shown in plate X. A thermograph was also obtained for mild steel at the stress level of 20 Tons/inch^2 - plate XI. A mild steel specimen was cyclicly loaded with the peak stress level of 20 Tons/inch^2 with a static mean of 10 Tons/inch^2, and a thermograph was obtained for the first ten thousand cycles. After the steel had undergone a total of 10^6 cycles, another thermograph was obtained. These two results are shown in plate XII.

(The theoretical stress concentration factors of the notched specimens are determined from Neuber's theory.)

Thin stainless steel foils for electron microscopy were produced in the following way:

The sheet material (18/8 stainless steel) was mechanically polished until about 0.010 inch thick. The edges of this plate were coated with Lacomit* and the sample was then transferred to an electro-

*This was done to prevent preferential polishing.

polishing cell in which the electrolyte was a 60/40 mixture of ortho-phosphoric and sulphuric acids. The current density in the cell was 2 amps/cm^2 and electropolishing was stopped as soon as a hole appeared in the sample. A small section of thin film was cut away from the side of this hole and examined in the electron microscope. The negative electrodes were pointed and spaced equally on either side of the positive metal specimen; adjustment of the distance between the probe and specimen enabled an equal distribution of electropolishing through the majority of the surface, so that when a hole was formed a large adjacent area of foil would be suitable for examination.

Discussion:

The review of metal fatigue has been centered, to a large extent, round a discontinuity which appears in the S/N curve of metals and alloys. It has been shown by Abdilla and Williams (ref. 26) that case carburising of both mild and 18/8 stainless steels can raise the fatigue limit to their respective discontinuities, but there is some doubt as to how this is achieved. Quenching and tempering carburised mild steel would cause a phase change from ferritic to the tetragonal structure martensite* and consequently it is possible that the increase in volume of the martensitic phase as compared to the original ferrite would cause residual compressive stresses in the surface layers. Consequently the applied load to obtain a stress would have to be larger to off-set these negative residual stresses. Thus it may be argued that the apparent increase in the fatigue limit of mild steel, due to carburising, is much larger than the real increase.

When, however, the carburising of a fully austensitic material - namely 18/8 stainless steel - also raises the fatigue limit to the level of the discontinuity, the residual stress argument breaks down since there is no phase change involved in this process. It can only be therefore, that the carburising causes an increase in the surface strength and as a result prevents the stage I initiation cracks and the associated stress concentration factor from forming below the level of the discontinuity.

It is, therefore, proposed that the discontinuity in a material represents the maximum stress to which the fatigue limit can be raised, above

*See Appendix C

which the associated strain causes irreparable damage - that is to say a continual structural collapse occurs and a "cyclic creep" results. The discontinuity may, therefore, be regarded as a critical stress level at which the transition occurs from low strain below to high strain above.

However, at stress levels above the discontinuity the higher strain gives rise to strain hardening in work hardening materials and so causes an increase in the resistance to fatigue crack propagation. This may, therefore, account for the shift to longer endurances found, for example, in mild steel at room temperature. In the case of age hardening aluminium alloys, however, it is possible that the strains above the discontinuity cause an overageing effect as shown by Forsyth. These result in a weakening of metal and a shift to lower endurances results at stress levels above the discontinuity.

Analysis of the results of annealed 70/30 brass, fatigue tested in a Rolls Royce rotating cantilever machine, reveals an endurance limit at 12.5 tons/inch^2 and a sudden change in the slope of the S/N curve at the stress level of 19 tons/inch^2 (see figure 10). The discontinuities reported by other researchers lie in the range of endurances from 10^3 to 10^5 cycles, and it is probable, therefore, that the change of slope in the S/N curve of 70/30 brass represents the discontinuity.

To investigate the effect of prestrain on the fatigue behaviour, the annealed material was given a longitudinal stretch to produce an

extension of 25% and the results of fatigue tests utilizing plain specimens tested in a Rolls Royce machine are shown in figure 11. Analysis of the fracture surfaces revealed a significant change in appearance from eccentric crack propagation at stress levels of 24.7 tons/inch^2 and below, to concentric crack propagation at 26 tons/inch^2 and above, (see plate XIII). These observations are similar to those reported by Williams, Hayden and Hallwood (ref. 6) for L65 aluminium alloy, and they associate the change in fracture with a discontinuity shown in the S/N curve.

Williams and Abdilla (ref. 26) have suggested that the discontinuity represents a change from crack propagation from slip band cracks below the discontinuity to a general 'grooving' process at stress levels above. The former process would tend to cause crack propagation from one source only, as suggested by Forsyth (ref. 7), whereas at stress levels above the discontinuity the 'grooving' process would not be localised but would completely affect the material, thus tending to cause crack propagation from all free surfaces. It is likely, therefore, that these are the reasons for eccentric and concentric crack paths.

A series of probability plots were also made for the cold stretched brass and these are shown in figure 12. The results produce a maximum slope at 26 tons/inch^2 indicating maximum scatter in endurance at this stress level. If, as Williams and Stevens suggest (ref. 3), the discontinuity corresponds to an increase in scatter, then, both by statistics and fracture

inspection, the discontinuity for the cold stretched brass is in the region of 24.7 to 26 tons/inch^2, which is a fairly good agreement.

Inspection of the S/N curve obtained from rotating cantilever testing of stretched 70/30 brass utilizing notched specimens reveals a discontinuity in the curve at the stress level of 25 tons/inch^2 (see figure 13). At the same stress level a change in the fracture appearance again reveals eccentric crack propagation below to concentric crack propagation at stress levels above 25 tons/inch^2 (see plate XIV). If, therefore, it can be assumed from the evidence so far presented that a change in appearance of the fracture surface of rotating cantilever specimens from eccentric to concentric propagation indicates the discontinuity, then it would be possible to indicate the region of the discontinuity in the S/N curve of a metal or alloy even though the plot of results showed no significant change in endurance.

Frost (ref. 8) has reported that the stress concentration factor, K_f, of a slip band crack in extruded aluminium alloy L65 is of the order 1.5. Now if between the stress levels of the fatigue limit, σ_L, and the discontinuity the fatigue process involves the initiation and propagation of slip band cracks then it may be anticipated that the minimum stress for crack propagation would be defined by the product of σ_L and K_f. If the K_f value of a slip band crack for 70/30 brass can be assumed to be 1.5 then it may be seen that the product $\sigma_L \times K_f$

yields a value of approximately 19 tons/inch^2, which is the level of the discontinuity. It may be seen from the plain fatigue tests of stretched brass that fatigue occurs only when $\sigma_L \times K_f \geq \sigma_D$ (where σ_D = stress level of the discontinuity; see figures 10 and 11).

Forsyth (ref. 7) has shown that slip band cracks can be produced at stress levels below the fatigue limit, but that the stage I (propagation) cracks do not form until the stress levels above the fatigue limit are attained. If the above equation is valid and the stress concentration of slip band cracks is around 1.5 then this evidence again indicates that the discontinuity is the minimum stress level required for crack propagation and the equation may be used to distinguish between propagating and non-propagating cracks.

Notched fatigue testing of stretched 70/30 brass with a theoretical stress concentration factor $K_\tau = 3$, yields a discontinuity at 25 tons/inch^2, which is the same as for plain specimens (c.f. figures 11 and 13). The endurance limit for the notched tests has fallen to approximately 8 tons/inch^2. It is at once apparent from these results that crack propagation occurs when $\sigma_L \times K_\tau$ is approximately 25 tons/inch^2.

The results of fatigue tests of 18/8 stainless steel cold rolled to give a reduction in area of 65% have yielded a fatigue limit with plain specimens at 36 tons/inch^2 and a discontinuity at 60 tons/inch^2 (figure 3). (σ_D is based on the fracture change from eccentric to concentric crack propagation). Williams and Stevens (ref. 3) report a fatigue limit of

22 tons/inch^2 and a discontinuity at 32 tons/inch^2 for annealed 18/8 stainless steel and it may be seen that each is substantially raised by the rolling. A further rolling reduction to 75% makes little if any difference to the discontinuity produced from 65% reduction in area, but the fatigue limit is raised to 45 tons/inch^2 (figure 5).

It is to be observed that for the 18/8 steel with a 65% reduction in area the value of σ_D/σ_L is 1.67 which is slightly above 1.5 originally suggested for the K_f value of a slip band crack. If, however, the material became more notch sensitive as a result of the rolling reduction then it is possible that a similar size of slip band crack would result in a larger stress concentration, than occurs in the annealed material. This would then account for the deviation in the K_f value.

From the results of 18/8 stainless steel with a 75% reduction in area (see figure 5) K_f is found to have the value 1.33 which is considerably below the value 1.5 found in the annealed condition. It is, however, interesting to notice that both for 65% and 75% reduction in area the discontinuities occur at the same stress level - namely 60 tons/inch^2. This would, therefore, indicate that one of the following is happening:- (a) the extra rolling has caused the slip plane cracks which are formed to have less severe stress concentration.

Or (b) the slip band cracks are not formed until the stress of 45 tons/inch^2 is reached in the 18/8 steel with 75% reduction in area.

It is difficult to postulate reasons which can explain a reduction in stress concentration but the relative reduction in grain diameter resulting in shallower slip band cracks could be a possible explanation. If, however, the extra prestraining caused a general increase in resistance to slip band formation then it is possible that this could result in the prevention of stage I cracks (as suggested in (b)) until the stress level of 45 tons/inch^2 is attained. Owing to the small quantity of material available for the tests on this 18/8 steel with a 65% reduction in area further experimental work was not possible. It would, however, provide valuable evidence on which to base or reject this argument if cycling just below the fatigue limit is carried out with the object of determining whether non propagating slip band cracks are produced.

Comparative notched testing of the rolled material with a 65% reduction has yielded a discontinuity between 35 and 40 tons/inch^2 with a corresponding fatigue limit at 18 tons/inch^2 (see figure 4), whereas notched fatigue testing of 75% rolled material has produced a discontinuity at 35 tons/inch^2 and a fatigue limit at 18 tons/inch^2 (see figure 6). The effect of an increased rolling reduction from 65 to 75% causes no significant change when the material is tested in the notched condition. The apparent benefit obtained with plain specimens is substantially reduced when notched fatigue tests are carried out, and compared with the discontinuity obtained from the annealed 18/8 steel (32 tons/inch^2) the improvement in the notched

condition is small, being only about 3 tons/inch^2. The difference in the discontinuity levels between the notched and plain fatigue tests is large and the reason why is not clear. Considerable difficulty, mainly in the form of bending, experienced during machining, indicates that the rolling produced considerable residual stresses, and it is possible that these are able to play a considerable part in plain test pieces, whereas the extra cut involved in the preparation of notched specimens may upset the residual stress patterns and apparently reduce the strength.

The result of giving a longitudinal stretch of 5% to 18/8 stainless steel with a reduction in area of 75% was to cause localized necking. Notched fatigue testing of this material in the rolled and stretched condition such that the highly stressed section of the test piece coincided with the necking revealed a fatigue limit at about 22 tons/inch^2 (see figures 7 and 8). Owing to the limited number of tests a discontinuity is not apparent, but analysis of the fracture surfaces indicated a change from eccentric to concentric crack propagation at the stress level of 44 tons/inch^2. If this is the discontinuity then rolling and stretching has raised it by approximately 12 tons/inch^2 above that of the annealed material.

It is interesting to notice that there is no sign of a collapse of the fatigue strength as reported by Frost (ref. 25) for mild steel. From his work it would seem that the improved fatigue strength produced from the

prior straining in compression is due to a metallurgical change rather than a physical change in the form of residual stress. This is fairly well justified by the fact that the specimens were machined from the core of prestrained blanks in such a way that the residual stress distributions would be grossly interrupted and be reduced to a negligible level.

The large amount of prestrain, necessary for the collapse of the fatigue strength in mild steel, will doubtless cause many microstructural changes in the form of dislocation networks but perhaps the most important consequence which may happen is the formation of microcracks which result from dislocation pile ups. An increased dislocation density would probably enhance the fatigue resistance, but once cracks are present they would provide ideal sources of stress concentration for triggering crack propagation and consequently reduce considerably the fatigue strength.

To reach the level at which microcracks are formed the amount of plastic deformation necessary would be more for 18/8 stainless steel than for mild steel, by virtue of the fact that 18/8 steel is a single and phased alloy as opposed to the structure of mild steel. But if it is the difference between the phases and structures which accounts for the differences in behaviour from prestrain in mild and 18/8 stainless steels then it will be necessary to take another similar single phase alloy, e.g. 70/30 brass, and subject it to a similar experimental programme in order to obtain more

definite proof. This was, however, not possible within the research programme of this thesis but will undoubtedly reveal useful information if it is carried out.

The small increase in the level of the discontinuity obtained from the notched fatigue tests of the 65% rolled 18/8 steel is possibly due to the strength increases brought about from the rolling and plate XV shows the martensitic transformation of the austenite which took place during the rolling.*

Impact tests undertaken on the 75% rolled stainless steel in an Hounsfield machine revealed a fairly low but constant level of energy absorption at about 8 lb.ft. (see page 112). Although no direct conversion can be made it is approximately equivalent to 20 lb.ft. on an Izod machine - a level considerably lower than for annealed stainless steel, but, nevertheless, not dangerously low for most engineering purposes. Plate IX shows some of the fractured specimens and it may be seen that they are of a cup and cone nature which indicates that plasticity has occurred.

From the notched fatigue tests of stretched 70/30 brass it has been shown that crack propagation ensues only when the stress at the notch base

*To determine whether the change was ferritic or martensitic stain etchant was used; no staining was apparent indicating the transformation to be purely martensitic. Stain Etchant: 16 gm. CrO_3: 145 ml. H_2O: 80 gm. NaOH Boiling Solution (ref. 29).

attains or exceeds the level of the discontinuity. It may also be noted from the results obtained from notched fatigue tests on the rolled 18/8 stainless steel that the product of $\sigma_L \times K_T$ is equal to the stress level of the discontinuity (see figures 4, 6 and 13). From these results it seems that crack propagation in notched bars, fatigue tested in a rotating cantilever machine, will occur when the stress level attained at the notch base is equal to or greater than the stress level of the discontinuity.

i.e. when $\sigma_L \times K_T \geq \sigma_D$

This relationship also applies to Finney's result for age-hardening aluminium 2024-T4 (ref. 12).

Plain Specimens:

σ_L	σ_D	σ_D/σ_L	Material	Condition
22	32	1.45	18/8 steel	annealed
36	60	1.67	18/8 steel	65% red
45	60	1.33	18/8 steel	75% red
12.5	19	1.52	70/30 brass	annealed
17	25	1.47	70/30 brass	25% ext.

Notched Specimens

σ_L	σ_D	$K_T \times \sigma_L$	K_T	Material	Condition
11	17	16.5	1.5	Aluminium Alloy 2024-T4	-
18	35-40	36	2.0	18/8 steel	65%red
18	35	36	2.0	18/8 steel	75% red.
22	44	44	2.0	18/8 steel	75% red + 5% ext.

From the above tables it may be seen that the criterion of crack propagation for notched specimens is consistently good for each of the three notches used. When, however, one examines the criterion for the propagation of cracks in plain specimens it is at once apparent that the experimental value σ_D/σ_L is very similar in the two annealed materials being approximately 1.5. The effect of plastic deformation is to cause significant but unpredictable changes from this value.

A cast of nominally 18/8 stainless steel with a high nitrogen content was found to contain 0.084% nitrogen. When this material was rolled to produce a reduction in area of 60% tensile tests revealed an average ultimate strength of 87.5 tons/inch^2, with a yield stress approximately 2 tons/inch^2 lower. The increase in the nitrogen level from the standard level of about 0.02% may be expected to stabilize the austenite during deformation, but thin film electron micropscopy revealed extensive acicular

martensite (see plates XVIII and XIX). Direct stress fatigue tests utilizing notched specimens with a $K_T = 2.37$ revealed a fatigue limit at the factored stress of 53 tons/inch^2 (see figure 9), whereas similar tests of annealed 18/8 stainless steel with a normal, low content (approximately 0.02%) revealed a fatigue limit at 27.5 tons/inch^2 (figure 14). It is at once apparent that the combination of rolling and an increase in the nitrogen content has caused the fatigue limit to be raised by 27.5 tons/inch^2 (assuming the frequency difference between the tests to have a negligible effect). The testing of notched specimens may reduce the residual stress benefits to a very small level as indicated by the results of rotating cantilever testing. If this is the case then the improvement is substantial and may be due to the effect of nitrogen preventing dislocation movement at interfaces of the martensite. A discontinuity is found at the typical endurance of 10^4 cycles but it is interesting to find that the ratio σ_D/σ_L is 1.65 which is considerably below the theoretical concentration of the notch. If the notch profile had changed it is possible that the K_T value may have been reduced, but no visual change was apparent and plasticity was not to be expected at stress levels below the yield stress of 85 tons/inch^2. It may, however, be possible for stage I cracks to be formed at the base of a notch as shown by Frost (ref.8) and this may be what is occurring, but without a considerable amount of further investigation it is not possible to be certain exactly what is happening.

It is, however, interesting to notice that the discontinuity occurs

at a factored stress level which is about the same stress as the yield stress of the rolled material. This would seem to indicate that the reversed stressing has not caused a strain softening to occur, which may be due to the role of nitrogen preventing dislocation movement. The absence of titanium and niobium stabilizers would enable the increase in notrogen content to be of maximum benefit.

From these preliminary results it seems that the role of nitrogen may play an important part in causing high fatigue strengths in 18/8 stainless steel. One possibility for further work in this field would be to change the alloy content by reducing the chromium and nickel by one or two percent but increasing the nitrogen content.

The Effect of Temperature on the S/N Curve of Mild and Stainless Steels

Shurmer (ref. 15) fatigue tested mild steel at room temperature and at -80°C and showed that the increase in endurance with an increase in stress found at the level of the discontinuity at room temperature was reversed when tested at -80°C, resulting in shorter lives at the higher stresses. He attributes the increase to strain ageing* which would not occur at -80°C. His results are reproduced in figure 1.

Similar testing of 18/8 stainless steel at -80°C has revealed that the overlap remains unchanged giving longer endurances at stress levels above the discontinuity (see figure 18). It would, therefore, seem that strain ageing does not play a significant part in the apparent increase

*See Appendix D

in the resistance to fatigue at the discontinuity.

Owing to the instability of the austenite in this steel considerable transformation to a high strength martensite can occur with plastic deformation, a transformation which is more easily achieved at the low temperature of -80°C rather than at room temperature (+ 20°C). Plate XVI taken from a region near the notch of a specimen fatigue tested at -80°C confirms that a considerable amount of martensite has been formed during the cyclic stressing. Now it has been suggested earlier that the discontinuity corresponds to the maximum strain which a material can withstand without fatigue occurring. Below this associated stress level microplastic strain from stress raisers causes crack propagation, but at levels above the discontinuity it seems that macro-plastic strain develops. The increase in the amount of deformation would be likely to cause an increase in the rate of and amount of transformation both at room temperature and at -80°C, and if it can be assumed that the martensite has an improved fatigue resistance compared with the austenite then its formation would tend to hinder both the rate of crack initiation and propagation hence resulting in an increase in endurance with the strain increase at the discontinuity.

From plate XVII it may be seen that extensive deformation of the steel has been caused during the machining of the central hole. This work hardened layer may substantially alter the fatigue behaviour and the

necessity to anneal specimens whenever possible after the machining process becomes very apparent.

Notched fatigue tests of mild steel at 350°C have revealed a fatigue limit at the stress level of 23.7 tons/inch^2 (see figure 21). Comparitive testing at room temperature revealed a fatigue limit at 21.8 tons/inch^2. Although the different frequencies of testing may contribute slightly to the difference, this is unlikely. The temperature of 350°C is probably the optimum for strain ageing to occur without creep, and it is possible for brittle fracture to occur during the tensile test of ferritic steels. The temperature is also conducive to oxidation of the surface which as a result turns to a blue colour and these are the reasons why the term "blue brittle" has come into use at this region of temperature. Since strain ageing can play such a significant role at this temperature the improved fatigue strength obtained is probably due to this effect.

MacKenzie and Benham (ref. 27) have convincingly shown that the fatigue strength of EN32B steel is considerably reduced by testing at 450°C compared with the results obtained at 20°C. The reason is not clear but it is possible that the role of creep as opposed to "cyclic creep" plays a significant part at this temperature and causes a reduction in strength which more than supervenes the benefit obtained from strain ageing.

If the results of high temperature tests of mild steel are examined it becomes apparent that there is no discontinuity. However, a small increase in scatter appears at the stress level of 21 tons/inch^2 with a corresponding

and typical endurance for the discontinuity of about 10^4 cycles. If this is taken to be the discontinuity then, with the fatigue limit at 9 tons/inch^2 the value of σ_D/σ_L is 2.33. The fatigue results of mild steel at room temperature yield values for σ_D and σ_L of 17 and 7 tons/inch^2 respectively (see figure 15), which produce a value of $\sigma_D/\sigma_L = 2.42$. Both of these figures of σ_D/σ_L are close to the theoretical stress concentration of the notch which is 2.5, and it would appear that mild steel in push pull fulfills the proposed criterion of propagation for rotating cantilever testing. However, Frost (ref.8) reports the K_f value of a slip band crack in mild steel to be around 2.0 and possibly higher. It may, therefore, be possible that the conditions here are similar to those mentioned earlier, for 18/8 stainless steel with a high nitrogen content, i.e. the effect of the notch is to cause a fairly even increase in the stress around the hole (notch) necessitating the production of initiation cracks as in the case of plain specimens. To clarify the situation further experiments will have to be carried out using different notches and plain specimens but this was not possible within the scope of this thesis.

The numerical difference for the ratio of σ_D/σ_L in the two tests is insufficiently large to be of any vital significance.

Investigations into the effect of high temperatures on the fatigue behaviour of 18/8 stainless steel revealed a discontinuity of

45 tons/inch^2 at 250°C whereas at 350°C the discontinuity was at the lower stress level of 41 tons/inch^2. The ratio of σ_D / σ_L in each of the curves at 250° and 350°C are 1.55 and 1.52 respectively, values which, within the limits of experimental error are very close to the K_f value of a slip band crack. Since, however, these tests were performed with notched specimens it would seem that the criterion for crack propagation in notched specimens is not valid for this type of testing - namely direct stress push-pull testing - since the theoretical value for the stress concentration of the notch is 2.37. It was shown in the review that it is sometimes necessary for stage I cracks to initiate the process of fatigue cracking in notched specimens and that the occurrence of such cracks depends largely on the notch profile. If, then, this is happening in the stainless steel this would provide explanation for the ratio of σ_D/σ_L being of the order 1.5 instead of 2.37.

It is, however, possible that the real stress concentration factor of the notch is not as high as 2.37, the theoretical concentration factor, but is instead of the order 1.5. This may come about through plastic deformation causing a changing of the notch profile and would so provide an alternative reason for the ratio σ_D/σ_L being much below 2.37. Without doubt there is much need for further investigations using direct stress systems and various notches in order to verify that the criteria of crack propagation proposed for rotating cantilever systems is

also valid for direct stress applications.

Further comparison of the curves obtained at 350°C and 250°C reveals the slopes to be considerably different, being steeper at 250°C. This would indicate that the crack propagation at 250°C is less easily achieved than at 350°C.

Plate XX of 18/8 stainless steel fatigue tested with a high stress and low endurance (10^3 cycles) shows slip lines which readily etched even after substantial mechanical polishing. The fact that these slip lines could be etched indicates that a considerable structural change must have occurred, and it is to be expected that the structure formed is martensite. Surface replicas examined by electron microscopy (see plate XXI) revealed a lathe-like structure typical of martensite produced in 18/8 stainless steel at room temperature.

The formation of martensite at 250°C as a result of deformation is not so surprising as at first it appears. Thomas and Krauss (ref.36) report that if 18/8 stainless steel is slightly sensitized it may have an m_s temperature at or just below room temperature; they say that the m_s temperature may also be raised by the presence of impurities.

Bressanelli and Moskowitz (ref. 32) report that 310 stainless steel contained 50% martensite which was caused by straining the annealed austenitic material to failure at a temperature of 100°C. They report that such high strain is less conducive to the production of martensite than smaller but repeated strain. Therefore it may be expected that the repeated stresses and corresponding plastic deformation caused by stress cycling would also produce a small percentage of martensite at 250°C and

even at higher temperatures.

From the above evidence it seems probable that martensite is formed at some stage during the fatigue process when at 250°C. However, at higher temperatures of 350°C the amount formed is negligible (see plate XXII taken from a specimen of 18/8 stainless steel fatigue tested at 350°C at high stress and corresponding low endurance of 10^3 cycles).

It may be assumed that martensite formed in 18/8 stainless steel as a result of plastic deformation has a greater resistance to further deformation than the original material (ref. 32). It is therefore, likely that martensite hinders the rate of crack propagation during fatigue. Hence the lack of martensite transformation at 350°C would result in the crack path being less interrupted than at 250°C and to cause shorter endurances.

It is also probable that the improvement obtained in the stress level of the discontinuity and the corresponding increase in the fatigue limit at 250°C by comparison with that obtained at 350°C is caused by the formation of martensite.

However, the improvement obtained at 250°C compared with room temperature testing is also of significance. Undoubtedly less percentage of the structure will transform to martensite at 250°C than at 20°C. It must, therefore, be that the increase in temperature causes some beneficial strength increase and is probably due to strain ageing of the martensite.

The theory proposed so far for the crack propagation in metals tested in rotating cantilever machines is based upon the existence of a

discontinuity which appears in the S/N curve. Now it is to be assumed that although a slightly different relationship may exist, the theory of crack propagation in direct stress systems also depends upon this phenomenon.

The research entailed to explain what relationship the discontinuity may have with respect to the static properties, is beyond the scope of this work, but it is possible that it is an equivalent parameter to the yield stress in a static tensile test for example. If this were true then it is possible that testing in tension only may reveal different results from reversed cycling.

The effect of the compressive stress cycle on the fatigue of metals has been shown to contribute to the striations found on the fracture surface (ref. 7) but few investigations have been undertaken to eliminate compression, tests usually being run about a specific mean stress level. From the results of L73 aluminium alloy, shown in figure 17, it may be seen that in the tension compression tests a discontinuity occurs at the typical endurance of 10^4 cycles and at the factored stress level of 30 tons/inch^2 which is coincident with the true ultimate tensile strength of this alloy. (The yield stress is almost coincident with the ultimate tensile stress owing to the ageing treatment.) This discontinuity may, therefore, be caused by a collapse of the notch profile. If, however, this is the case, then it is to be expected that a decrease in stress would occur and consequently a corresponding increase in endurance, but this is not observed.

At this stage it is interesting to notice that with a discontinuity at 30 tons/inch^2 and a fatigue limit at 12 tons/inch^2 the ratio of σ_D/σ_L is 2.5 which is the theoretical concentration factor of the notch. It would, therefore, seem that the criterion for crack propagation proposed for rotating cantilever testing is valid for direct stress testing of this aluminium alloy.

At the endurance of about 10^2 cycles the clear existence of another discontinuity may be seen, but it is not possible to know what this represents without further investigations. A similar change was also found from high stress testing of 18/8 stainless steel (see figure 14). In each of these cases notched specimens were used and they were mounted in the machine in such a way that the length between the grips was 0.5 inch. If the buckling load for such a length is calculated (see below) an approximate value for the critical Euler force is 7×10^3 lbs., which is considerably more than the applied load of 290 lbs. It is, therefore, improbable that this step in the S/N curve is due to buckling.

The Euler critical load, $E = \frac{\pi^2 EI}{\lambda^2}$

where E = Young's Modulus (for steel) = $30. \ 10^6$ lb/inch^2.

I = 2nd moment of area = $\frac{b.d^3}{3}$ inch^4

λ = Equivalent length of strut = 0.25 inch

Therefore, $E = \frac{9.9 \times 30 \times 10^6 \times 0.069 \times (0.064)^3}{(0.25)^2 \times 12}$

$= 7.1 \times 10^3$ lbs.

From the comparison of the alternating tension-compression and fluctuating tension tests of the aluminium alloy it may be noted that near the endurance limits the endurances differ by less than an order of magnitude and it appears that the endurance limits are forming at approximately the same stress level, the fluctuating tension being possibly higher. Bauschinger proposed a theory that if a metal or alloy were strained above its yield stress in tension, then the resulting strain hardening would only be advantageous in tension, the compressive yield being lowered, and the elastic range from compression to tension would remain unchanged. It has been shown, however, by Broom and Ham (ref. 30) that both the tensile and the compressive yield stresses can be raised by reversed cyclic stressing. In a material such as L73 aluminium alloy, being in the optimum aged condition, it is unlikely that strain hardening would occur during stress cycling, and if little or no strain softening were to occur then it may be expected that, providing the compressive cycle does not initiate damage but only contributes to the rate of crack growth, then eliminating compression will have a negligible effect on the endurance limit apart from changing the endurance at which it occurs.

There is a marked absence of a discontinuity in the fluctuating tension tests which may be attributed to the elimination of compressive stresses. As a result, it is impossible to discuss the effect of the eliminating of compression on the discontinuity of this alloy; since the fatigue limits are the same for reversed stressing and fluctuating

tension it may be expected that the discontinuities are also the same.

Compressive stress cycling of this L73 aluminium alloy reveals that fatigue cracks can propagate in the absence of applied tensile stresses (see figure 17). Notched specimens were used (mainly to circumvent the problem of buckling in the sheet specimens) and except at unfactored stress levels below 28 tons/inch^2 change in the notch profile could be observed. It is also possible that plasticity was occurring at 23 tons/inch^2 thus causing a change in the profile of the notch. Once this had changed the K_T value may fall to as low as unity and this could explain the shift in endurance found at this stress level.

Similar testing of 18/8 stainless steel has shown that a considerable improvement is found from fluctuating tension cycling as compared to reversed stress cycling, there being nearly a factor of two between the ratio of the fatigue limits. This alloy has a large capacity for strain and it is possible that there is a Bauschinger-fatigue effect. This is indicated by the way the discontinuities are at substantially different stress levels, being 68 tons/inch^2 for reversed cycling, and 90 tons/inch^2 for the fluctuating tension results. The ratio σ_D/σ_L for each type of testing are respectively 2.42 and 1.8, and the theoretical stress concentration factor of the notch is 2.37. It is immediately apparent that in reversed stress cycling the ratio of σ_D/σ_L is very near to the K_T value of the notch, whereas the fluctuating tension tests have yielded a much lower ratio.

The improvement in the fatigue limit found from fluctuating

tension testing of mild steel is about 65% compared with the fatigue limit obtained from the reversed cycling results. This increase is fairly comparable with the obtained improvement of 18/8 stainless steel, being an increase of approximately 90%. Both of these improvements are respectively proportional to the amount of strain hardening each material is able to undergo; the results are also consistent for the L73 aluminium alloy which exhibits no ability to strain hardening and does not have an increase in the endurance limit owing to the elimination of the compressive stresses.

Each of these results, therefore, indicates that when a material has the ability to strain harden it will also have improved fatigue properties when cycled in fluctuating tension as opposed to reversed stress cycling.

There is, again, an absence of a discontinuity in the fluctuating tension tests of mild steel which makes comparison of the discontinuities from each type of testing impossible.

The possibility of obtaining fatigue results caused by a changing value of stress compared with those obtained under sinusoidal loading provides a field for an intense amount of investigation. The effect of occasional stresses in a generally low stress distribution may cause a significant change in fatigue characteristics and the relative importance of the applications of stress levels either above or below the discontinuity in the conventional S/N curve must surely be of importance.

Random stress loading* of L73 aluminium alloy has revealed remarkably little scatter except at the unfactored R.M.S. of peak stress of 4 tons/inch^2 and at about 1.3 tons/inch^2 (see figure 22). Using Mitchell's values for the Peak/R.M.S. ratio it may be seen that the increase in scatter at 4 tons/inch^2 occurs when the unfactored peak stresses have the value

$$4 \times \frac{3.0}{1.414} = 8.5 \text{ tons/inch}^2$$

(Peak/R.M.S. ratio = 3.0)

Comparative testing of this material with sinusoidal loading has revealed a discontinuity at the unfactored stress of 8 tons/inch^2. This testing was undertaken by Mitchell and mean values are shown in the plot in figure 32. The implication, therefore, is that when occasional peak stresses in the random distribution exceed the level of the discontinuity in the constant amplitude curve, then an increase in scatter is produced.

The greatest significance of this result is that a discontinuity appears in the random curve and that it is produced by only a very small

---

*Previous investigations by Abdilla (ref. 11) and Mitchell (ref. 24) have shown that the peak distribution obtained from the resonant beam fatigue machine (described earlier) approximates closely to a Rayleigh distribution. Mitchell has also shown that the ratio of Peak/R.M.S. of stress varies depending on the R.M.S. level. These latter results are shown in figure 33.

number of peak stress, 18.0%*, which are above the conventional discontinuity found in constant stress testing. Therefore the mechanism required for the formation of a discontinuity in random loading is such that only occasional stresses are required and that these appear to be sufficient to enable lower stresses to take an active part in contributing to the phenomenon.

From figure 22 it may be seen that an endurance limit occurs at the R.M.S. of peak stress of approximately 1.2 tons/inch^2. The value of the maximum peak stresses at this R.M.S. is

$$1.2 \times \frac{3.5}{1.414} = 3.0 \text{ tons/inch}^2$$

Again where a small number of peak stresses in the random loading distribution exceed the endurance limit obtained from sinusoidal loading, then fatigue occurs.

Comparison of the sinusoidal and random curves reveals that there is a fairly considerable difference between the discontinuity endurances in each type of testing, the sinusoidal endurances being much less. A similar situation exists at the endurance limits.

In the random curve a considerable quantity - indeed the

---

*The proportion of stresses above a specified stress S in a Rayleigh distribution which has an R.M.S. of peak = σ is given by

$$E(S) = e^{-\frac{(S/\sigma)^2}{2}}$$

when $S = 8.0$ and $\sigma = 4/\sqrt{2}$

$$E(S) = 0.\emptyset 18 \quad (0.18)$$

majority of stresses will be below the peak stress level, and, if considering the endurance limit, below this also. It is, however, the peak stress level of the random results which compares with the sinusoidal loading curve. The difference in endurances between each curve is about an order of magnitude. Therefore only about 1/10 of the number of stress reversals can be said to contribute to the difference in endurances between the two tests. Theoretically it may be expected that approximately only one in a hundred should cause crack propagation at that stress level. It may, therefore, be deduced that stress levels below the endurance limit will contribute to damage in a stress spectrum which contains peak stresses above the fatigue limit.

If the theory which proposes that the discontinuity is the fundamental stress level necessary for crack propagation is valid, then it is to be expected that any stresses in a random stress distribution which attain or exceed the stress level of the endurance limit (an applied stress level which results in the stress level of the discontinuity being attained in part of the specimen) in sinusoidal loading will contribute to damage. This explains the close relationship found between the stresses in sinusoidal and random loading curves at the endurance limits and discontinuities.

Sequence effects are factors which have been shown to cause significant changes in endurance from those predicted by Miner's rule (ref. 23). However, it is interesting and important to notice that if a sequence is reversed then the average experimental endurance is approxi-

mately the same as the predicted value. It may be, therefore, that in the case of random loading sequence effects do not play a significant role.

However, the potential role of low stresses which are below the conventional endurance limit in the S/N curve is high when they are accompanied by high stresses. If it may be assumed that crack propagation can only occur when the stress level of the discontinuity is reached, then crack propagation can only commence if stresses above the conventional S/N curve endurance limit exist. Once, however, a crack is formed by such stresses then the associated stress concentration of the crack will enable applied stresses with magnitude just below the sinusoidal endurance limit to attain the stress level of the discontinuity at the crack tip.

These stresses will, therefore, contribute to crack propagation and so give rise to shorter endurances under random loading than would otherwise be anticipated.

High-low sequence tests would be one means of verifying this theory using low stresses which are below the endurance limit of the material.

During the application of cyclic stress to metals heat may be generated. It has been thought that at stress levels below the fatigue limit this heat generation is due to the non-linearity of the so-called elastic portion of the stress-strain diagram, a part which on complete reversal of stress can yield a hysteresis loop in the stress strain diagram.

Measurement of the area of hysteresis loop is an indication of the amount of damping a material possesses and it is believed that measurement of the temperature rise at stresses below the fatigue limit of a material also indicates the damping capability of a material.

The cause of heat generation and hysteresis loops is thought to be due to atomic movement probably in the form of dislocations. If, therefore, cyclic stressing of material is performed above the fatigue limit an increase in the output of heat is to be expected and if correlation could be made between the level of fatigue activity and the amount of heat generated a rapid method of measuring fatigue damage would be obtained.

Temperature measurement could easily be obtained with the use of thermocouples, but their presence at the surface of a metal under cyclic stress is questionable. The use of an infra red camera, however, provides a remote method of temperature measurement which could be used in conjunction with rotating machinery.

Preliminary investigations of a qualitative nature* were carried out on mild steel and 18/8 stainless steel because the level of heat generated in these materials was found to be large compared with most metals. Tests undertaken on L73 aluminium alloy revealed an

---

*The infra red camera available was not equipped with any form of instrumentation which would enable any accurate quantitative measurements.

undetectable temperature rise during low endurance fatigue testing.

Plate XI shows a thermograph obtained for mild steel with cyclic stress of 20 tons/inch^2 and an endurance of 8 x 10^4 cycles. It may be seen that a fairly constant level of heat generation was achieved soon after the onset of the test and that no significant change occurred until the last few seconds of the specimen's life. At this stage the rate of crack propagation would be high and the actual stress level would rise accordingly.

From the thermograph obtained from mild steel with a dynamic stress level of 10 tons/inch^2 and a static stress also 10 tons/inch^2 (see plate XII) it may be seen that a significant change in heat intensity is found between the onset of stress cycling and after 10^6 stress reversals. This stress continuation is doubtless below the fatigue limit of the steel; the decrease in heat generation indicates that the hysteresis loop is closing and the amount of general atomic movement is at a much reduced level. In other words a reduction in heat generation indicates that work hardening is occurring. It would seem, therefore, that this technique can be suitably applied to detect the presence of metal fatigue in ferrous alloys.

It is to be anticipated that if heat is generated in an alloy during fatigue then an increase in the dynamic stress would result in an increase in the heat generation. Plate X shows the thermograph obtained from a sequence test on 18/8 stainless steel. The temperature rise at the onset of the high stress level of 36 tons/inch^2 was almost immediate,

and at the stress level change it may clearly be seen that a lower amount of heat radiation was produced from the low stress of 28 tons/ $inch^2$ until very near the time of fracture when the heat intensity rose considerably.

Lack of availability of the infra-red camera resulted in being unable to consider the change in heat produced over a small stress range which would include the stress level of the discontinuity. If, however, this could be undertaken and proof obtained that the discontinuity itself is responsible for the major heat increase found, then infra-red thermography could be used as a quick method of detecting the discontinuity in the S/N curve, and hence using the theory of crack propagation the fatigue limit could be predicted.

CONCLUSIONS

From the rotating cantilever testing both with notched and plain specimens of 70/30 brass and 18/8 stainless steel a change in fracture appearance was found at the stress level of the discontinuity from eccentric crack propagation paths below to concentric crack propagation paths above. Coupled with statistics this fracture change provides a reliable method for the determination of the discontinuity.

The results of plain fatigue tests obtained conform closely to the relationship $\sigma_L \times K_T = \sigma_D$, where σ_L is the fatigue limit, σ_D is the discontinuity and K_f is the stress concentration factor of a slip bond crack, a value which is normally about 1.5. Experiments with 18/8 stainless steel have shown that values of K_f from as low as 1.33 to as high as 1.67 may be obtained and that these variations are caused by the cold rolling.

The following criterion is proposed to predict the propagation of fatigue cracks in notched specimens tested in a rotating cantilever machine:-

$$\sigma \times K_T \geq \sigma_D$$

where σ is the applied unfactored stress level, σ_D is the discontinuity and K_T is the elastic stress concentration factor of a notch. The experimental results obtained indicate that this criterion will provide an accurate and reliable method for the determination of crack propagation.

The effect of prestrain on the fatigue of 18/8 stainless steel was to raise both the fatigue limits and the discontinuities obtained in the

notched and plain tests. The discontinuities obtained in the notched tests were raised by a lesser amount than those obtained with plain specimens. The effect of a longitudinal stretch of 5% was to further improve the fatigue strength obtained with notched testing of 18/8 stainless steel with a 75% reduction in area. No collapse in fatigue strength was found from the extensive prestrain. It is suggested that the improvement in fatigue strength obtained from the plastic deformation is owing to the phase transformation from austenite to martensite which occurs during cold work. The inability of the whole material to transform to martensite resulted in the reasonably high equivalent Izod impact value of 20 lb.ft. throughout the temperature range -196°C to +100°C for the stainless steel with a 75% reduction in area.

The result of a 25% extension of 70/30 brass was to raise both the discontinuity and the fatigue limit in plain specimens. The discontinuities in the notched and plain specimens of 25% stretched 70/30 brass were found to be the same in contradistinction to the prestrained 18/8 stainless steel. Residual stresses are proposed to account for the stainless steel behaviour.

The effect of an increase in nitrogen content to 0.084% and the omission of the titanium stabilizer in 18/8 stainless steel was to enable the high ultimate tensile strength of 87.5 tons/inch^2 to be achieved resulting from a 60% rolling reduction. The fatigue limit was also raised to 55 tons/inch^2. The quantity of nitrogen added was insufficient to prevent the formation of acicular martensite and it is

suggested that the combination of martensite and nitrogen is responsible for the improvements in fatigue strength.

Fatigue testing of 18/8 stainless steel (at -80°C) resulted in the stress of the discontinuity being raised but the overlap remained with longer endurances at the higher stress levels; the overlap remaining the same as found at room temperature is attributed to the formation of extensive amounts of martensite, which forms more readily at the lower temperature.

The improvement in fatigue strength obtained by testing mild steel at 350°C is attributed to the effect of strain ageing. A serious reduction in resistance to fatigue at higher temperatures is discussed and thought to be due to the onset of creep.

Optical and electron microscopy show clearly that martensite may be formed by very high stress cycling in 18/8 stainless steel at 250°C. This finding is discussed in detail and is supported with evidence from literature.

The effect of fatigue tests of 18/8 stainless steel at 250°C was to cause an increase in the fatigue limit which is accounted for by strain ageing. Further increase in temperature to 350°C caused a reduction in strength and this is accounted for by the lack of martensite - a transformation which is shown to occur at 250°C but not at 350°C.

The discontinuity found in L73 aluminium alloy was found to exist at a stress which was the same as the ultimate tensile strength

of the alloy. A second discontinuity was also found at the endurance of 10^2 cycles; this could not be attributed to buckling or any other testing factors. The ratio of σ_D/σ_L was found to be 2.5, the theoretical concentration factor of the notch, thus indicating that the criterion for crack propagation in direct stress may be similar to that proposed for rotating cantilever systems.

The amount by which the fatigue limits of 18/8 stainless steel, mild steel and L73 aluminium alloy may be raised, purely by the elimination of the compressive part of the stress cycle is indicated by the work hardening properties of each material, e.g. L73 aluminium alloy shows no work hardening ability and there is no fatigue benefit obtained from eliminating compression.

While fatigue which is caused by fluctuating compression in L73 aluminium alloy is only at very high stresses the compressive part of the cycle in tension-compression cycling can contribute to the rate of damage at stresses well below the fatigue limit in pure compression.

A significant change in the ratio of σ_D/σ_L resulting from the elimination of compression indicates that if a relationship exists similar to the one proposed for rotating cantilever testing to determine the fatigue limit in notched specimens in direct stress systems then substantial modifications will have to be made to allow for the different types of testing.

From the random loading fatigue data a discontinuity was found at the unfactored R.M.S. of stress of 4.0 tons/inch^2. It occurred when

the peak stresses of the distribution attained the stress level of the discontinuity obtained in sinusoidal testing. An endurance limit was found in the random curve at 1.2 tons/inch^2 when the peak stresses attained the value of the endurance limit in the sinusoidal curve. It is proposed that crack propagation in random loading occurs when the microstress in the structure attains or exceeds the level of the discontinuity attained in sinusoidal loading.

Generally the scatter in random loading is small compared with that obtained in sinusoidal loading and it is proposed that the majority of stresses below the endurance limit in sinusoidal loading contribute to the damage when accompanied by stresses above the endurance limit.

Qualitative experiments indicate that it may be possible to use an infra-red camera to indicate the presence of fatigue in inaccessible structures. It may also provide a rapid method of detecting the discontinuity and so enable a rapid assessment of fatigue properties.

REFERENCES

1.
2. The Fatigue of Materials and Structures, Douglas Aircraft Co., 1954.

3. Williams, T.R.G. Stevens, D.T. — Nature, 1964, 201, 1181.

4. Frost, N.E. — J.Mech. Eng. Sci., 1959, 1, 151.

5. Benham, P. Ford, H. — J. Mech. Eng. Sci., 1961, 3, 119.

6. Williams, T.R.G. Hallwood, S. Hayden, R. — Metal Indus., 1961, 99, 182.

7. Forsyth, P.J. — Crack Prop. Symposium, Cranfield, September 1961.

8. Frost, N.E. — Aero. Quarterly, 1957, 8, 1.

9. Frost, N.E. — Nature, 1961, 192, 446.

10. Porter, J. Levy, J.R. — J.I.M., 1960, 88, 86.

11. Abdilla, J. — M.Sc. Thesis, Southampton University, 1965.

12. Finney, J.M. — J.I.M., 1964, 94, 11.

13. Porter, J. Levy, J.R. — J.I.S.I., 1961, 197, 296.

14. Adair, A.M. Lipsitt, H.A. — Trans.Met.Soc., A.I.M.E., 1966, 236, 1235.

15. Shurmer, C.R. — B.Sc. Thesis, Southampton University, 1965.

16. Cina, B. — Metallurgia, 1957, 55, 11.

17. Frost, N.E. — Metallurgia, 1962, 65, 287.

18. Coombs, A.G.H. Sherratt, A. Pope, J. — Int. Conference on Fatigue of Metals, November 1956.

19. Miner, M.A. — J. Appl. Mech. A.S.M.E. 1945, 12, 3.

20.	Marsh, K.J.	N.E.L. Report, 1965, No. 204.
21.	Pope, J. Foster, B. Bloomer, N.	Engineering, 1957, 184, 236.
22.	Williams, T.R.G. Lowcock, M.	Engineering, 1965, 200, 571.
23.	Wood, W.A. Reimann, W.H.	J.I.M., 1966, 94, 66.
24.	Mitchell, P.J.	M.Sc. Thesis, Southampton University, 1966.
25.	Frost, N.E.	Metallurgia, 1960, 62, 85.
26.	Williams, T.R.G. Abdilla, J.	The Engineer, 1964, 218, 325.
27.	MacKenzie, C.T. Benham, P.	Pro. Inst. Mech. Eng., 1965-6, 180, 1, 30.
28.	Serensen, S.V.	Maschgiz, Moscow, 1963, 166.
29.	Reed, R.P.	Acta Met., 1962, 10, 865.
30.	Broom, T. Ham	Proc. Roy. Soc. 1959, A251, 186.
31.	Weibull, W.	Fatigue Testing and the Analysis of Results, published by Pergamon Press.
32.	Owen, W.S.	The Metallurgist, 1961, 1, 238.
33.	Baird, J.D.	Iron and Steel, 1963, 36, 186.
34.	Irvine, J.	J.I.S.I., 1959, 192, 218.
35.	Hundy, B.	J.I.S.I., 1954, 178, 34
36.	Kaufman, L. Cohan, M.	Progress in Metal Physics, 1958, 7, 165.

APPENDIX I

Under the heading Fatigue Testing Apparatus, section (b), mention was made that an air bearing is used to prevent buckling of the column which may result in bending of the test piece. One of the major problems in the design of direct stress fatigue machines is the prevention of bending stresses which can result in a substantial change of the applied stress from that which is required. In most direct stress fatigue machines bending can easily be caused by misaligned grips. In the machine mentioned in section (b) a very careful procedure was adopted to re-align the grips whenever the bearing was removed:-

A rigid plate specimen was loosely fixed in the grips, a static tensile load of about 50 lb. was applied, all the flex-plate bolts securing the column were loosened and the bearing securing screws were undone until the bearing with the air supply on was free to move. The imposed tensile load lined up the items and the plate specimen was then firmly secured as was the flex-plate. The air bearing was held by hand in the correct position and was secured with the fixing bolts, but care had to be taken not to cause deformation of the bearing by applying too much torque to the fixing screws. (The applied torque to the bearing fixing screws was 5 lb. ft.).

Suppose a bending moment of 1 lb.in. is applied to a specimen of the type shown in figure 30 in such a way as to cause the maximum stress.

The nominal surface stress, f, is related to the bending

moment, M, the second moment of area, I, and the distance from the neutral axis, y, by the following formula:-

$$f = \frac{M.y}{I}$$

Now $M = 1$ lb.in.

$y = 0.032$ in.

$I = \frac{1}{12} (0.1 - 0.031) \times (0.064)^3$ in.^{4}

$$f = \frac{1 \times 0.032 \times 12}{2240 \times (0.069) \times (0.064)^3}$$

$= 8.1$ tons/inch^2.

i.e. a bending moment of 1 lb.in. results in a nominal stress of 8.1 tons/inch^2.

This stress would be more than sufficient to cause a substantial change in the applied stress pattern which may give rise to very different fatigue characteristics from those obtained in 'pure' push pull fatigue.

APPENDIX A

The Statistical Evaluation of Fatigue Results -(ref. 31)

When fatigue tests have been undertaken it is often necessary to indicate statistically how the amount of scatter produced changes with the applied stress level. It is usual to present the information graphically and for one particular stress level, endurance is plotted against probability on graph paper which has a logarithm scale on the 'y' axis and a probability scale on the 'x' axis. For any one stress level this plot produces a straight line graph if the scatter is evenly distributed and the slope of the line is proportional to the amount of scatter; i.e. an increase in slope signifies an increase in scatter.

There are various ways in which probability can be obtained, and the following method although very slightly inaccurate is simple, easy to remember and gives adequate results:

If x specimens are tested at a given stress level and arranged in order of endurance such that:

$$n_1 > n_2 > n_3 \ldots\ldots > n_x$$

where n_1 is the endurance of specimen no. 1, etc.

then the probability p is given by the relationship:

$$p = \frac{m}{x + 1}$$

where m is the specimen number.

i.e. m is an integer whose value lies in the range 1 to x.

It can be seen that if there are x specimens then there are also x probabilities.

APPENDIX B

The Stress Strain Diagram

It is conventional when plotting the stress strain diagram to calculate the values of stress and strain in the following ways:

$$\text{stress} = \frac{\text{instantaneous load}}{\text{original cross section area}}$$

$$\%\text{ age strain} = \frac{\text{change in length}}{\text{original length}} \times 100$$

The stress strain diagram evolved this way is sometimes called the 'engineers' stress-strain diagram.

For the purpose of correlating certain phenomena, which may occur under conditions of fatigue with the stress strain diagram, it may be necessary to use "true stress" and "true strain" axes instead of the conventional ones. These true stresses and strains may be calculated as follows:

$$\text{True stress} = \frac{\text{load}}{\text{instantaneous cross sectional area}}$$

$$\text{True strain (up to the point of necking)} = \log_e \left(\frac{\text{instantaneous length}}{\text{original length}}\right)$$

$$\text{True strain (during necking)} = \log_e \left(\frac{\text{original cross sectional area}}{\text{instantaneous cross section area}}\right)$$

APPENDIX C

Martensite

Rapid cooling, such as water quenching, as shown by curve D, produces the complex structure known as martensite. This is a solid solution of carbon in ferrite and as such the carbon causes an expansion in volume of the ferrite which as a result changes to become tetragonal instead of cubic. (See diagram below.)

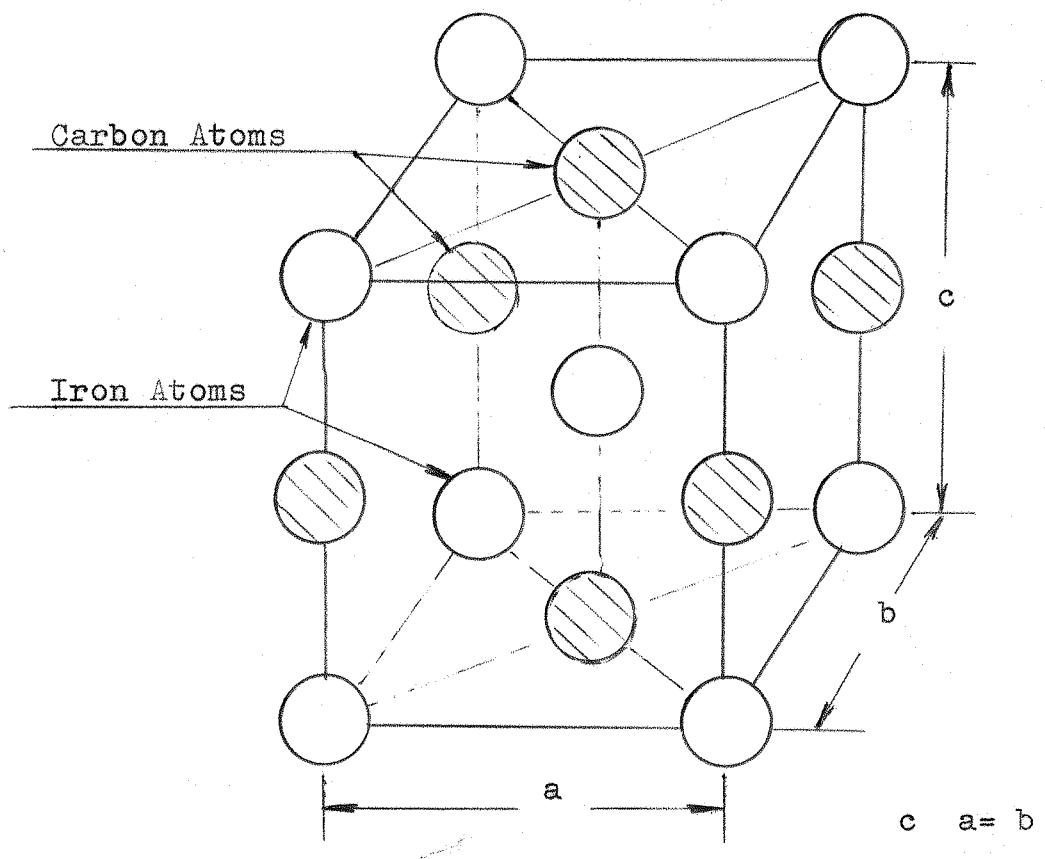

If the martensite obtained by quenching is heated to 300°C it may undergo further transformation to a structure known as tempered martensite, which

is very similar to the bainite produced as per cooling curve C.

The effect of alloying steel can result in a very significant change of the TTT diagram. The 'knee' or 'S' shaped portion is moved to the right with an increase in alloy content; this may lead to a considerable change in shape; the M_s and M_f temperatures are lowered by an increase in alloy content. There exists another critical temperature known as the M_d temperature below which martensite may be produced by deformation of the otherwise stable gamma phase, the M_d temperature being above that of the M_s temperature. This M_d temperature is also affected by the alloy content in a similar way to the M_s and M_f temperatures. Below is given a table which indicates approximately by how much 1% of an alloying element lowers the M_s, M_f and M_d temperatures in iron (ref. 34).

Element	Temp. Decrease per % age ^{o}C
Ni	10
N	200
Cr	8
C	300
Mn	50
Cn	5

The conception of an M_s temperature is one which suggests that martensite is only produced when a sufficiently large energy difference exists between the gamma and martensitic phases. Hence the existence of an M_d temperature may be realized. This occurs at a higher temper-

ature than the M_s temperature and consequently energy in the form of deformation is necessary to produce the extra energy required for the transformation to martensite to occur.

The martensitic structure can occur in two distinct forms:-

(a) Massive martensite which has a "lath-like" appearance and is typical of martensite produced by quenching high carbon steel.

(b) Acicular martensite. This appears as plates or slabs when viewed by the electron microscope. The plates may be twinned. This type of martensite is sometimes called "lenticular" or "unclapp" martensite.

It is acicular martensite which is formed by the deformation process but little is known except that it forms very rapidly. Below is given a proposed model of how this martensite may be produced from the austenite in 18/8 chromium-nickel steel.

It has been proposed and it is widely believed that a second type of martensite can be produced which is hexagonal and not tetragonal. This is called ε martensite, and is produced in materials which have a low stacking fault energy - say of the order 10 ergs per $cm.^2$ It is likely that the martensite produced in 18/8 stainless steel is therefore an hexagonal structure and not the body centered tetragonal variety.

The plain carbon steel martensites are extremely hard and this is thought to be due to a high twin density and also to the interstitial atoms which occur at twin interfaces, where there are high dislocation networks. Consequently there exists at twin interfaces barriers which

A.

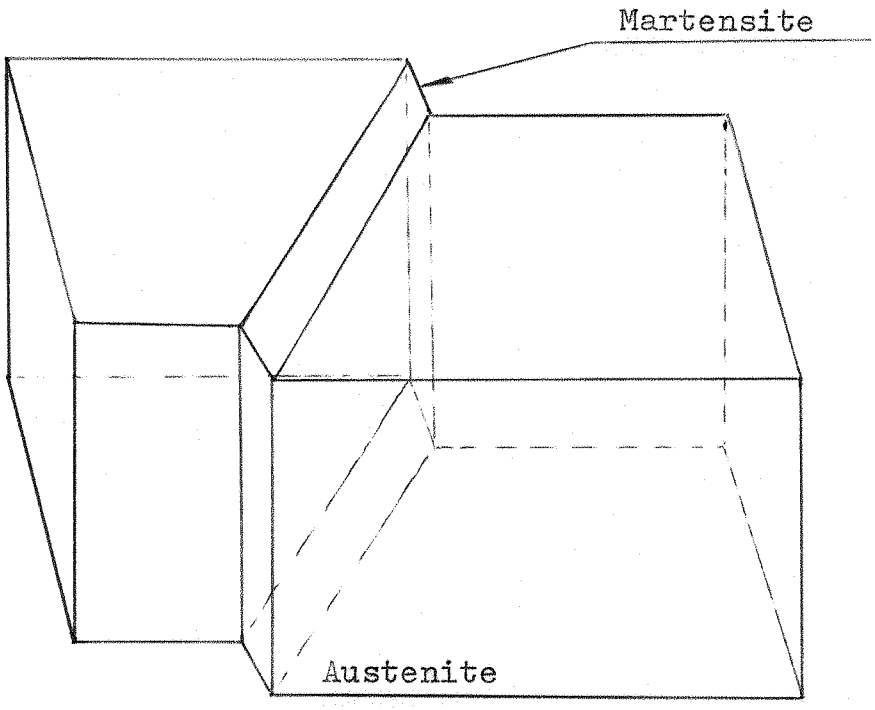

B.

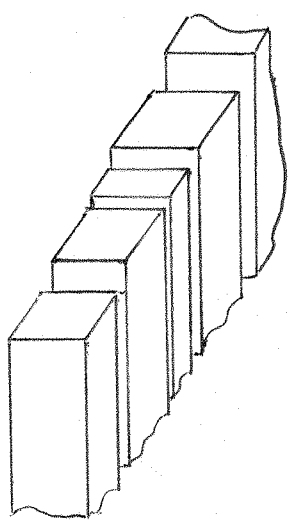

A - Primary Displacement

B - Secondary Displacement

prevent atomic movement. These conditions are ideal for high fatigue strengths. If the locking of dislocations at twin interfaces can be prevented by using a non-ageing material, then a ductile martensite can be produced under the correct conditions (maraging steel) but this is possibly not very good for high fatigue strength, since the action of reversed stressing may cause the disentangling of dislocations in a structure which may be considered equivalent to that of a work-hardened metal.

APPENDIX D

Strain Ageing

This is responsible for some of the changes in mechanical properties of ferritic steels, containing carbon and nitrogen, which take place after the steels have been plastically deformed. These property changes are:-

1. The yield stress rises and upper and lower yield points form.
2. The yield elongation falls.

It has been established that the strain ageing mechanism is caused by the presence of interstitial atoms migrating to and pinning dislocations. Since these solute atoms are responsible for the mechanism it is necessary that they be soluble in the material, have high diffusion rates and severely lock the dislocations. Carbon and nitrogen atoms are the best elements to fulfill this role but, as will be explained later, other elements can have an appreciable effect on strain ageing.

When a dislocation is pinned it requires a higher stress to move than in the unpinned condition, but once torn away from its atmosphere the stress required falls to its original value and correspondingly the lower yield point occurs in the stress strain diagram. When stressed beyond the elastic limit the discontinuous yield phenomenon disappears and returns after a lapse of time when held at room temperature. This is because the dislocations in their new positions are not anchored by the solute atoms and ageing is necessary to allow the diffusion of the

carbon and nitrogen atoms to re-lock the dislocations and so restore the discontinuous yielding.

Since strain ageing is a diffusion process it is both time and temperature dependent and these parameters are related by the following equation (ref. 35):-

$$\log_{10} \frac{tr}{t} = 4400 \left\{ \frac{1}{Tr} - \frac{1}{T} \right\} - \log_{10} \frac{T}{Tr}$$

where tr = ageing time at room temperature, Tr

t = ageing time at temperature T,

the temperature being expressed in ^{o}K.

It may be deduced from this equation that at a temperature -80°C the effect of strain ageing can be completely ignored since the time factor involved compared with that at room temperature is increased by a factor of 10^{7}.

To produce significant ageing effects evidence suggests that 0.0001% nitrogen is sufficient but that, in general, the amount of strain ageing at room temperature increases with an increase in nitrogen content until saturation occurs. Owing to a lower equilibrium solubility carbon tends to produce but little strain ageing at room temperature. As the temperature is increased to 200°C and above, experiments show that strain ageing owing to carbon is very pronounced. In ferritic steels only 0.0001% carbon is necessary to give measurable ageing at 100°C and the amount of ageing again increases with an increase in carbon until the amount of free ferrite begins to fall causing a corresponding decrease in ageing.

Other elements, which do not contribute directly to the process of strain ageing but affect it in other ways, can be classified into four categories:

(a) Elements which react weakly or not at all with carbon or nitrogen - copper, nickel, manganese, phosphorous.

(b) Nitride formers - aluminium, silicon, boron.

(c) Carbide formers - molybdenium.

(d) Nitride and Carbide formers - chromium, vanadium, niobium, titanium.

(a) Copper and nickel which do not react with carbon or nitrogen may cause an increase in strain ageing; there is no decrease owing to their presence. Manganese and phosphorous which attract nitrogen atoms when in solid solution may slow down the rate of low temperature strain ageing in steels, but they will not prevent it.

(b) Elements which form stable nitrides, e.g. aluminium, silicon, boron, decrease strain ageing caused by nitrogen. The effect is very pronounced when heat treatment is carried out at such temperatures that the nitrogen is completely precipitated.

(c) The available evidence is limited, but suggests that carbide formers such as molybdenum do not have any effect on high or low temperature strain ageing.

(d) Carbides and nitrides are formed by chromium, vanadium, niobium and titanium and may completely eliminate strain ageing at all

temperatures up to 250°C. It has been shown that 0.56% chromium in a low carbon steel substantially reduces strain ageing, and that at temperatures up to 250°C, 6.1% chromium prevents strain ageing from occurring.

(Much of the above review was taken from a critical review of strain ageing - ref. 33).

RESULTS

Rotating cantilever testing of cold rolled 18/8 stainless steel with 65% reduction in area - plain specimens.

Test No.	Stress (Tons/inch^2)	Endurance (cycles)	No.	Stress	Endurance
1	36	$9.5\ 10^6$ (unbroken)	11	53	$4.6\ 10^4$
2	39	$1.7\ 10^5$	12	60	$2.8\ 10^4$
3	39	$1.6\ 10^5$	13	60	$1.2\ 10^4$
4	41	$2.4\ 10^5$	14	60	$2.0\ 10^4$
5	41	$3.1\ 10^5$	15	65	$1.2\ 10^4$
6	45	$3.1\ 10^5$	16	65	$2.2\ 10^4$
7	45	$5.4\ 10^5$	17	65	$1.0\ 10^4$
8	49	$1.1\ 10^5$	18	75	$4.8\ 10^3$
9	49	$1.9\ 10^4$	19	75	$3.6\ 10^3$
10	53	$4.0\ 10^4$			

Rotating cantilever testing of cold rolled 18/8 stainless steel with 65% reduction in area - notched specimen $K_t = 2.0$.

No.	Unfactored Stress	Endurance	No.	Unfactored Stress	Endurance
1	18	$1.2\ 10^7$	12	26	$7.3\ 10^4$
2	18.5	$1.7\ 10^5$	13	26	$4.6\ 10^4$
3	19	$2.2\ 10^5$	14	30.8	$1.8\ 10^4$
4	19	$2.2\ 10^5$	15	30.8	$1.9\ 10^4$
5	19.5	$1.4\ 10^5$	16	35.3	$8.9\ 10^3$
6	19.5	$2.7\ 10^5$	17	35.3	$9.3\ 10^3$
7	21.5	$1.6\ 10^5$	18	40	$5.1\ 10^3$
8	21.5	$2.2\ 10^5$	19	40	$5.2\ 10^3$
9	21.5	$1.6\ 10^5$	20	45	$2.8\ 10^3$
10	21.5	$8.0\ 10^4$	21	50	$1.6\ 10^3$
11	26	$5.4\ 10^4$			

Rotating cantilever testing of cold rolled 18/8 stainless steel with 75% reduction in area - plain specimens.

No.	Stress	Endurance	No.	Stress	Endurance
1	42	$1.3\ 10^7$ (unb.)	14	62.5	$9.4\ 10^3$
2	46	$1.0\ 10^5$	15	62.5	$6.1\ 10^3$
3	46	$2.0\ 10^7$ (unb.)	16	62.5	$8.9\ 10^3$
4	49	$2.3\ 10^5$	17	67	$1.7\ 10^4$
5	49	$6.2\ 10^5$	18	67	$1.0\ 10^4$
6	49	$4.3\ 10^5$	19	67	$2.8\ 10^3$
7	52	$2.3\ 10^4$	20	72	$2.9\ 10^3$
8	52	$4.1\ 10^4$	21	72	$2.2\ 10^3$
9	53.5	$3.7\ 10^4$	22	72	$3.9\ 10^3$
10	53.5	$3.6\ 10^4$	23	76.5	$2.6\ 10^3$
11	58	$6.5\ 10^4$	24	76.5	$1.8\ 10^3$
12	58	$5.0\ 10^4$	25	76.5	$1.5\ 10^3$
	58	$1.6\ 10^4$	26	76.5	$3.3\ 10^3$

Rotating cantilever testing of cold rolled 18/8 stainless steel with 75% reduction in area - notched specimens $K_t = 2.0$

No.	Unfactored Stress	Endurance	No.	Unfactored Stress	Endurance
1	18	$1.4\ 10^7$ (ub.)	15	28	$5.0\ 10^4$
2	19.5	$4.5\ 10^5$	16	30.5	$1.5\ 10^4$
3	19.5	$6.0\ 10^5$	17	30.5	$2.6\ 10^4$
4	21.5	$2.5\ 10^5$	18	30.5	$2.3\ 10^4$
5	21.5	$1.1\ 10^6$	19	32.5	$2.3\ 10^4$
6	21.5	$7.2\ 10^4$	20	32.5	$1.4\ 10^4$
7	24	$7.1\ 10^4$	21	35	$7.8\ 10^3$
8	24	$3.0\ 10^5$	22	35	$6.2\ 10^3$
9	24	$4.1\ 10^4$	23	35	$7.9\ 10^3$
10	26	$7.4\ 10^4$	24	40	$3.9\ 10^3$
11	26	$3.9\ 10^4$	25	40	$3.4\ 10^3$
12	26	$7.7\ 10^4$	26	44	$1.6\ 10^3$
13	28	$3.1\ 10^4$	27	44	$2.3\ 10^3$
14	28	$4.2\ 10^4$			

Rotating cantilever testing of cold rolled 18/8 stainless steel with 75% reduction in area and stretched 5% - notched specimens $K_t = 2.0$

No.	Unfactored Stress	Endurance	No.	Unfactored Stress	Endurance
1	35.5	$9.2\ 10^3$	7	40	$1.8\ 10^4$
2	35.5	$1.2\ 10^4$	8	40	$1.8\ 10^4$
3	26	$3.8\ 10^5$	9	44.5	$3.2\ 10^3$
4	26	$1.1\ 10^5$	10	44.5	$1.6\ 10^4$
5	21.5	$1.3\ 10^6$	11	49	$4.3\ 10^3$
6	21.5	$4.3\ 10^7$(unb.)	12	31	$1.9\ 10^5$

Composition of nominally 18/8 stainless steel with a raised nitrogen content:

Chromium	16.82%
Nickel	9.18%
Nitrogen	0.084%
Iron	remainder

Direct stress testing of the above steel cold rolled to 60% reduction in area - notched specimens $K_t = 2.37$.

Test	Fac. Stress	Endurance	Test	Fac. Stress	Endurance
1	115	$1.4\ 10^3$	21	92	$1.3\ 10^4$
2	115	$1.2\ 10^3$	22	92	$8.7\ 10^3$
3	115	$1.1\ 10^3$	23	88	$6.0\ 10^3$
4	115	$1.6\ 10^3$	24	88	$1.9\ 10^4$
5	106	$2.4\ 10^3$	25	88	$6.0\ 10^3$
6	106	$3.0\ 10^3$	26	88	$1.9\ 10^4$
7	106	$3.6\ 10^3$	27	86	$9.0\ 10^3$
8	106	$3.0\ 10^3$	28	85	$1.8\ 10^4$
9	102.4	$6.8\ 10^3$	29	82.5	$1.2\ 10^4$
10	102.1	$6.2\ 10^3$	30	82.5	$2.0\ 10^4$
11	102.1	$5.6\ 10^3$	31	82.3	$2.0\ 10^4$
12	100	$3.6\ 10^3$	32	80	$1.8\ 10^4$
13	100	$1.4\ 10^4$	33	77	$2.6\ 10^4$
14	100	$8.4\ 10^3$	34	76	$2.9\ 10^4$
15	100	$3.0\ 10^3$	35	75.1	$3.0\ 10^4$
16	97.5	$7.4\ 10^3$	36	73.6	$6.5\ 10^4$
17	96.5	$8.6\ 10^3$	37	73.5	$4.8\ 10^4$
18	96	$7.4\ 10^3$	38	72.4	$8.3\ 10^4$
19	96	$7.2\ 10^3$	39	70.3	$9.8\ 10^4$
20	93.5	$9.3\ 10^3$	40	67.1	$2.4\ 10^5$

cont/d...

Test	Fac. Stress	Endurance
41	66	$6.2\ 10^4$
42	64.3	$1.8\ 10^5$
43	62.0	$5.8\ 10^4$
44	62.0	$5.0\ 10^5$
45	61.7	$3.2\ 10^5$
46	59.8	$1.5\ 10^5$
47	57.5	$4.6\ 10^5$
48	57.5	$4.2\ 10^5$
49	57.5	$1.6\ 10^5$
50	54	$1.8\ 10^6$
51	54	$6.4\ 10^6$ (unbroken)

Rotating cantilever testing of annealed 70/30 brass.

No.	Stress	Endurance	No.	Stress	Endurance
1	32.5	$1.0\ 10^3$	23	20.5	$3.2\ 10^3$
2	32.5	$8.8\ 10^2$	24	20.5	$1.7\ 10^3$
3	32.5	$1.1\ 10^3$	25	19.5	$6.4\ 10^3$
4	32.5	$1.3\ 10^3$	26	19.5	$5.0\ 10^3$
5	30.5	$1.1\ 10^3$	27	19.5	$2.9\ 10^3$
6	30.5	$9.0\ 10^2$	28	19	$8.1\ 10^3$
7	30.5	$9.3\ 10^2$	29	19	$8.4\ 10^3$
8	29.0	$8.6\ 10^2$	30	18.7	$1.1\ 10^4$
9	29.0	$1.1\ 10^3$	31	18.7	$1.2\ 10^4$
10	29.0	$1.1\ 10^3$	32	18.7	$1.3\ 10^4$
11	27.0	$1.5\ 10^3$	33	18.0	$2.3\ 10^4$
12	27.0	$1.0\ 10^3$	34	18.0	$2.8\ 10^4$
13	27.0	$1.2\ 10^3$	35	18.0	$2.9\ 10^4$
14	25	$1.7\ 10^3$	36	17.0	$2.2\ 10^4$
15	25	$1.3\ 10^3$	37	17.0	$2.0\ 10^4$
16	25	$1.2\ 10^3$	38	16.0	$2.4\ 10^5$
17	23.5	$1.7\ 10^3$	39	16.0	$1.6\ 10^5$
18	23.5	$2.2\ 10^3$	40	16	$6.8\ 10^4$
19	23.5	$2.4\ 10^3$	41	14	$3.7\ 10^5$
20	21.5	$2.4\ 10^3$	42	14	$9.3\ 10^5$
21	21.5	$2.3\ 10^3$	43	14	$2.1\ 10^6$
22	21.5	$1.8\ 10^3$	44	12.5	$7.7\ 10^7$

Rotating cantilever tests of stretched 70/30 brass with 25% extension.

No.	Stress	Endurance	No.	Stress	Endurance	No.	Stress	Endurance
1	37.0	5.0 10^2	21	28.8	2.2 10^3	41	24.7	8.6 10^4
2	37.0	5.0 10^2	22	28.8	1.7 10^3	42	24.7	2.7 10^4
3	37.0	5.0 10^2	23	28.8	3.2 10^3	43	24.7	1.7 10^4
4	34.2	7.0 10^2	24	28.8	4.0 10^3	44	24.7	3.7 10^4
5	34.2	7.0 10^2	25	28.8	2.0 10^3	45	24.7	2.0 10^4
6	34.2	6.0 10^2	26	28.8	1.6 10^3	46	23.4	1.0 10^5
7	34.2	7.0 10^2	27	27.5	6.3 10^3	47	23.4	9.2 10^4
8	34.2	7.0 10^2	28	27.5	3.9 10^3	48	23.4	8.4 10^4
9	31.5	1.2 10^3	29	27.5	6.0 10^3	49	23.4	5.0 10^4
10	31.5	1.1 10^3	30	27.5	4.2 10^3	50	23.4	1.2 10^5
11	31.5	9.0 10^2	31	27.5	3.1 10^3	51	23.4	2.0 10^5
12	31.5	1.2 10^3	32	27.5	7.5 10^3	52	23.4	7.9 10^4
13	31.5	9.0 10^2	33	26.0	1.3 10^4	53	22.0	3.1 10^5
14	30.5	1.2 10^3	34	26.0	1.0 10^4	54	22.0	3.6 10^5
15	30.5	1.0 10^3	35	26.0	1.0 10^4	56	22.0	2.0 10^5
16	30.5	1.1 10^3	36	26.0	4.5 10^3	57	20.5	4.1 10^6
17	30.5	9 10^2	37	26.0	2.1 10^4	58	20.5	5.0 10^6
18	30.5	1.4 10^3	38	26.0	2.1 10^4	59	19.6	2.0 10^7
19	30.5	1.2 10^3	39	26.0	2.0 10^4	60	18.0	4.4 10^7
20	28.8	2.1 10^3	40	24.7	3.4 10^4	61	18.0	1.0 10^8

Rotating cantilever tests of stretched 70/30 brass with 25% extension - notched specimens $K_t = 3.0$.

No.	Unfactored Stress	Endurance	No.	Unfactored Stress	Endurance
1	28.0	$4.5\ 10^3$	21	21.3	$1.7\ 10^4$
2	28.0	$2.7\ 10^3$	22	21.3	$1.2\ 10^4$
3	28.0	$4.8\ 10^3$	23	21.3	$1.3\ 10^4$
4	28.0	$3.6\ 10^3$	24	19.0	$5.3\ 10^4$
5	28.0	$2.9\ 10^3$	25	19.0	$2.7\ 10^4$
6	25.8	$5.4\ 10^3$	26	19.0	$3.6\ 10^4$
7	25.8	$3.2\ 10^3$	27	19.0	$4.8\ 10^4$
8	25.8	$4.0\ 10^3$	28	17.0	$7.3\ 10^4$
9	25.8	$2.9\ 10^3$	29	17.0	$5.3\ 10^4$
10	25.8	$2.9\ 10^3$	30	17.0	$8.4\ 10^4$
11	24.5	$9.6\ 10^3$	31	17.0	$4.5\ 10^4$
12	24.5	$7.3\ 10^3$	32	17.0	$8.3\ 10^4$
13	24.5	$1.3\ 10^4$	33	17.0	$8.0\ 10^4$
14	24.5	$7.6\ 10^3$	34	14.4	$1.2\ 10^5$
15	23.5	$9.5\ 10^3$	35	14.4	$1.5\ 10^5$
16	23.5	$1.4\ 10^4$	36	14.4	$3.0\ 10^5$
17	23.5	$1.6\ 10^4$	37	14.4	$2.2\ 10^5$
18	23.5	$1.7\ 10^4$	38	12.5	$3.0\ 10^5$
19	21.3	$1.2\ 10^4$	39	12.5	$2.1\ 10^5$
20	21.3	$2.0\ 10^4$	40	12.5	$3.2\ 10^5$

cont/d...

No.	Unfactored Stress	Endurance
41	12.5	$5.5\ 10^5$
42	12.5	$2.2\ 10^5$
43	9.6	$5.1\ 10^5$
44	9.6	$1.2\ 10^6$
45	7.6	$6.7\ 10^6$
46	7.6 (unbroken)	$9.0\ 10^7$

Direct stress testing of annealed 18/8 stainless steel - notched specimens $K_t = 2.37$.

No.	Fac. Stress	Endurance	No.	Stress	Endurance
1	86.0	$3.0\ 10^1$	15	51.5	$1.9\ 10^3$
2	86.0	$5.0\ 10^1$	16	47.3	$6.1\ 10^3$
3	86.0	$4.0\ 10^1$	17	47.3	$1.1\ 10^4$
4	79.5	$1.0\ 10^2$	18	47.3	$5.0\ 10^4$
5	79.5	$7.5\ 10^1$	19	40.8	$7.7\ 10^4$
6	73.0	$2.2\ 10^2$	20	40.8	$5.4\ 10^4$
7	73.0	$2.0\ 10^2$	21	40.8	$7.5\ 10^4$
8	73.0	$1.6\ 10^2$	22	32.3	$1.3\ 10^5$
9	64.5	$1.9\ 10^2$	23	32.3	$2.9\ 10^5$
10	64.5	$2.6\ 10^2$	24	32.3	$5.0\ 10^4$
11	64.5	$2.8\ 10^2$	25	28.0	$3.7\ 10^5$
12	56.0	$9.0\ 10^2$	26	28.0(unb.)	$6.5\ 10^6$
13	56.0	$1.6\ 10^3$	27	23.7(")	$1.4\ 10^7$
14	52.5	$1.3\ 10^3$			

Fluctuating tension testing of annealed 18/8 stainless steel - notched specimens $K_t = 2.37$.

No.	Fac. Stress	Endurance	No.	Fac. Stress	Endurance
1	102.0	$1.4\ 10^3$	12	74.2	$1.4\ 10^4$
2	102.0	$4.8\ 10^3$	13	74.2	$1.7\ 10^4$
3	102.0	$1.8\ 10^3$	14	66.3	$2.3\ 10^4$
4	95.5	$8.0\ 10^3$	15	60.0	$3.8\ 10^4$
5	95.5	$2.4\ 10^3$	16	60.0	$3.4\ 10^4$
6	88.6	$8.0\ 10^3$	17	60.0	$7.7\ 10^4$
7	88.1	$6.0\ 10^3$	18	53.8	$8.2\ 10^4$
8	83.0	$6.5\ 10^3$	19	53.8	$9.0\ 10^4$
9	83.0	$4.5\ 10^3$	20	53.8	$6.0\ 10^4$
10	78.2	$1.0\ 10^4$	21	49.5(unb)	$2.8\ 10^6$
11	78.2	$6.0\ 10^3$	22	47.4(unb.)	$1.0\ 10^7$

Direct stress tests of annealed mild steel - notched specimens

$K_t = 2.5$

No.	Unf. Stress	Endurance	No.	Unf. Stress	Endurance
1	31.8	$3.5\ 10$	22	24.2	$2.3\ 10^2$
2	31.8	$2.5\ 10$	23	24.2	$2.1\ 10^2$
3	31.8	$2.3\ 10$	24	24.2	$2.1\ 10^2$
4	29.8	$4.0\ 10$	25	23.4	$2.6\ 10^2$
5	29.8	$4.0\ 10$	26	23.4	$2.6\ 10^2$
6	29.8	$3.5\ 10$	27	23.4	$3.7\ 10^2$
7	28.5	$7.5\ 10$	28	22.3	$4.5\ 10^2$
8	28.5	$6.0\ 10$	29	22.3	$3.7\ 10^2$
9	28.5	$5.0\ 10$	30	22.3	$4.2\ 10^2$
10	27.3	$7.5\ 10$	31	21.6	$4.5\ 10^2$
11	27.3	$9.0\ 10$	32	21.6	$4.6\ 10^2$
12	27.3	$9.0\ 10$	33	21.6	$6.2\ 10^2$
13	26.1	$1.1\ 10^2$	34	20	$1.1\ 10^3$
14	26.1	$1.1\ 10^2$	35	20	$1.3\ 10^3$
15	26.1	$1.2\ 10^2$	36	20	$1.1\ 10^3$
16	25.5	$1.0\ 10^2$	37	17.9	$2.8\ 10^3$
17	25.5	$1.5\ 10^2$	38	17.9	$3.2\ 10^3$
18	25.5	$1.3\ 10^2$	39	17.9	$2.9\ 10^3$
19	24.8	$1.4\ 10^2$	40	16.1	$4.4\ 10^3$
20	24.8	$1.5\ 10^2$	41	16.1	$5.9\ 10^3$
21	24.8	$1.6\ 10^2$	42	16.1	$9.4\ 10^3$

cont/d..

No.	Unf. Stress	Endurance	No.	Unf. Stress	Endurance
43	16.5	$6.1\ 10^3$	53	13.0	$5.9\ 10^4$
44	16.5	$3.7\ 10^3$	54	12.1	$5.9\ 10^4$
45	16.5	$4.0\ 10^3$	55	12.1	$1.1\ 10^5$
46	15.5	$2.3\ 10^4$	56	12.1	$1.1\ 10^5$
47	15.5	$2.3\ 10^4$	57	10.8	$3.5\ 10^5$
48	15.2	$1.4\ 10^4$	58	10.8	$4.6\ 10^5$
49	14.2	$3.3\ 10^4$	59	9.6	$7.1\ 10^5$
50	14.2	$1.9\ 10^4$	60	9.6	$7.2\ 10^5$
51	14.2	$2.9\ 10^4$	61	8.8(unb.)	$7.9\ 10^6$
52	13.0	$1.1\ 10^5$			
53					

Fluctuating tension tests of annealed mild steel - notched specimens

$K_t = 2.5$

No.	Unf. Stress	Endurance	No.	Unf. Stress	Endurance
1	33.6	$4.0\ 10^3$	12	24.2	$4.5\ 10^4$
2	33.6	$4.0\ 10^3$	13	22.6	$6.9\ 10^4$
3	32.5	$5.0\ 10^3$	14	22.6	$9.0\ 10^4$
4	32.5	$7.0\ 00^3$	15	20.5	$2.4\ 10^5$
5	30.0	$1.0\ 10^4$	16	20.5	$1.5\ 10^5$
6	30.0	$1.1\ 10^4$	17	18.1	$6.9\ 10^5$
7	28.6	$1.5\ 10^4$	18	18.1	$3.6\ 10^5$
8	28.6	$1.7\ 10^4$	19	17.3	$1.0\ 10^6$
9	26.2	$2.9\ 10^4$	20	17.3	$1.3\ 10^6$
10	26.2	$2.4\ 10^4$	21	16.3(unb)	$1.6\ 10^7$
11	24.2	$4.2\ 10^4$			

Direct stress tests of L73 aluminium alloy-notched specimens $K_t = 2.5$

No.	Fac. Stress	Endurance	No.	Fac. Stress	Endurance
1	66.3	$3.0\ 10$	23	42.6	$5.5\ 10^2$
2	66.0	$2.7\ 10$	24	42.6	$8.1\ 10^2$
3	65.0	$3.0\ 10$	25	42.6	$8.9\ 10^2$
4	65.0	$2.5\ 10$	26	38.4	$1.7\ 10^3$
5	63.3	$4.0\ 10$	27	38.4	$1.5\ 10^3$
6	62.5	$4.0\ 10$	28	38.4	$1.3\ 10^3$
7	61.5	$4.0\ 10$	29	33.8	$3.1\ 10^3$
8	61.5	$5.0\ 10$	30	33.8	$3.1\ 10^3$
9	61.4	$4.0\ 10$	31	33.8	$2.8\ 10^3$
10	60.0	$1.0\ 10^2$	32	29.6	$4.8\ 10^3$
11	57.2	$1.3\ 10^2$	33	29.6	$1.2\ 10^4$
12	57.2	$1.0\ 10^2$	34	29.6	$3.8\ 10^3$
13	56.4	$1.4\ 10^2$	35	25.6	$1.9\ 10^4$
14	54.5	$2.1\ 10^2$	36	25.6	$1.4\ 10^4$
15	54.5	$1.6\ 10^2$	37	25.6	$1.3\ 10^3$
16	54.5	$1.7\ 10^2$	38	19.0	$6.3\ 10^4$
17	52.5	$2.5\ 10^2$	39	19.0	$5.2\ 10^4$
18	52.5	$2.8\ 10^2$	40	19.0	$1.3\ 10^4$
19	52.5	$2.3\ 10^2$	41	14.8	$8.4\ 10^4$
20	47.7	$4.3\ 10^2$	42	14.8	$4.0\ 10^5$
21	47.7	$4.2\ 10^2$	43	14.8	$1.2\ 10^5$
22	47.7	$4.5\ 10^2$			

Fluctuating tension tests of L73 aluminium alloy - notched specimens

$K_t = 2.5$

No.	Fac. Stress	Endurance	No.	Fac. Stress	Endurance
1	74.0	$4.0\ 10$	22	42.6	$8.5\ 10^3$
2	74.0	$3.35\ 10$	23	42.6	$7.6\ 10^3$
3	71.0	$2.6\ 10$	24	41.4	$1.2\ 10^4$
4	71.0	$4.3\ 10$	25	41.4	$1.2\ 10^4$
5	70.0	$5.6\ 10$	26	40.0	$1.4\ 10^4$
6	67.5	$6.3\ 10$	27	39.2	$1.6\ 10^4$
7	67.5	$6.2\ 10$	28	39.2	$1.6\ 10^4$
8	62.4	$9.5\ 10$	29	39.2	$2.0\ 10^4$
9	62.4	$1.3\ 10$	30	35.0	$2.6\ 10^4$
10	61.0	$1.2\ 10$	31	34.8	$2.7\ 10^4$
11	60.3	$1.2\ 10$	32	31.0	$3.9\ 10^4$
12	58.8	$2.1\ 10$	33	30.7	$4.7\ 10^4$
13	58.4	$1.8\ 10$	34	28.8	$6.1\ 10^4$
14	55.3	$2.4\ 10$	35	28.8	$6.2\ 10^4$
15	55.3	$2.5\ 10$	36	24.6	$1.1\ 10^5$
16	51.8	$3.5\ 10$	37	24.6	$9.3\ 10^5$
17	51.8	$3.8\ 10$	38	21.8	$2.0\ 10^5$
18	47.7	$5.8\ 10$	39	21.8	$1.8\ 10^5$
19	47.7	$5.8\ 10$	40	18.3	$3.4\ 10^5$
20	44.2	$7.3\ 10$	41	14.6	$7.4\ 10^5$
21	43.4	$1.0\ 10$	42	14.4	$3.1\ 10^6$

Fluctuating compression tests of L73 aluminium alloy-notched specimens

$K_t = 2.5$

No.	Fac. Stress	Endurance	No.	Fac. Stress	Endurance
1	86.5	$1.3\ 10^4$	16	58.4	$1.1\ 10^5$
2	86.5	$8.0\ 10^3$	17	57.5	$7.5\ 10^4$
3	80	$2.9\ 10^4$	18	56.2	$3.9\ 10^4$
4	79	$2.5\ 10^4$	19	54.5	$1.3\ 10^5$
5	77.5	$2.5\ 10^4$	20	54.0	$2.4\ 10^5$
6	76.6	$2.7\ 10^4$	21	53.3	$6.3\ 10^4$
7	72.5	$4.9\ 10^4$	22	53.2	$8.0\ 10^4$
8	72	$2.0\ 10^4$	23	51.8	$9.7\ 10^4$
9	71.5	$4.1\ 10^4$	24	51.8	$4.4\ 10^4$
10	70.8	$3.6\ 10^4$	25	49.4	$1.3\ 10^5$
11	68.2	$6.2\ 10^4$	26	49.4	$1.9\ 10^5$
12	68.2	$7.4\ 10^4$	27	47.7	$1.8\ 10^5$
13	63.2	$7.6\ 10^4$	28	47.7	$2.8\ 10^5$
14	63.2	$2.3\ 10^4$	29	39.2	$2.2\ 10^5$
15	58.4	$1.5\ 10^5$	30	39.2(unb.)	$1.2\ 10^6$

Direct stress tests of annealed 18/8 stainless steel at -80°C -

notched specimens $K_t = 2.37$

No.	Fac. Stress	Endurance	No.	Fac. Stress	Endurance
1	87.2	$1.56\ 10^3$	18	79.3	$6.0\ 10^2$
2	87.2	$4.7\ 10^2$	$1\frac{1}{4}$	77.4	$3.0\ 10^3$
3	87.2	$1.2\ 10^3$	20	77.4	$3.9\ 10^3$
4	87.2	$1.2\ 10^3$	21	77.4	$2.9\ 10^2$
5	85.2	$3.6\ 10^3$	22	75.5	$2.4\ 10^3$
6	85.2	$2.2\ 10^3$	23	75.5	$2.4\ 10^3$
7	85.2	$4.7\ 10^3$	24	75.5	$4.8\ 10^3$
8	83.2	$6.0\ 10^2$	25	75.5	$4.8\ 10^3$
9	83.2	$3.0\ 10^3$	26	73.6	$9.6\ 10^3$
10	83.2	$1.6\ 10^3$	27	73.6	$1.4\ 10^4$
11	83.2	$2.3\ 10^3$	28	73.6	$1.8\ 10^3$
12	81.3	$8.4\ 10^2$	29	73.6	$6.6\ 10^3$
13	81.3	$3.6\ 10^3$	30	72.6	$8.6\ 10^3$
14	81.3	$1.8\ 10^3$	31	72.6	$9.2\ 10^3$
15	81.3	$1.4\ 10^3$	32	72.6	$6.0\ 10^3$
16	79.3	$1.8\ 10^3$	33	72.6	$7.2\ 10^2$
17	79.3	$9.6\ 10^2$	34	69.7	$1.7\ 10^4$

Direct stress tests of annealed D.T.D. 18 stainless steel at 250°C - notched specimens $K_t = 2.37$

No.	Fac. Stress	Endurance	No.	Fac. Stress	Endurance
1	58.0	$1.3\ 10^3$	14	42.5	$1.4\ 10^4$
2	58.0	$1.1\ 10^3$	15	42.5	$9.1\ 10^3$
3	58.0	$6.8\ 10^2$	16	38.6	$2.5\ 10^4$
4	54.0	$1.3\ 10^3$	17	38.6	$2.8\ 10^4$
5	54.0	$2.8\ 10^3$	18	38.6	$3.7\ 10^4$
6	54.0	$2.1\ 10^3$	19	34.8	$8.2\ 10^4$
7	50.2	$6.8\ 10^3$	20	34.8	$5.7\ 10^4$
8	50.2	$6.2\ 10^3$	21	34.8	$7.4\ 10^4$
9	50.2	$3.2\ 10^3$	22	31.0	$2.0\ 10^6$
10	46.3	$4.0\ 10^3$	23	31.0	$1.2\ 10^6$
11	46.3	$3.4\ 10^3$	24	31.0	$2.1\ 10^6$
12	46.3	$6.8\ 10^3$	25	29.0	$5.5\ 10^6$
13	42.5	$4.8\ 10^4$	26	29.0(unb.)	$1.1\ 10^7$

Direct stress tests of annealed 18/8 stainless steel at 350°C - notched specimens $K_t = 2.37$

No.	Fac. Stress	Endurance	No.	Fact. Stress	Endurance
1	50.3	$3.3\ 10^2$	16	36.7	$1.8\ 10^4$
2	50.3	$4.4\ 10^2$	17	36.7	$1.8\ 10^4$
3	46.4	$5.5\ 10^2$	18	34.8	$5.3\ 10^4$
4	42.6	$3.9\ 10^3$	19	34.8	$1.2\ 10^4$
5	42.6	$5.0\ 10^3$	20	34.8	$3.4\ 10^4$
6	42.6	$2.8\ 10^3$	21	31.0	$2.2\ 10^5$
7	40.7	$5.5\ 10^3$	22	31.0	$5.4\ 10^4$
8	40.7	$8.8\ 10^3$	23	31.0	$1.8\ 10^5$
9	40.7	$2.8\ 10^3$	24	29.0	$3.3\ 10^4$
10	40.7	$5.5\ 10^3$	25	29.0	$1.0\ 10^5$
11	38.7	$3.9\ 10$	26	29.0	$2.2\ 10^5$
12	38.7	$2.8\ 10^3$	27	27.1(unb.)	$1.0\ 10^7$
13	38.7	$5.5\ 10^3$	28	28.1	$2.1\ 10^6$
14	38.6	$2.7\ 10^4$	29	28.1(unb.)	$2.7\ 10^7$
15	36.7	$8.8\ 10^3$			

Direct stress tests of annealed mild steel at 350°C notched specimens

$K_t = 2.5$

No.	Unf. Stress	Endurance	No.	Unf. Stress	Endurance
1	21.8	$1.1\ 10^3$	16	15.1	$1.9\ 10^4$
2	21.8	$9.1\ 10^2$	17	14.2	$4.7\ 10^4$
3	21.0	$2.9\ 10^3$	18	14.2	$2.9\ 10^4$
4	21.0	$1.4\ 10^3$	19	13.3	$4.1\ 10^4$
5	19.9	$1.8\ 10^3$	20	13.3	$8.7\ 10^4$
6	19.9	$2.3\ 10^3$	21	12.3	$1.5\ 10^5$
7	18.9	$3.4\ 10^3$	22	12.3	$7.3\ 10^4$
8	18.9	$3.4\ 10^3$	23	11.4	$1.2\ 10^5$
9	18.0	$6.2\ 10^3$	24	11.4	$2.6\ 10^5$
10	18.0	$5.7\ 10^3$	25	10.4	$1.0\ 10^5$
11	17.0	$8.5\ 10^3$	26	10.4	$4.4\ 10^5$
12	17.0	$9.1\ 10^3$	27	9.9	$4.1\ 10^6$
13	16.1	$1.2\ 10^4$	28	9.9	$5.4\ 10^5$
14	16.1	$1.7\ 10^4$	29	9.5	$4.9\ 10^5$
15	15.1	$2.6\ 10^4$	30	9.5(unb.)	$1.8\ 10^7$

Direct stress-random loading tests of L73 aluminium alloy - factored static mean load = 15 tons/inch^2 - notched specimens K_t = 2.5

No.	R.M.S. of Peak Stress (Factored)	Endurance	No.	R.M.S. of Peak Stress (Factored)	Endurance
1	18.2	$4.4\ 10^3$	24	7.9	$1.8\ 10^5$
2	18.2	$4.5\ 10^3$	25	7.7	$5.0\ 10^4$
3	18.2	$4.8\ 10^3$	26	7.7	$2.2\ 10^5$
4	16.5	$5.0\ 10^3$	27	7.3	$1.5\ 10^5$
5	16.5	$6.0\ 10^3$	28	6.7	$3.1\ 10^5$
6	16.5	$4.4\ 10^3$	29	6.3	$3.5\ 10^5$
7	16.5	$5.7\ 10^3$	30	6.0	$3.2\ 10^5$
8	15.4	$5.4\ 10^3$	31	5.7	$7.0\ 10^5$
9	13.5	$8.1\ 10^3$	32	5.7	$5.1\ 10^5$
10	13.2	$1.1\ 10^4$	33	5.6	$8.0\ 10^5$
11	12.5	$1.2\ 10^4$	34	5.1	$1.1\ 10^6$
12	12.3	$1.6\ 10^4$	35	4.7	$1.6\ 10^6$
13	12.2	$1.1\ 10^4$	36	4.4	$3.0\ 10^6$
14	12.2	$1.1\ 10^4$	37	4.4	$2.9\ 10^6$
15	12.1	$2.7\ 10^4$	38	4.3	$1.2\ 10^6$
16	10.9	$4.7\ 10^4$	39	4.3	$2.1\ 10^6$
17	10.6	$1.4\ 10^4$	40	4.3	$1.4\ 10^6$
18	10.4	$4.5\ 10^4$	41	4.0	$3.1\ 10^7$
19	9.7	$9.6\ 10^4$	42	3.3	$3.2\ 10^7$
20	9.3	$4.3\ 10^4$	43	3.3	$1.3\ 10^8$
21	9.1	$6.5\ 10^5$	44	3.3	$5.2\ 10^6$
22	8.9	$1.6\ 10^5$	45	3.3	$6.2\ 10^6$
23	8.1	$1.4\ 10^5$			

Tensile Test Results:-

Material	Field Stress (Tons/inch^2)	True Ultimate Stress (Tons/inch^2)
Annealed Mild Steel	17.3	41.6
L73 aluminium alloy	-	29.3
70/30 brass after 25% extension	27.8	40.0
18/8 stainless steel cold rolled 75% reduction in area	-	98
18/8 stainless steel with raised nitrogen content, cold rolled 60% reduction in area	-	87.5 (average of three results)

Impact Test Results performed on cold rolled 18/8 stainless steel with a reduction in area of 75%

Temperature ^{o}C	-196	-70	-70	-50	-50	-25	+10	+50	+100
Energy absorbed lb.ft.	6.7	6.0	8.5	7.8	6.0	8.1	8.5	9.2	9.2

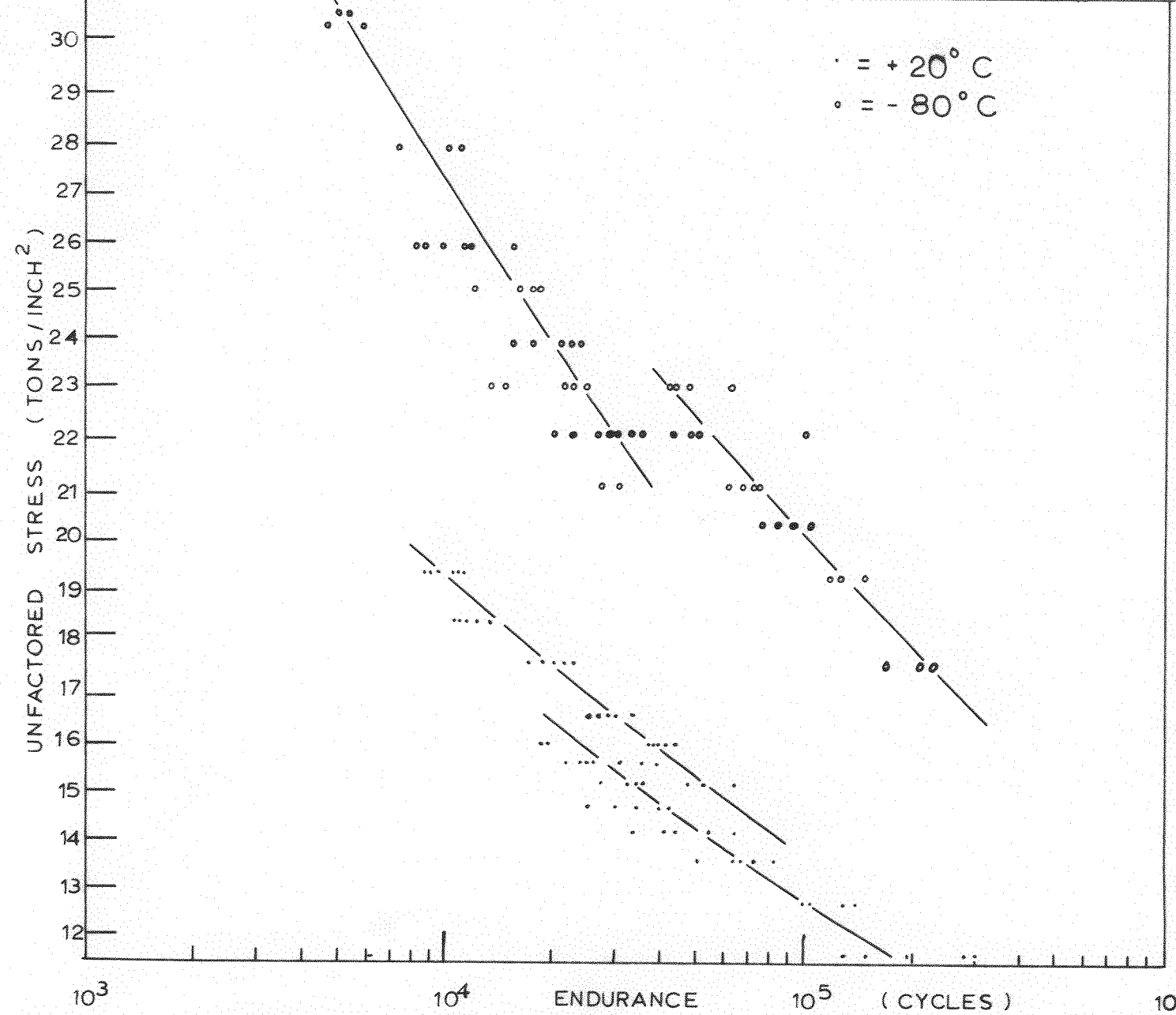

FREQ.=120 C.P.S.

FIG. 1 . COMPARATIVE FATIGUE TESTS OF ANNEALED MILD STEEL AT + 20°C & - 80°C. DIRECT STRESS TESTING OF NOTCHED SPECIMENS $K_t = 2.5$.

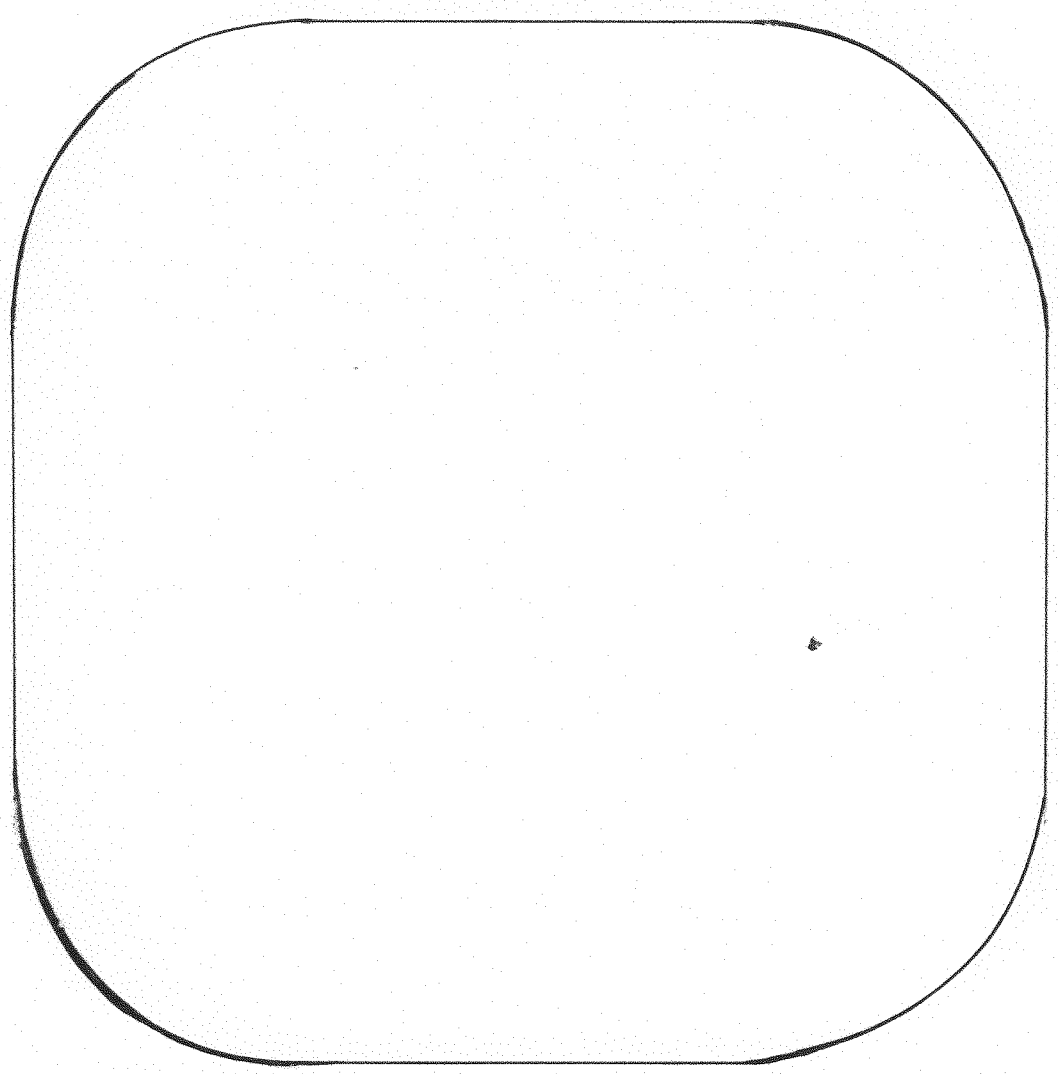

FIG. 2. SHAPE OF ROLLED 18/8 STEEL BAR.
(NOT TO SCALE)

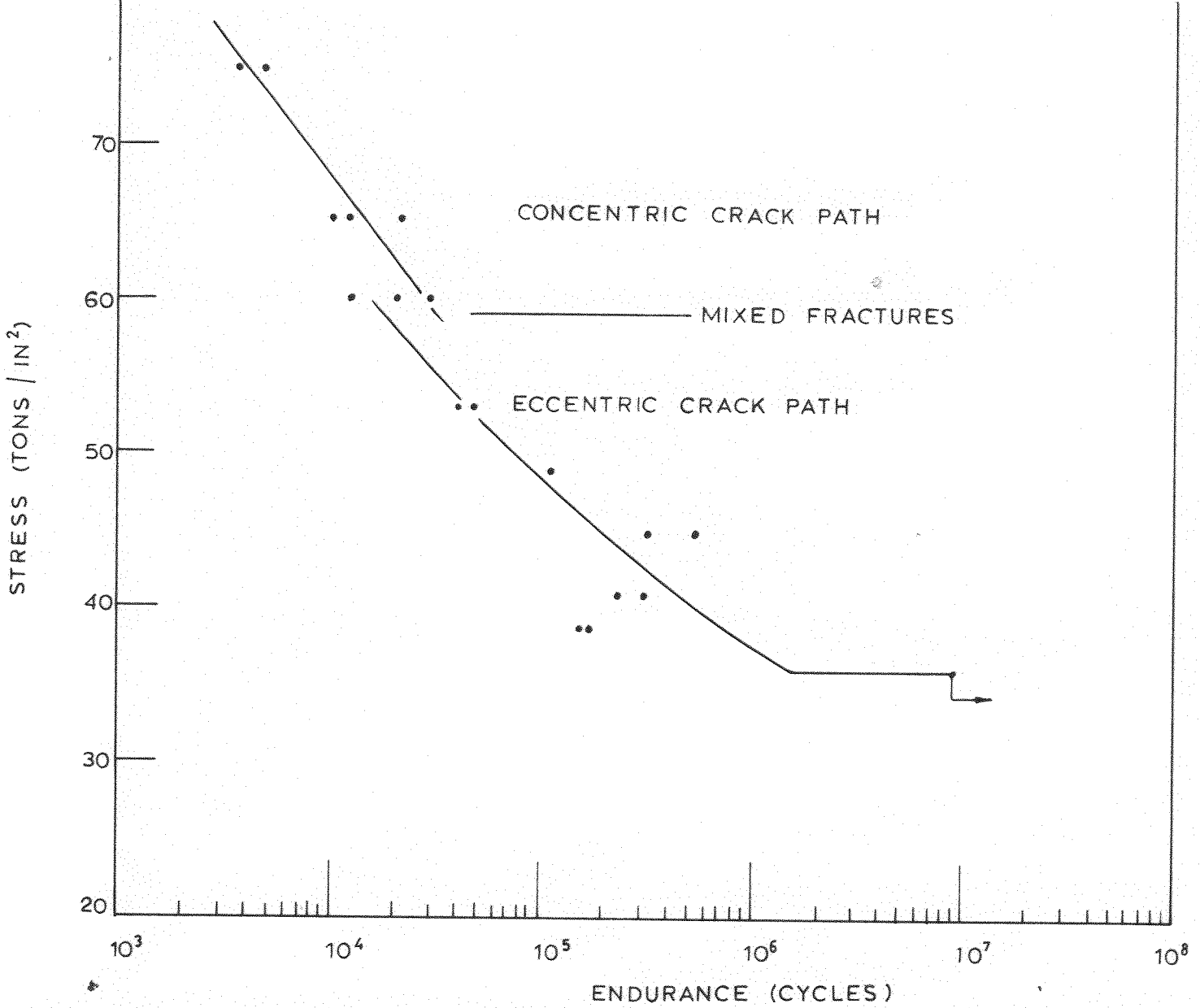

FIG. 3. S/N CURVE OF 18/8 STEEL COLD ROLLED 65% REDUCTION IN AREA. ROTATING CANTILEVER TESTING OF PLAIN SPECIMENS.

FREQ. = 80 C.P.S..

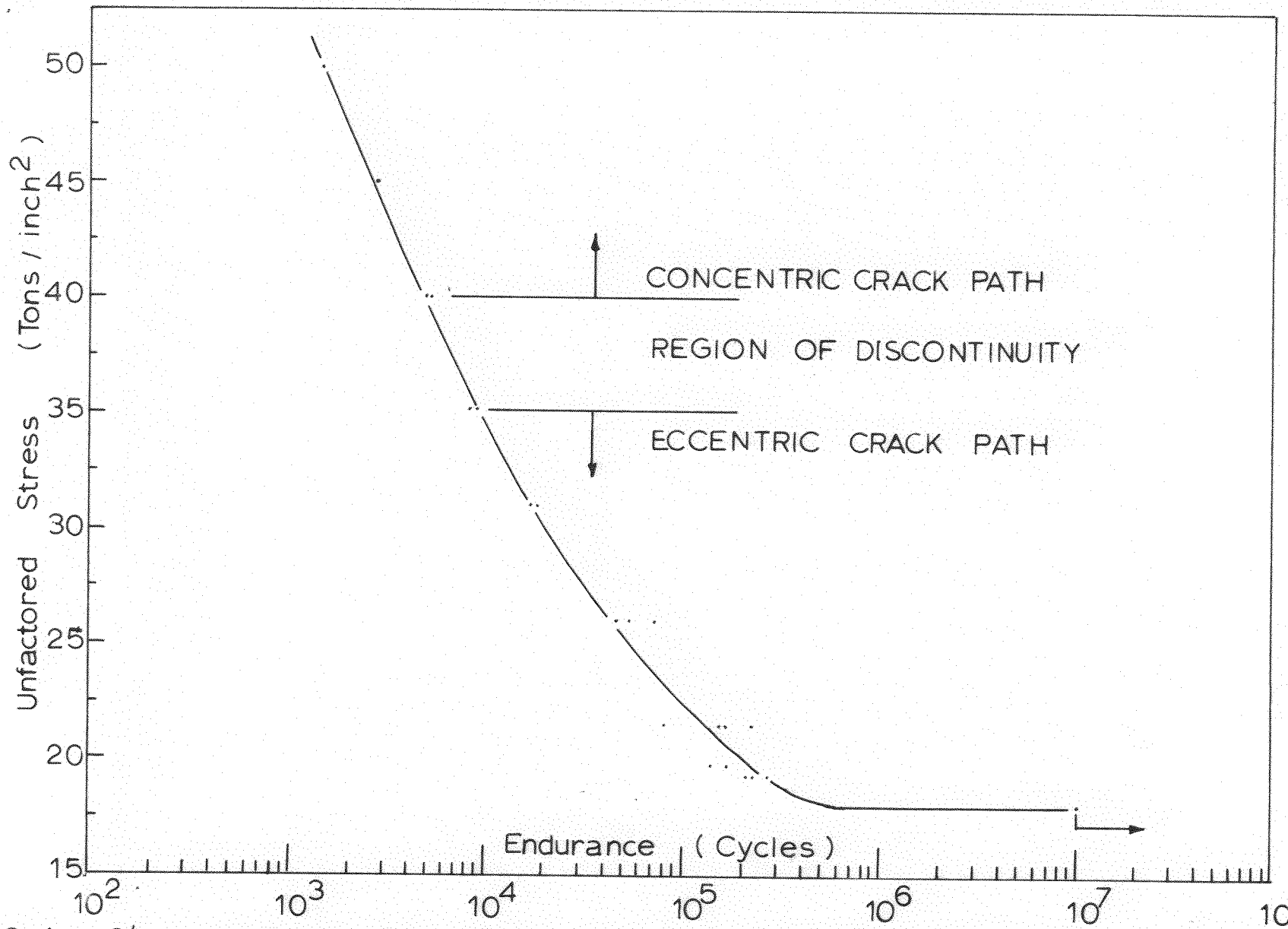

FIG. 4. S/N CURVE OF 18/8 STEEL COLD ROLLED 65% REDUCTION IN AREA. ROTATING CANTILEVER TESTING OF NOTCHED SPECIMENS $K_t = 2{\cdot}0$. FREQ. = 80 C.P.S.

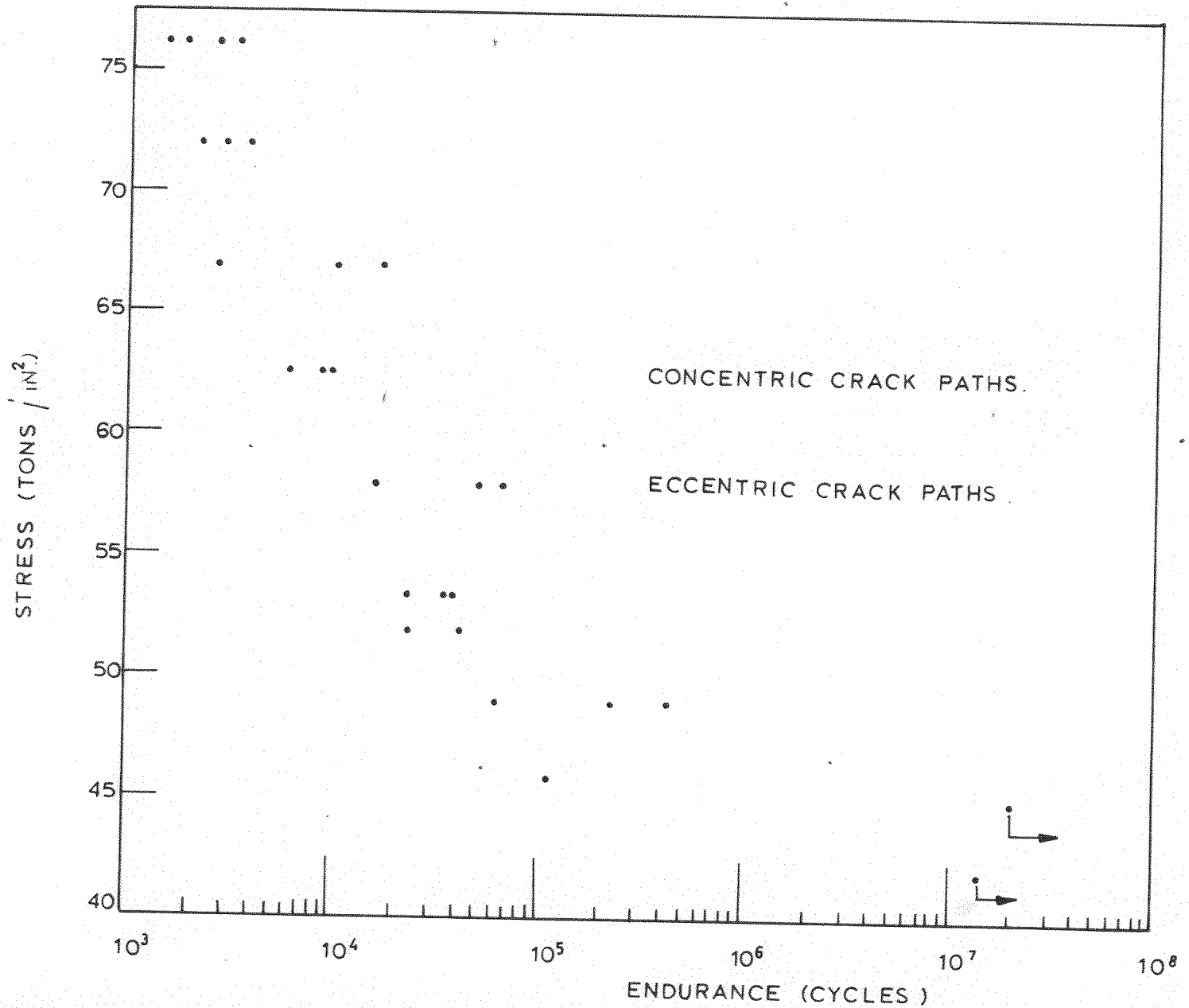

FIG. 5. S/N CURVE OF 18/8 STEEL COLD ROLLED 75% REDUCTION IN AREA. ROTATING CANTILEVER TESTING OF PLAIN SPECIMENS. FREQ. = 80 C.P.S..

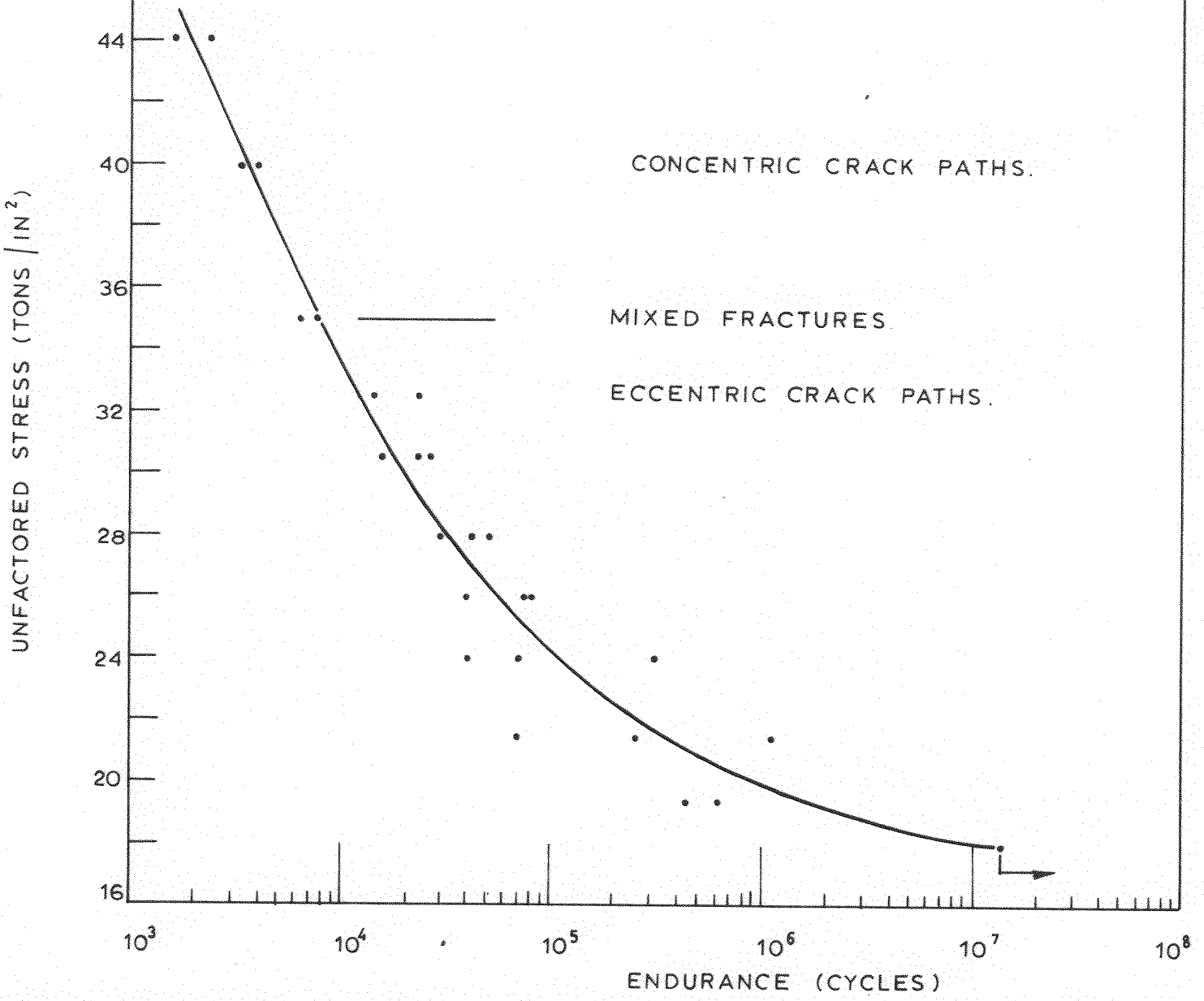

FIG. 6. S/N CURVE OF 18/8 STEEL COLD ROLLED 75 % REDUCTION IN AREA. ROTATING CANTILEVER TESTING OF NOTCHED SPECIMENS $K_t = 2 \cdot 0$. FREQ. = 80 C.P.S..

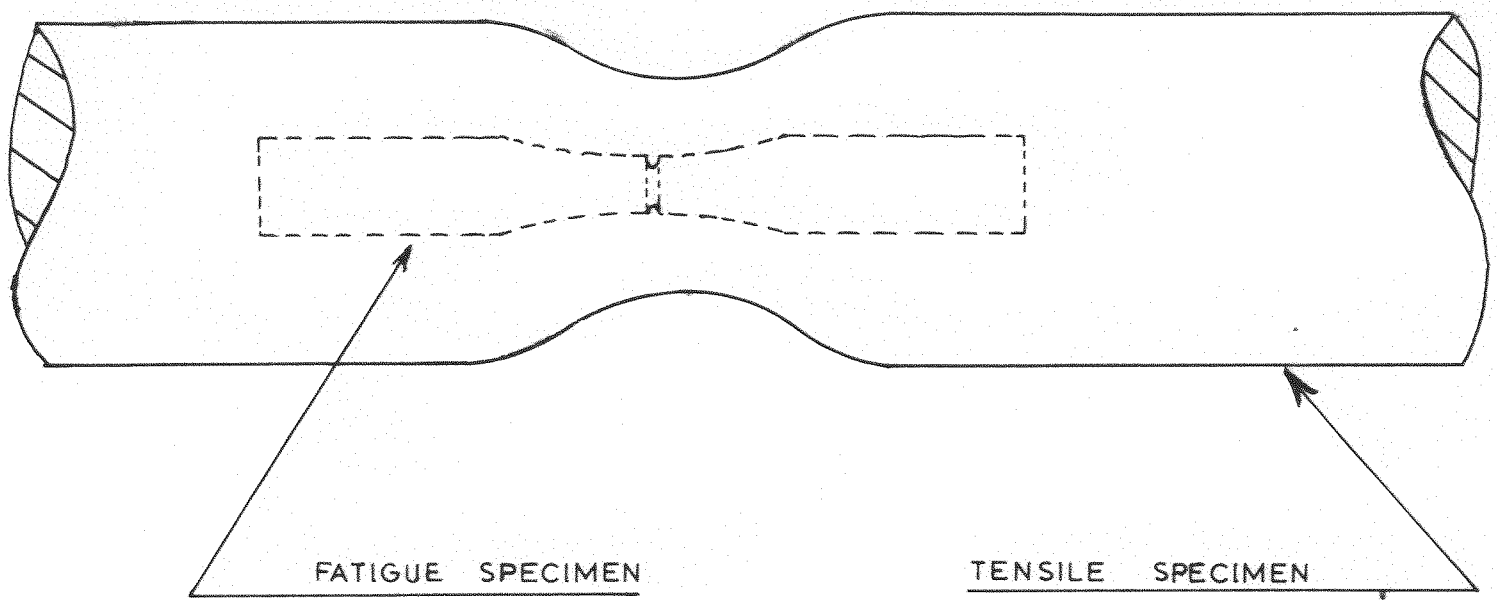

FIG. 7. SCHEMATIC DIAGRAM SHOWING SPECIMEN PREPARATION FROM TENSILE SPECIMEN.

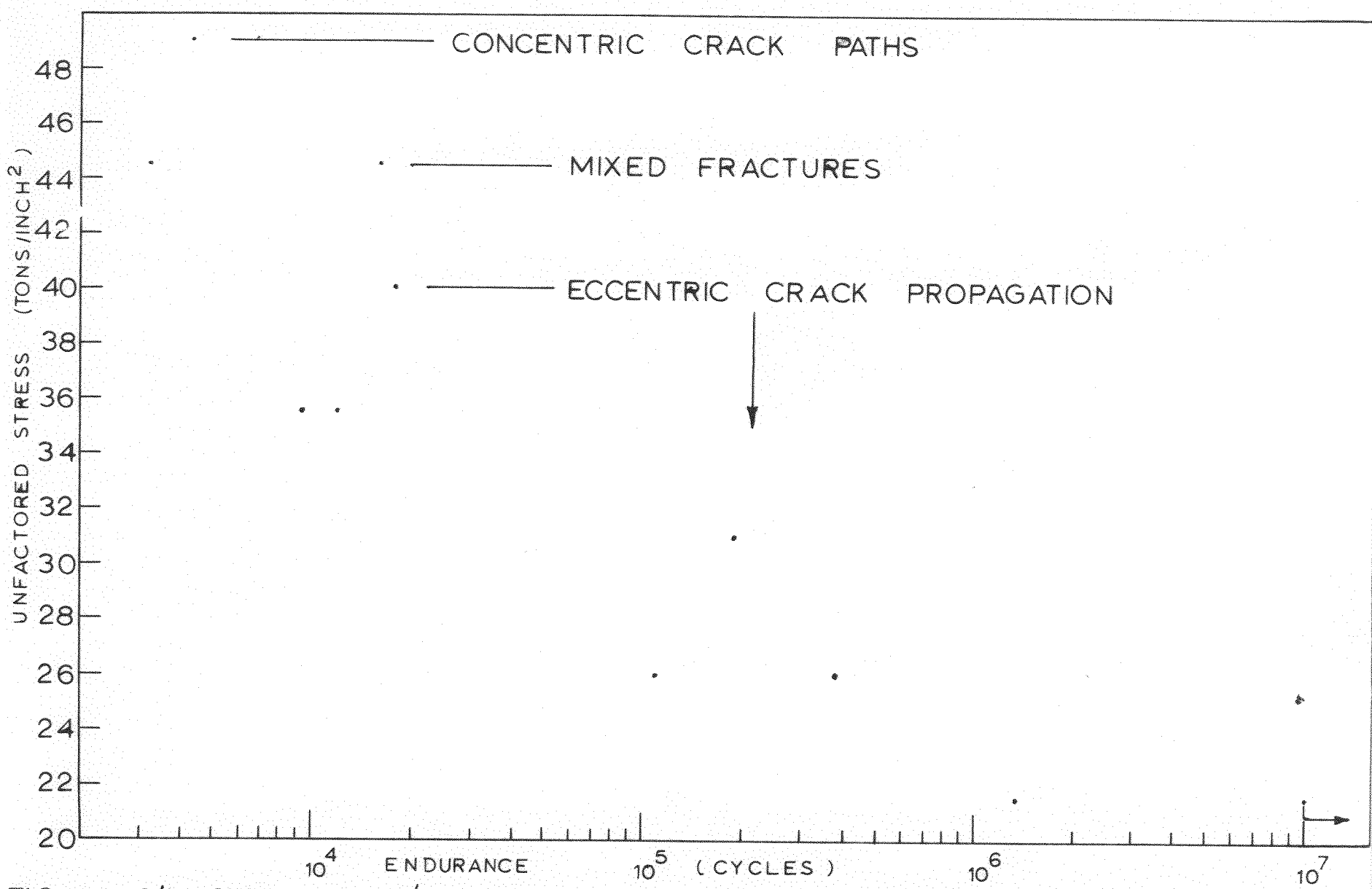

FIG. 8. S/N CURVE OF 18/8 STEEL COLD ROLLED 75% REDUCTION + 5% EXTENSION. ROTATING CANTILEVER TESTING OF NOTCHED SPECIMENS $K_t = 2 \cdot 0$. FREQ. = 80 C.P.S..

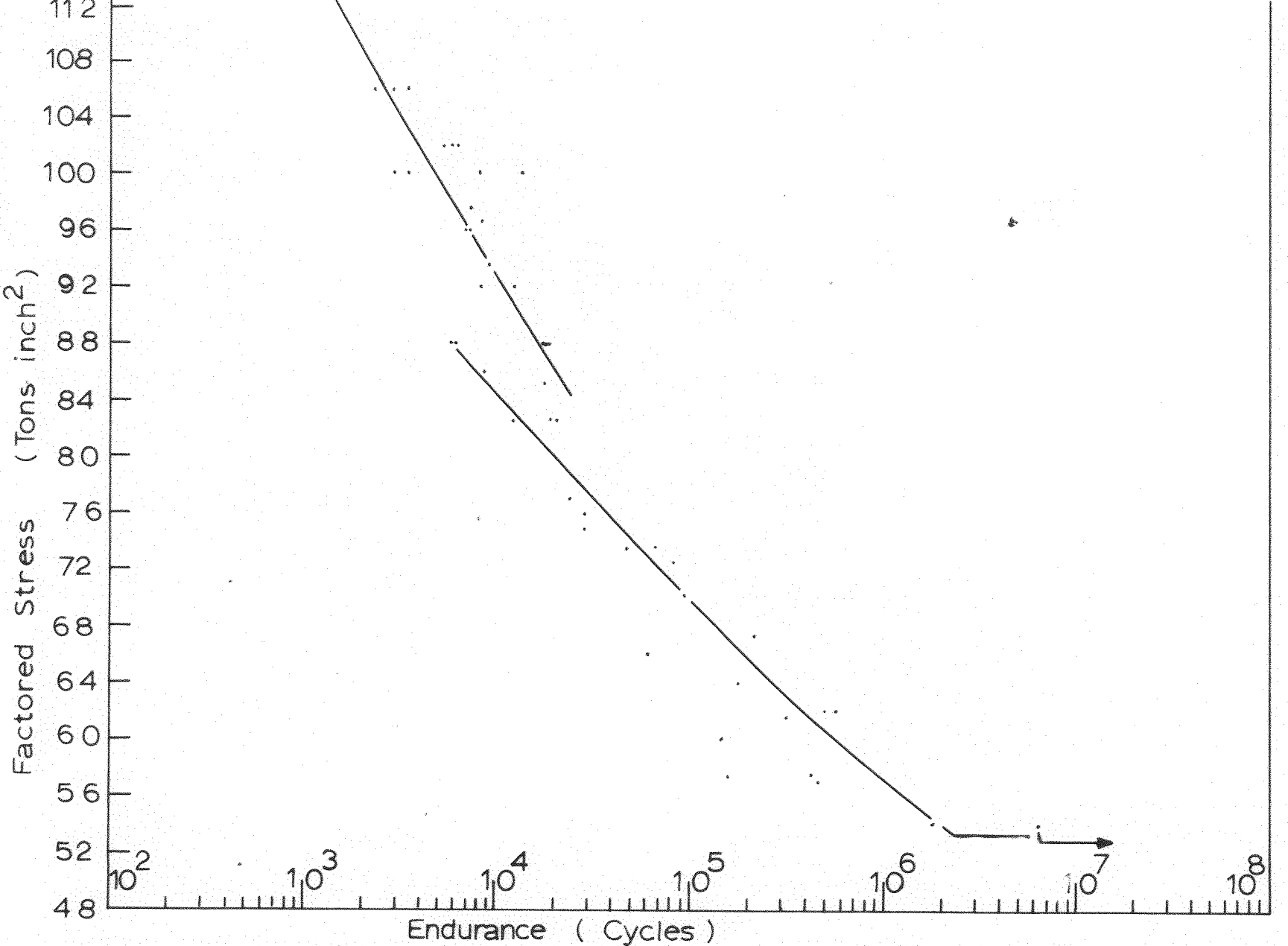

FIG. 9. S/N CURVE OF 18/8/N STEEL COLD ROLLED 60% REDUCTION IN AREA. DIRECT STRESS TESTING OF NOTCHED SPECIMENS K_t = 2·37. FREQ.=120C.P.S.

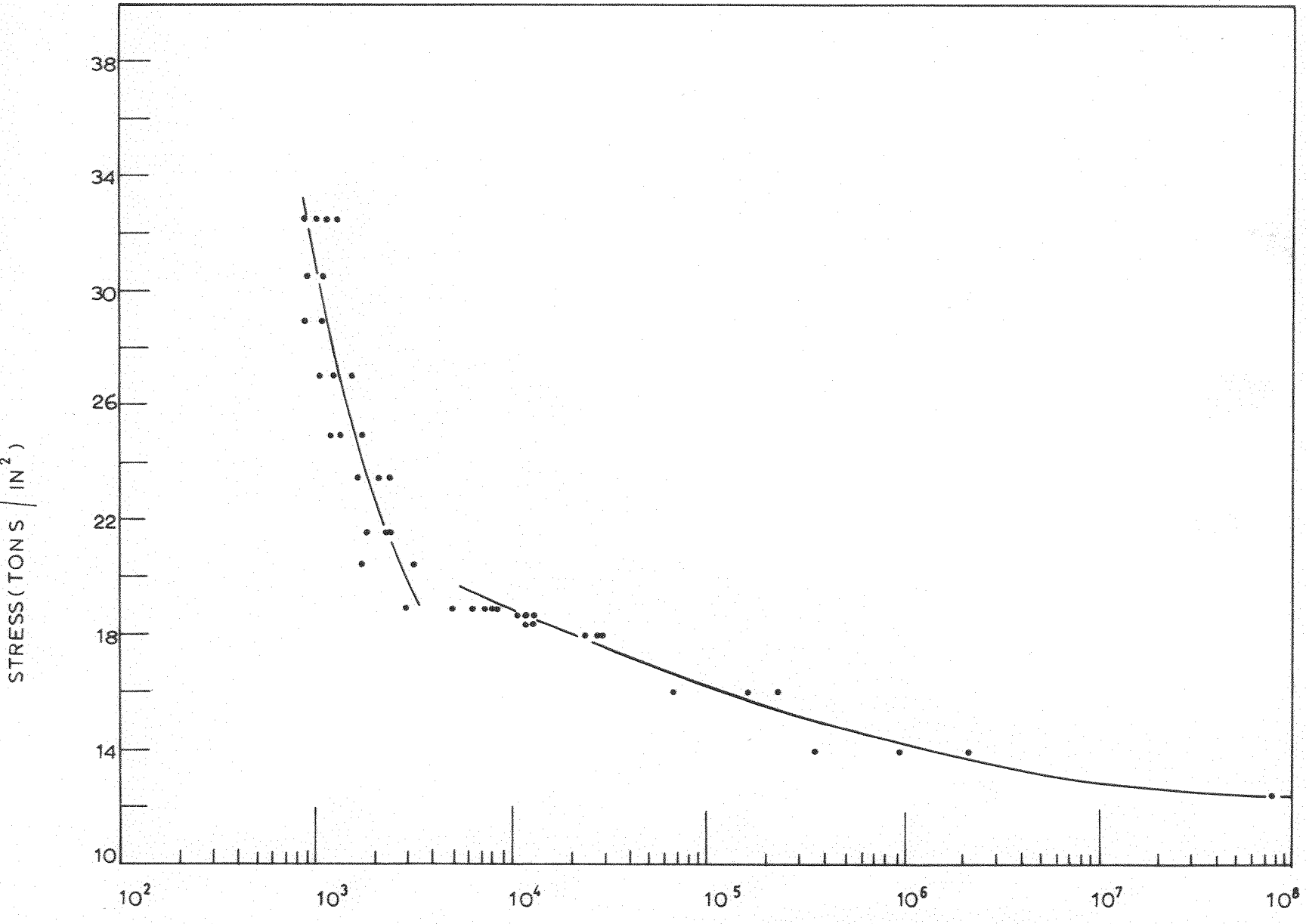

FIG.10. S/N CURVE OF ANNEALED 70/30 BRASS. ROTATING CANTILEVER TESTING OF PLAIN SPECIMENS. FREQ. = 80 C.P.S.

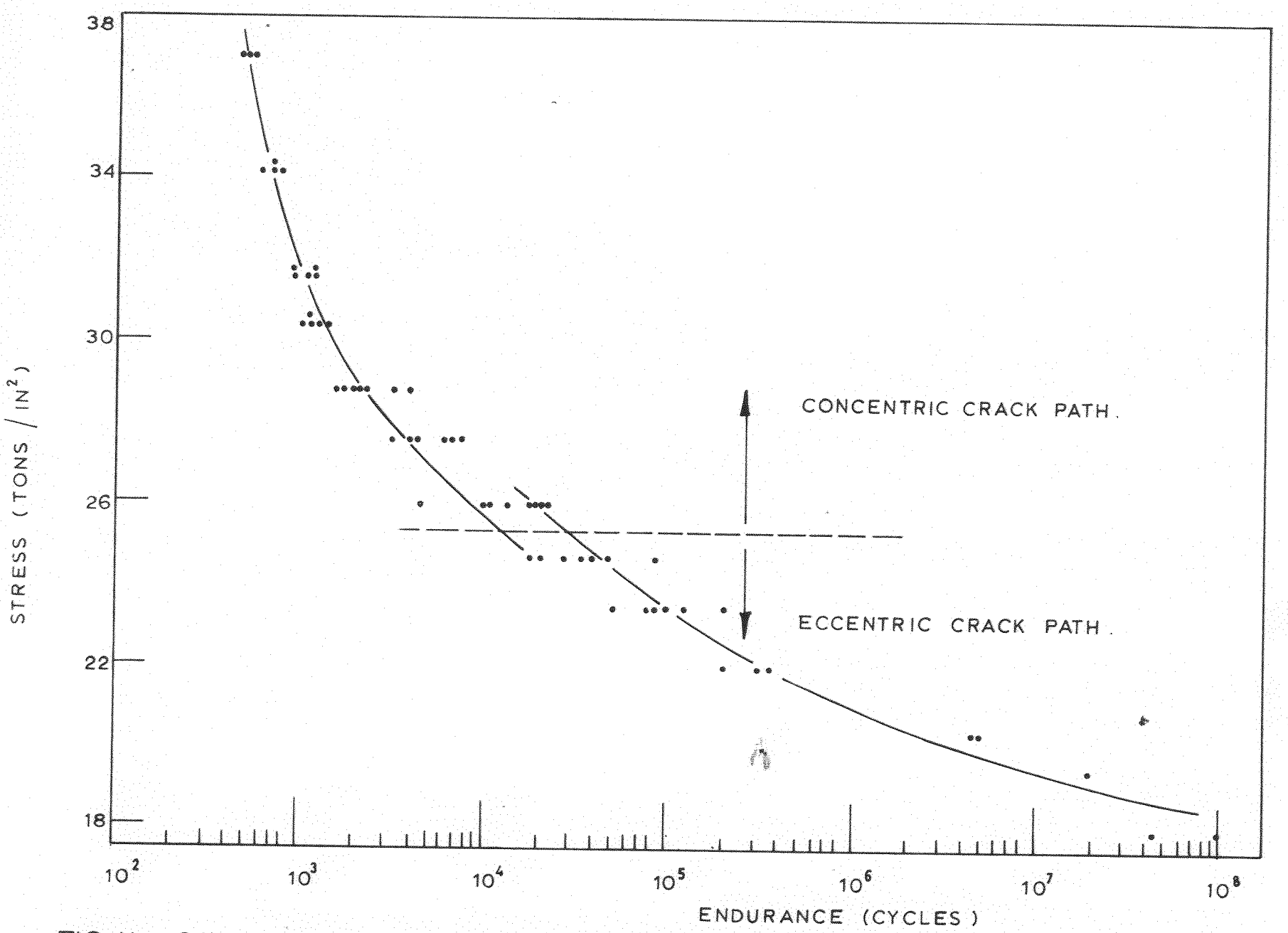

FIG. 11. S/N CURVE OF 70/30 BRASS COLD STRETCHED 25%. ROTATING CANTILEVER TESTING OF PLAIN SPECIMENS. FREQ. = 80 CPS

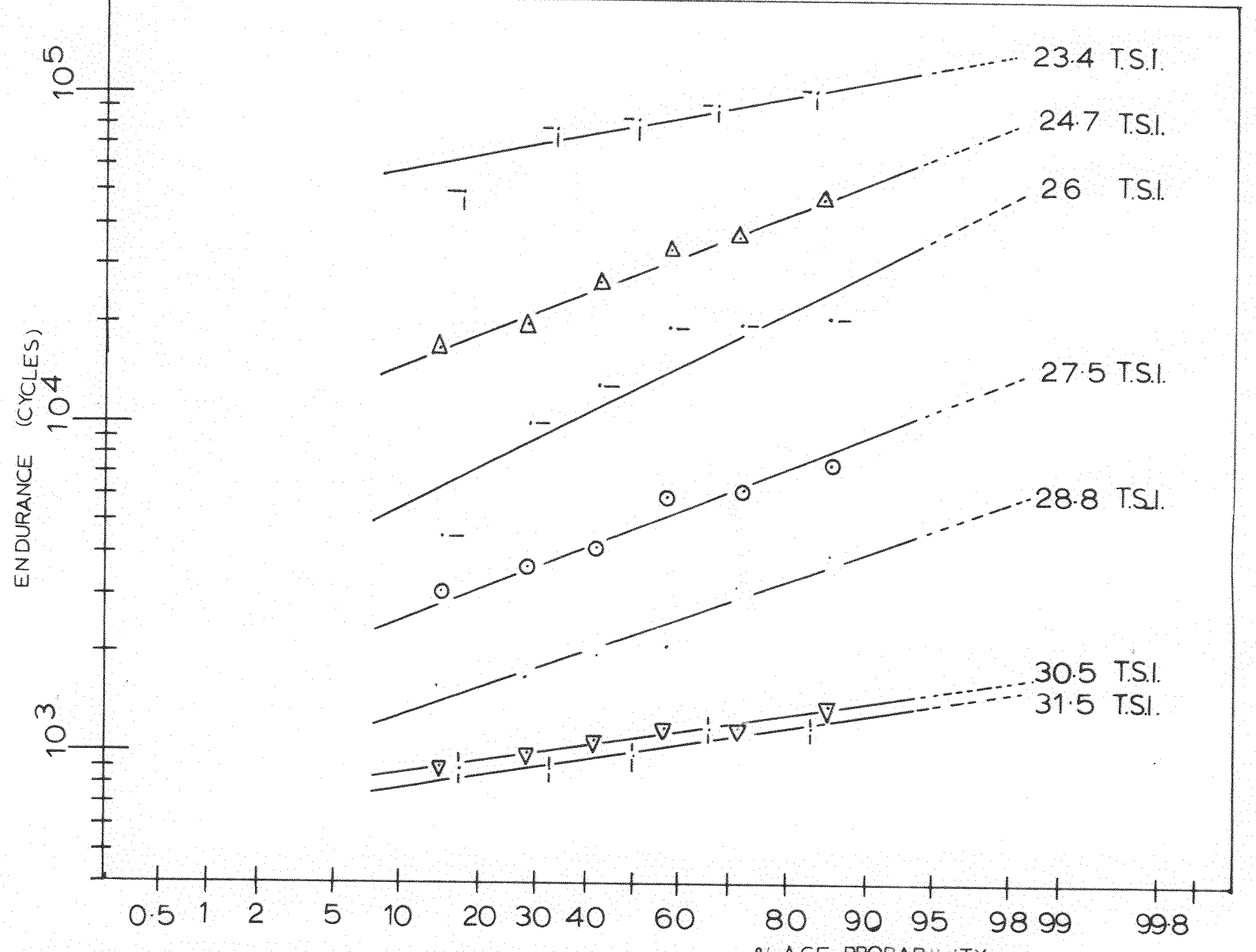

FIG.12. ENDURANCE — PROBABILITY FOR COLD STRETCHED BRASS.

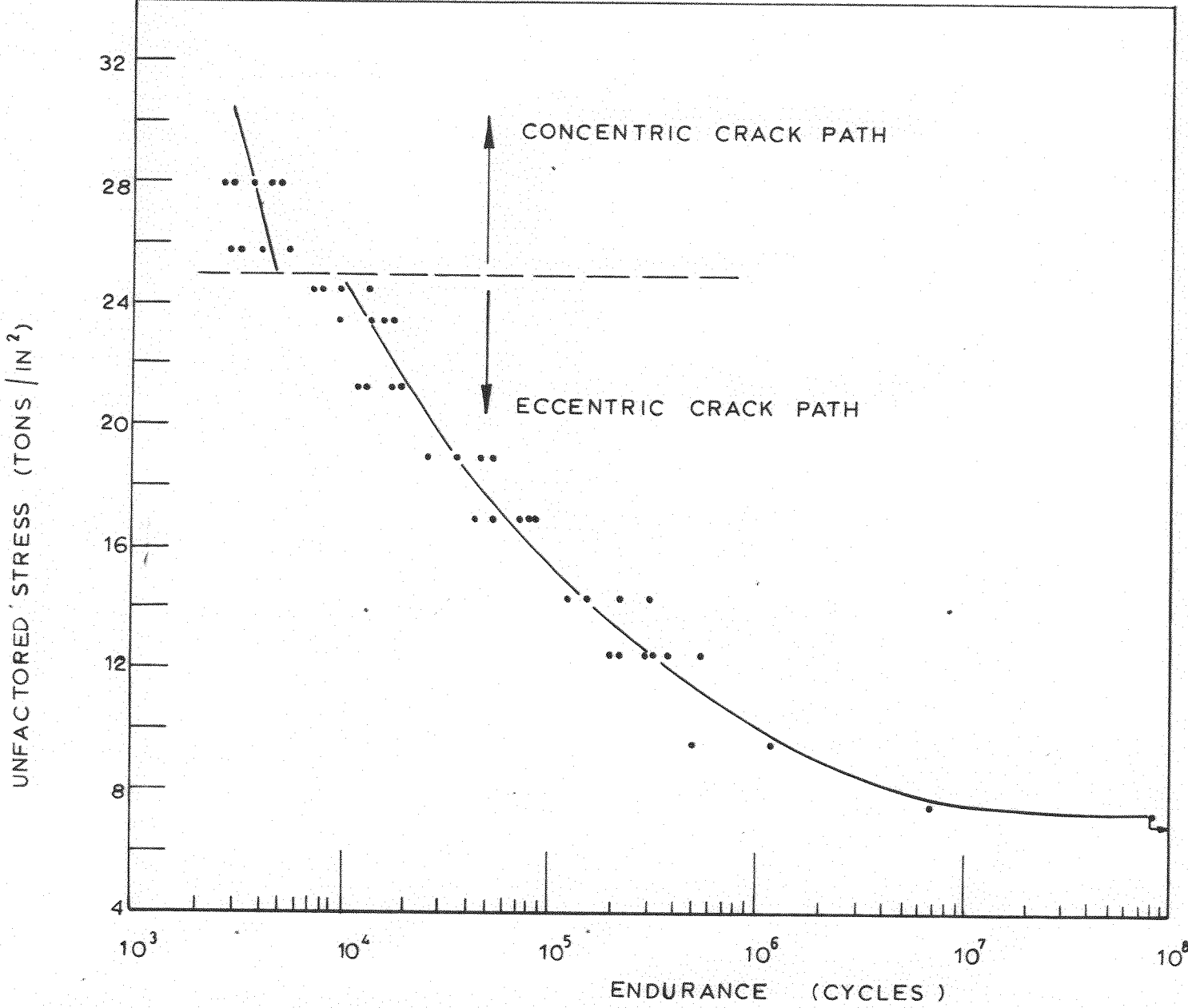

FIG.13. S/N CURVE OF 70/30 BRASS COLD STRETCHED 25 %. ROTATING CANTILEVER TESTING OF NOTCHED SPECIMENS $K_t = 3.0$. FREQ. = 80 C.P.S..

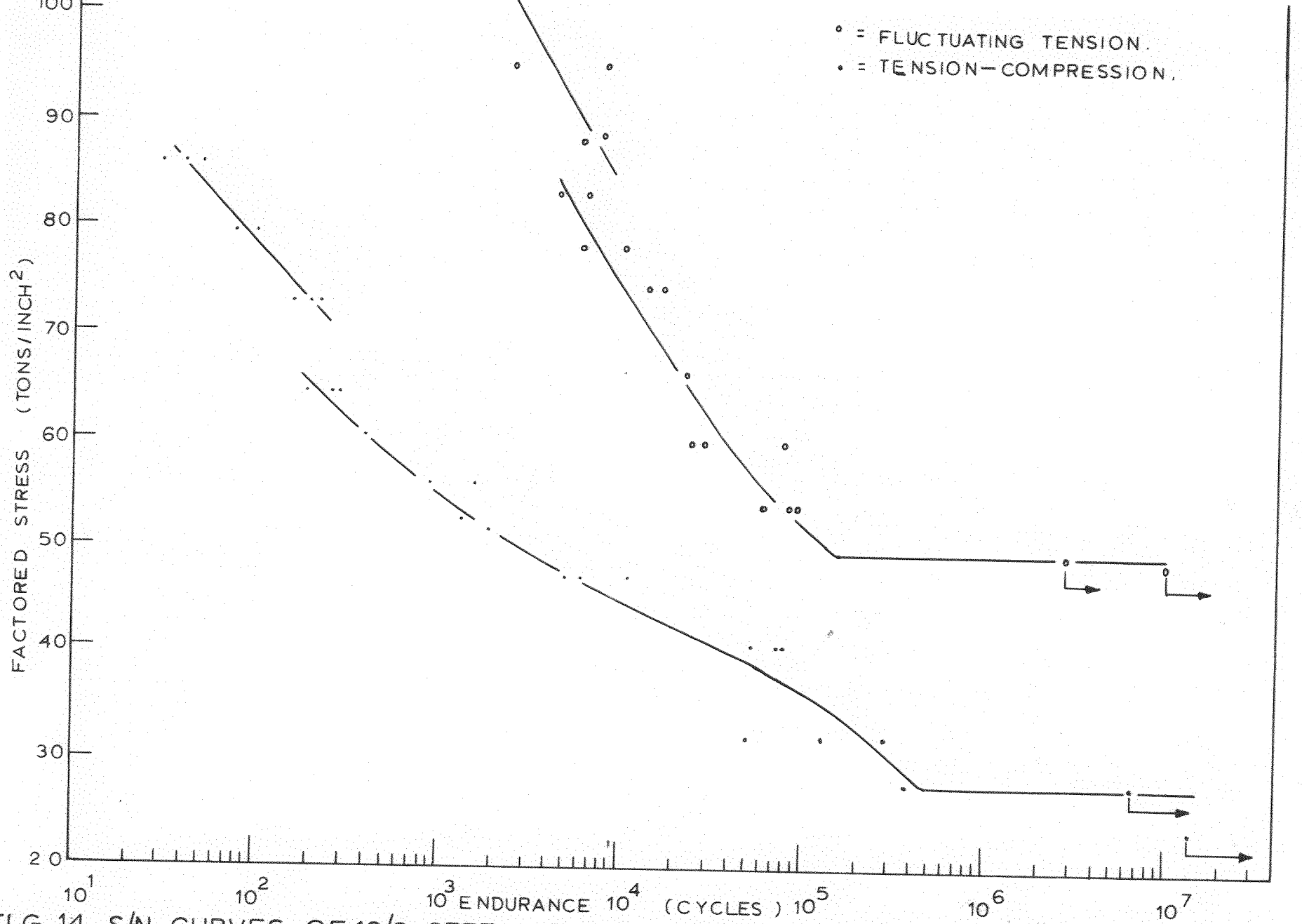

FIG. 14. S/N CURVES OF 18/8 STEEL. DIRECT STRESS TESTING OF NOTCHED SPECIMENS $K_t = 2{\cdot}37$. TENSION-COMPRESSION & FLUCTUATING TENSION. FREQ. = 50 C.P.S..

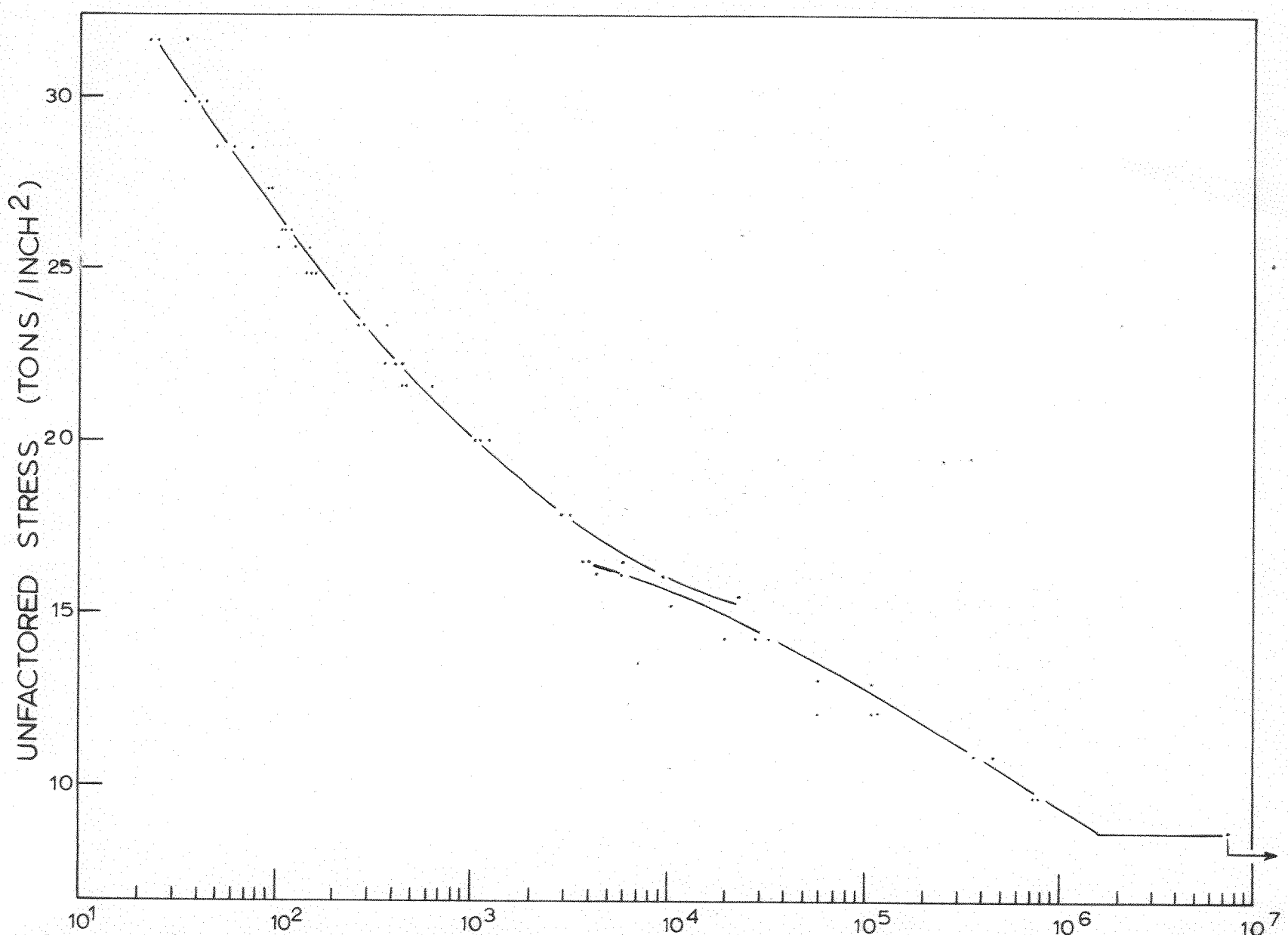

FIG. 15. S/N CURVE OF ANNEALED MILD STEEL. DIRECT STRESS TESTING OF NOTCHED SPECIMENS $K_t = 2{\cdot}5$ FREQ. = 50 C.P.S..

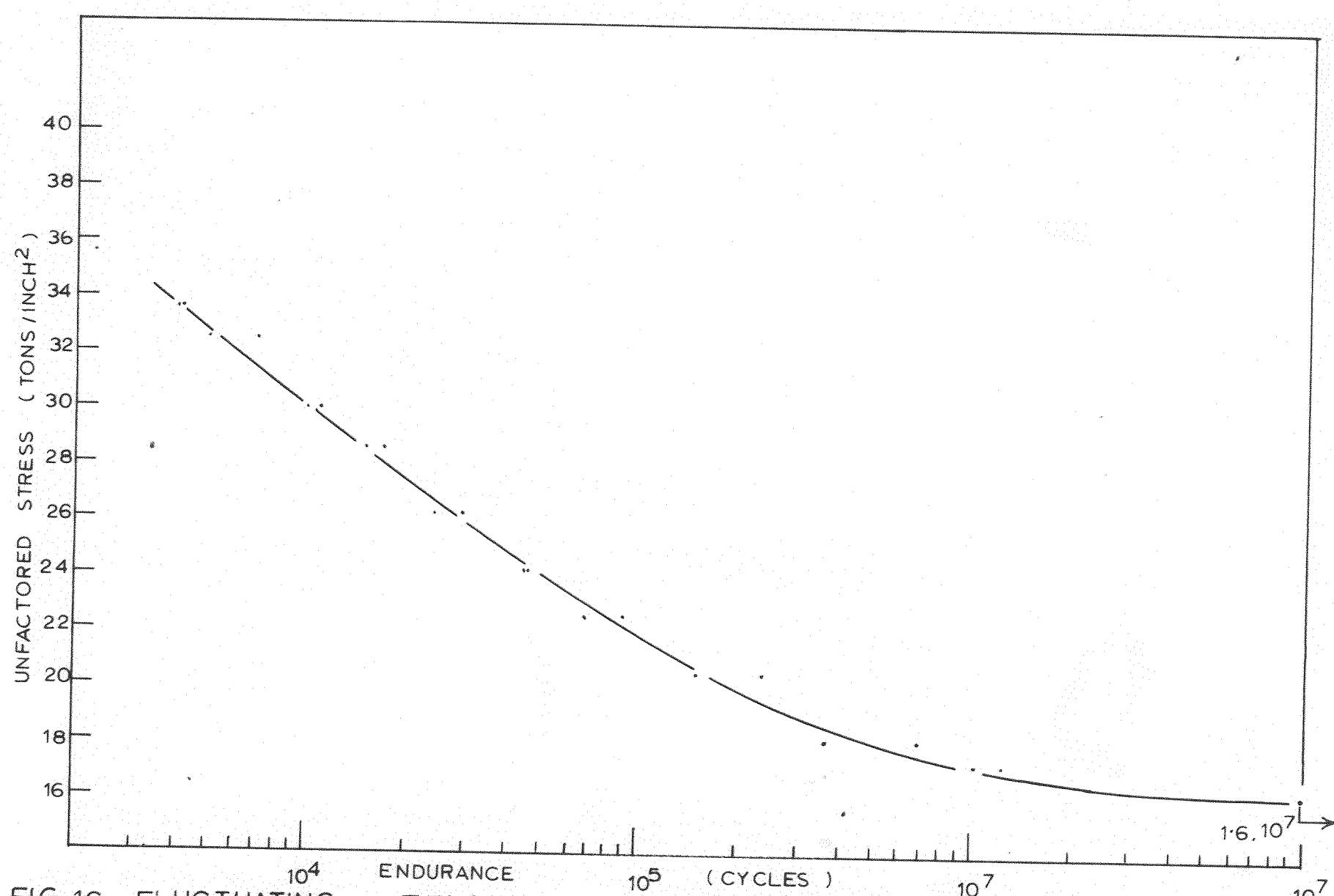

FIG. 16. FLUCTUATING TENSION TESTS OF ANNEALED MILD STEEL. DIRECT STRESS TESTING OF NOTCHED SPECIMENS $K_t = 2{\cdot}5$. FREQ. = 50 C.P.S..

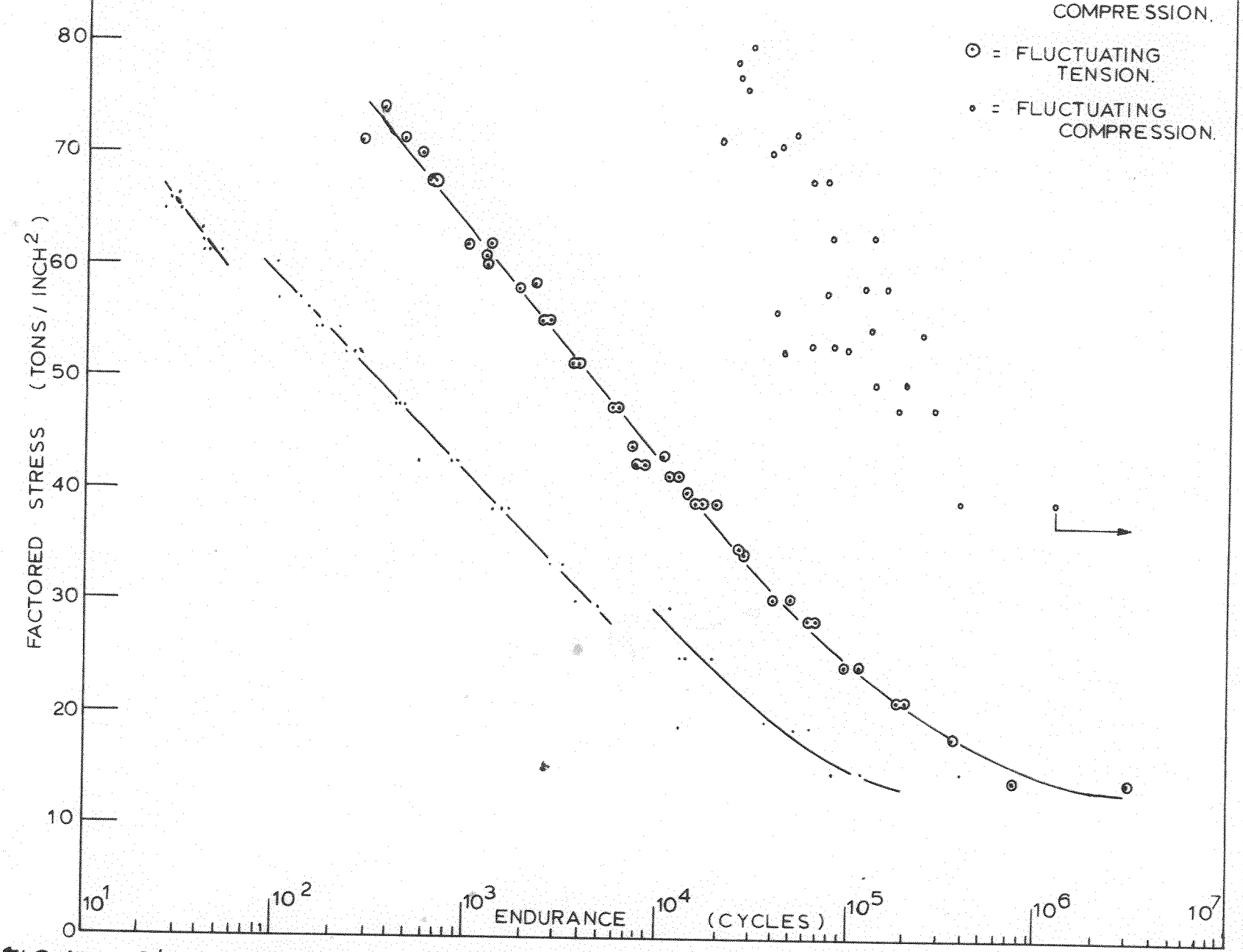

FIG. 17. S/N CURVES OF L 73 ALUMINIUM ALLOY. DIRECT STRESS TESTING OF NOTCHED SPECIMENS K_t = 2·5. FREQ. = 50 C.P.S..

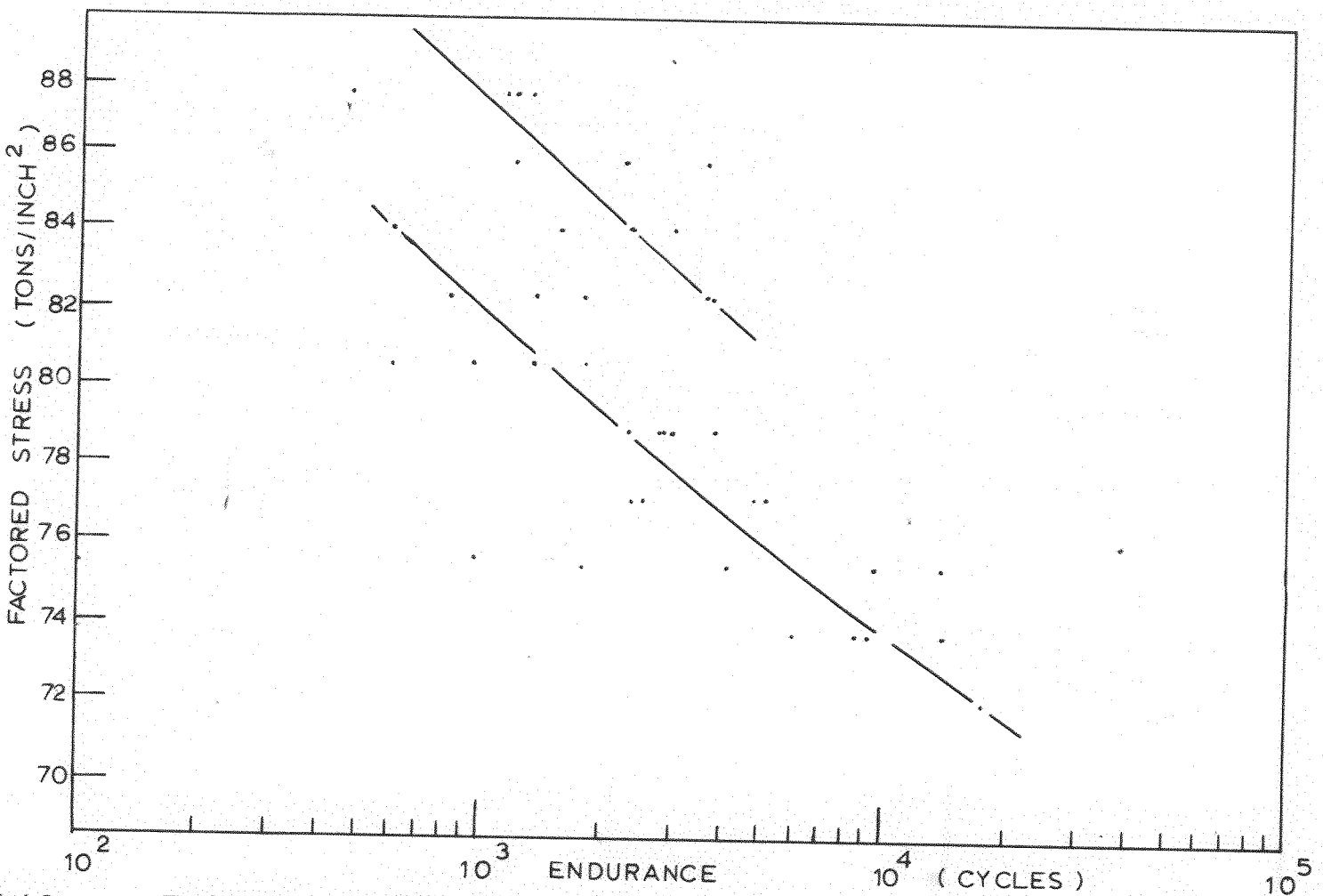

FIG.18 . FATIGUE TESTS OF 18/8 STEEL AT -80°C. FREQ. =120 C.P.S.. DIRECT STRESS TESTING OF NOTCHED SPECIMENS $K_t = 2{\cdot}37$.

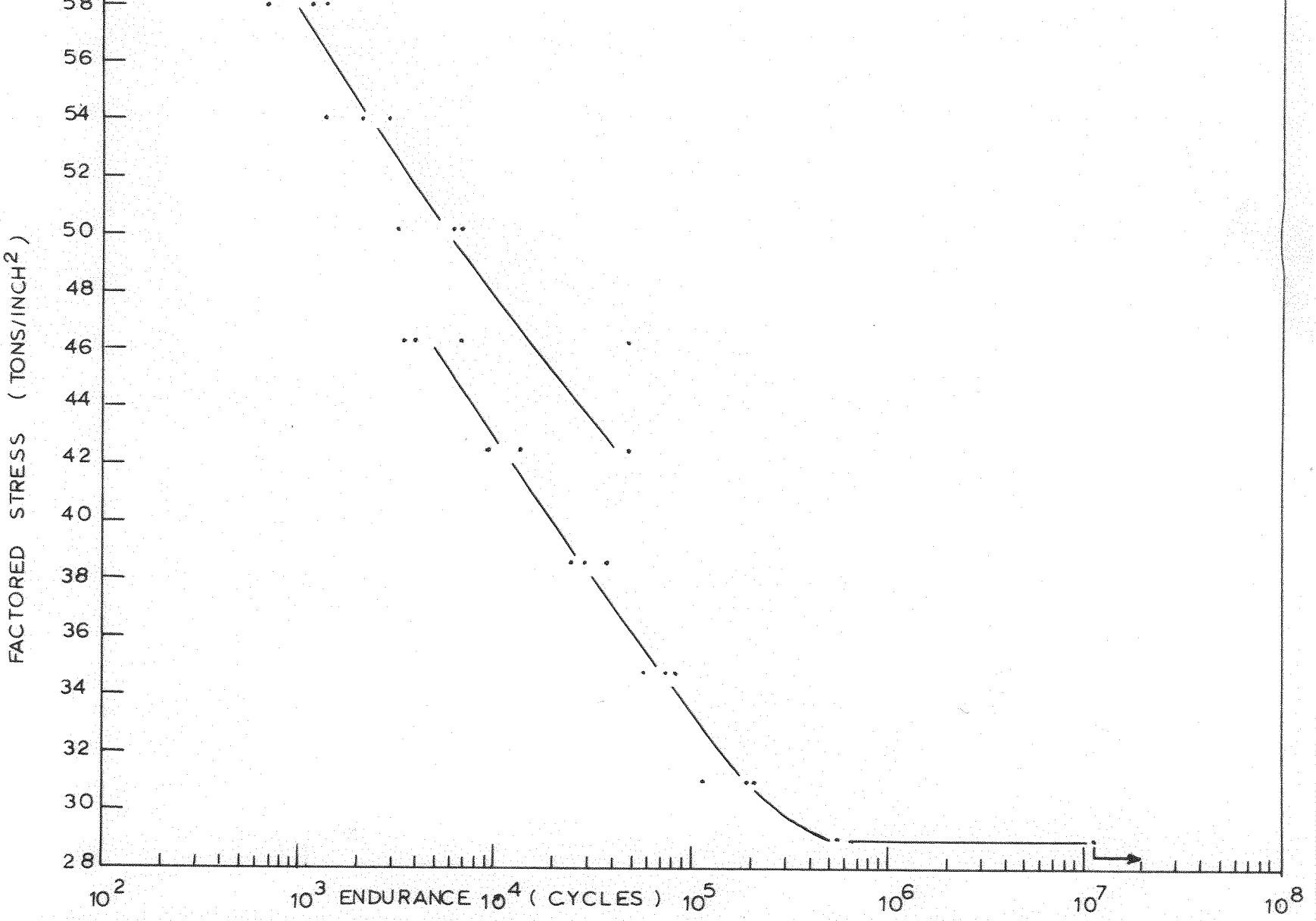

FIG.19. S/N CURVE OF ANNEALED 18/8 STEEL. DIRECT STRESS TESTING OF NOTCHED SPECIMENS $K_t = 2{\cdot}37$ TEMPERATURE = 250° C. FREQ.=120 C.P.S..

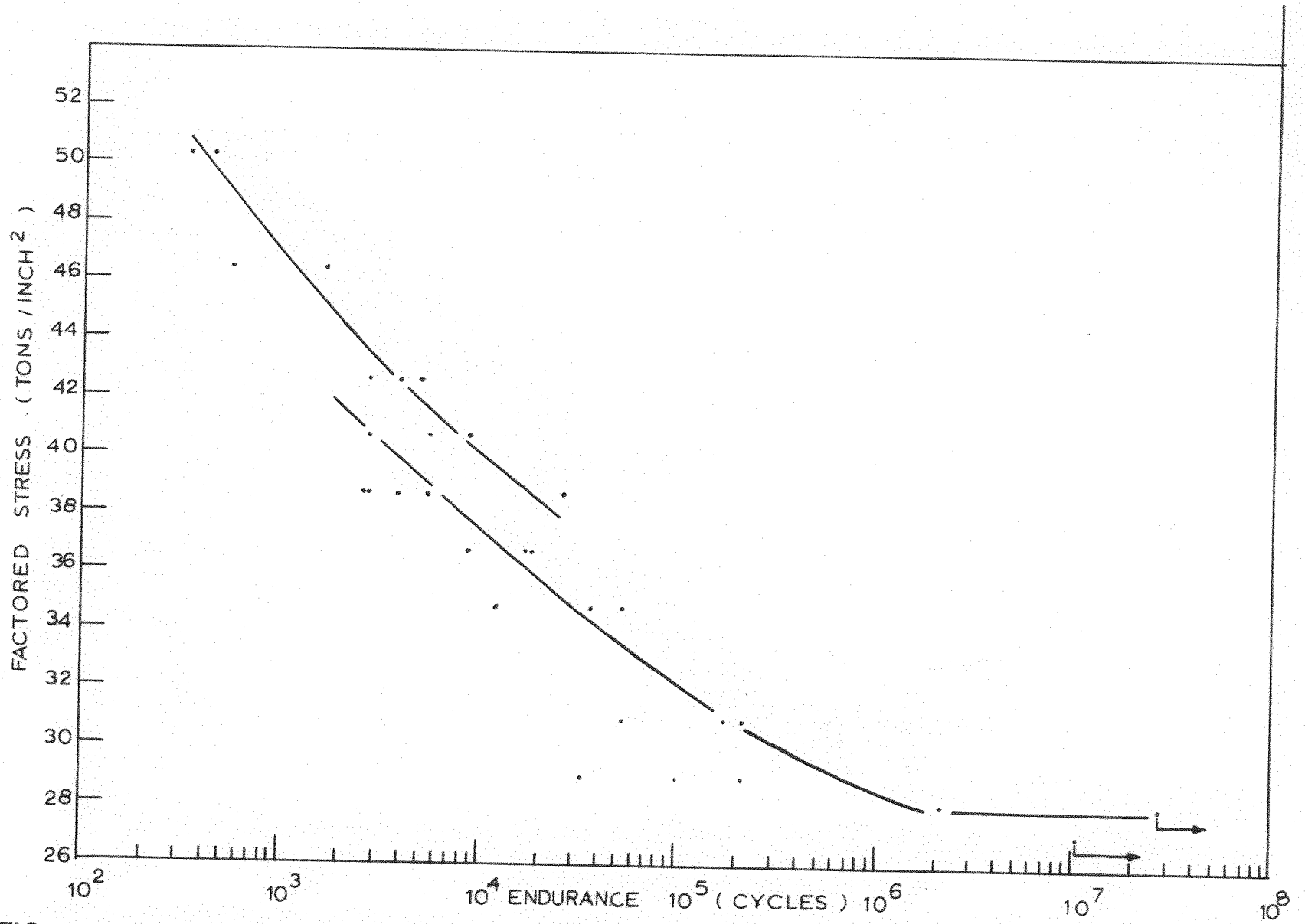

FIG. 20. S/N CURVE OF ANNEALED 18/8 STEEL. DIRECT STRESS TESTING OF NOTCHED SPECIMENS $K_t = 2{\cdot}37$. TEMPERATURE = 350°C. FREQ. = 120 C.P.S..

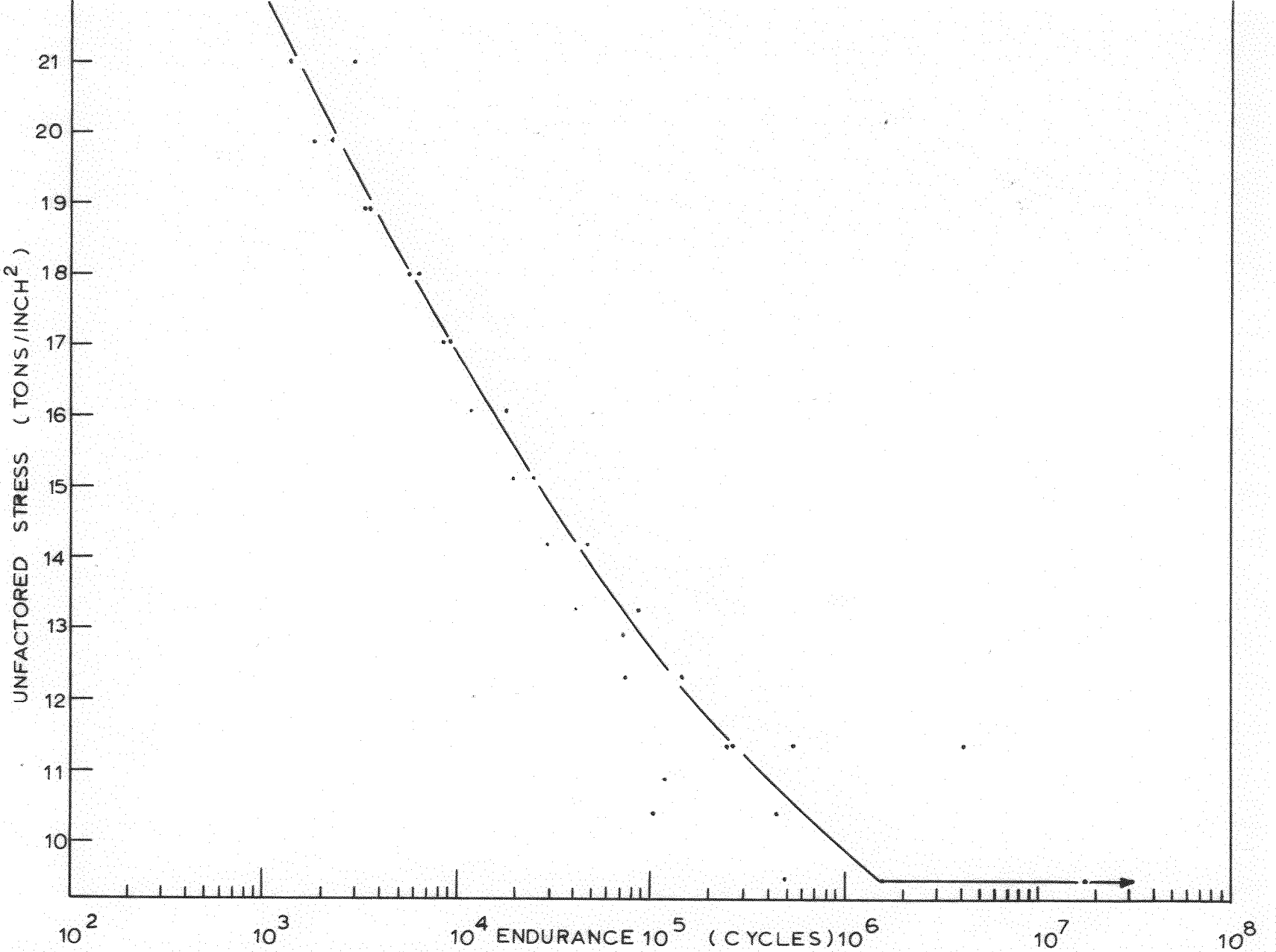

FIG. 21. S/N CURVE OF ANNEALED MILD STEEL. DIRECT STRESS TESTING OF NOTCHED SPECIMENS K_t=2·5 TEMPERATURE=350°C. FREQ.=120 C.P.S..

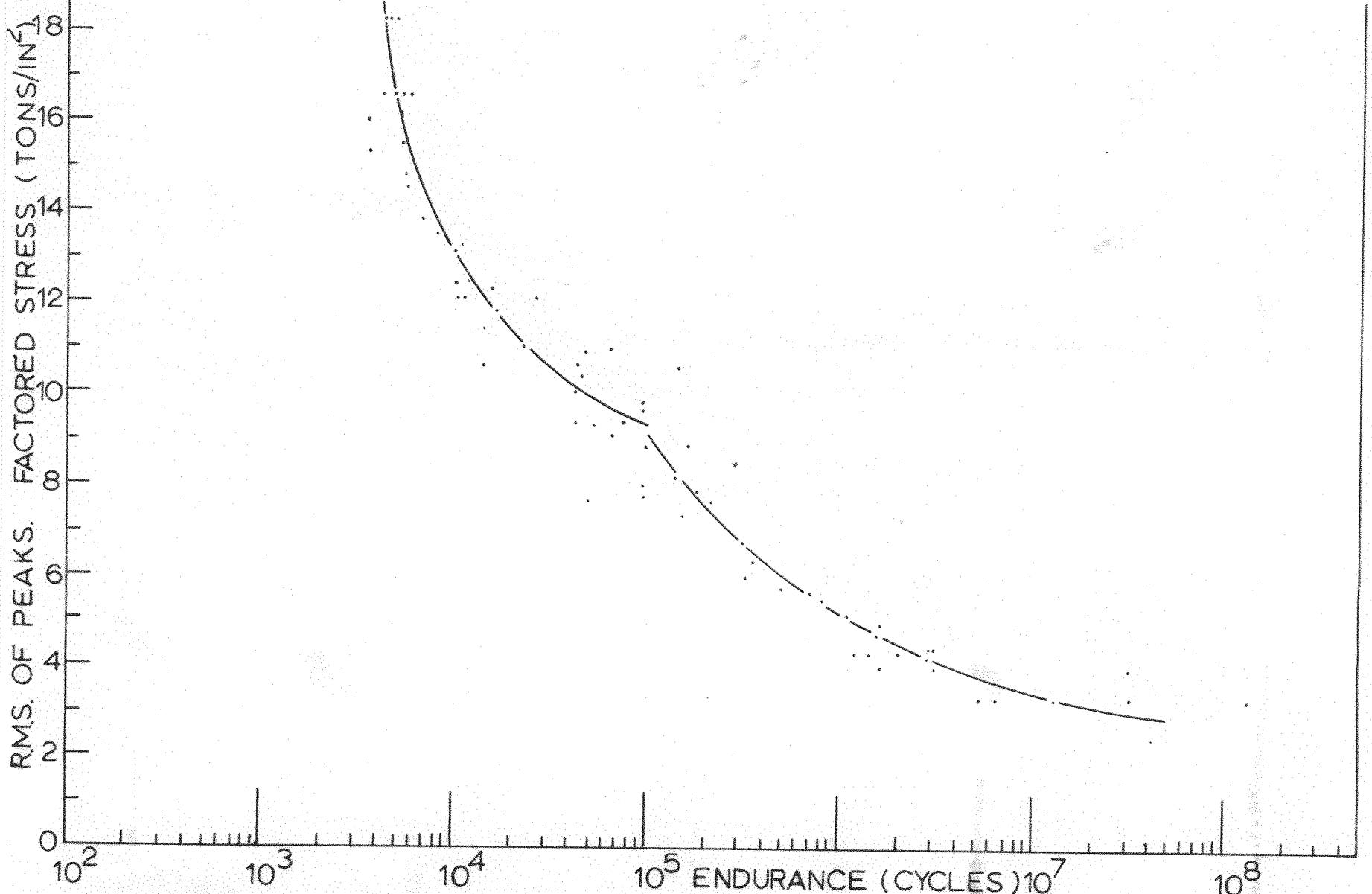

FIG. 22 . RANDOM LOADING FATIGUE TESTS OF L73 ALUMINIUM ALLOY. DIRECT STRESS TESTING OF NOTCHED SPECIMENS $K_t = 2{\cdot}5$. FACTORED STATIC MEAN LOAD = 15 TONS/INCH FREQ. = 90 CYCLES / SEC.

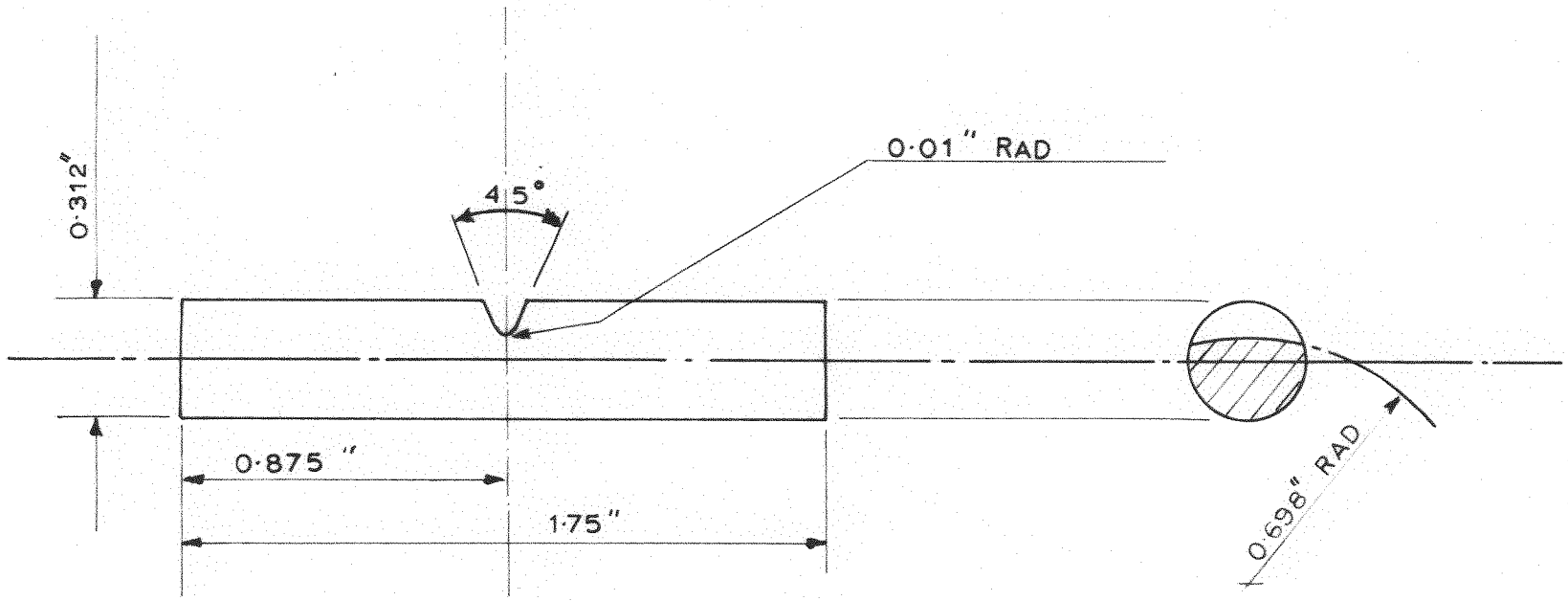

FIG. 23. HOUNSFIELD IMPACT SPECIMEN.

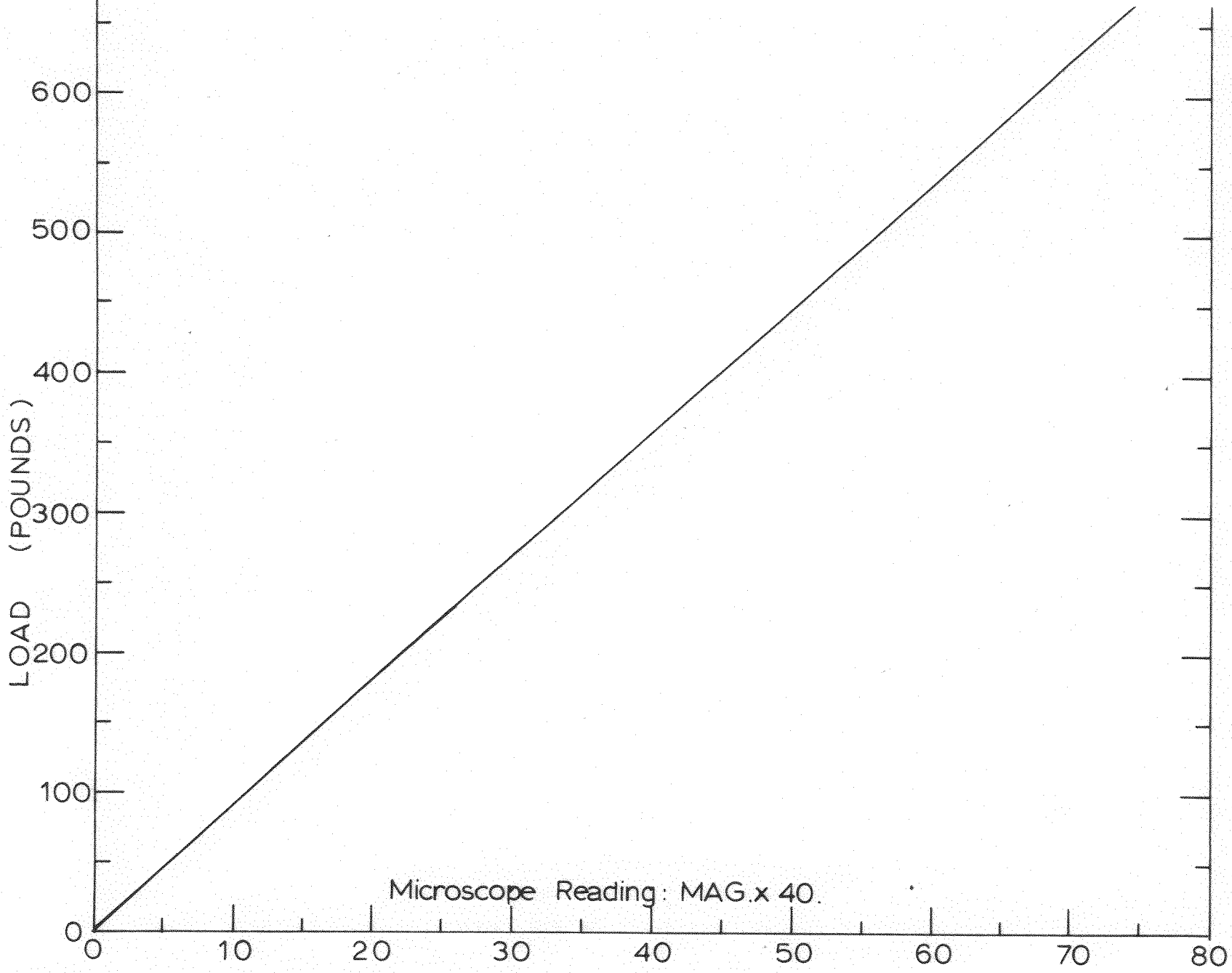

FIG. 24. CALIBRATION OF AVERY MIDGET PULSATOR.

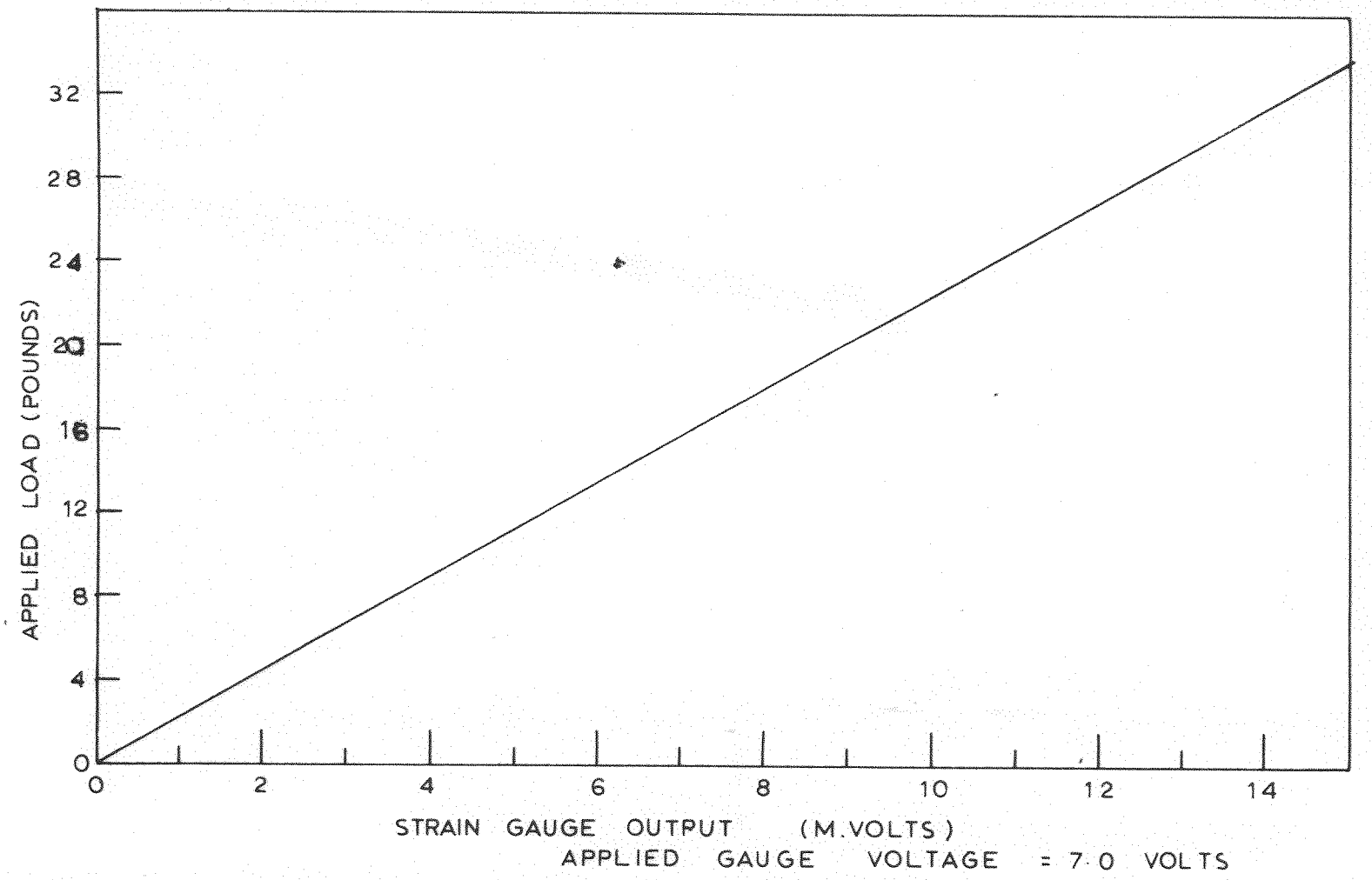

FIG. 25. CALIBRATION OF STRAIN GAUGES OF RANDOM LOADING FATIGUE MACHINE.

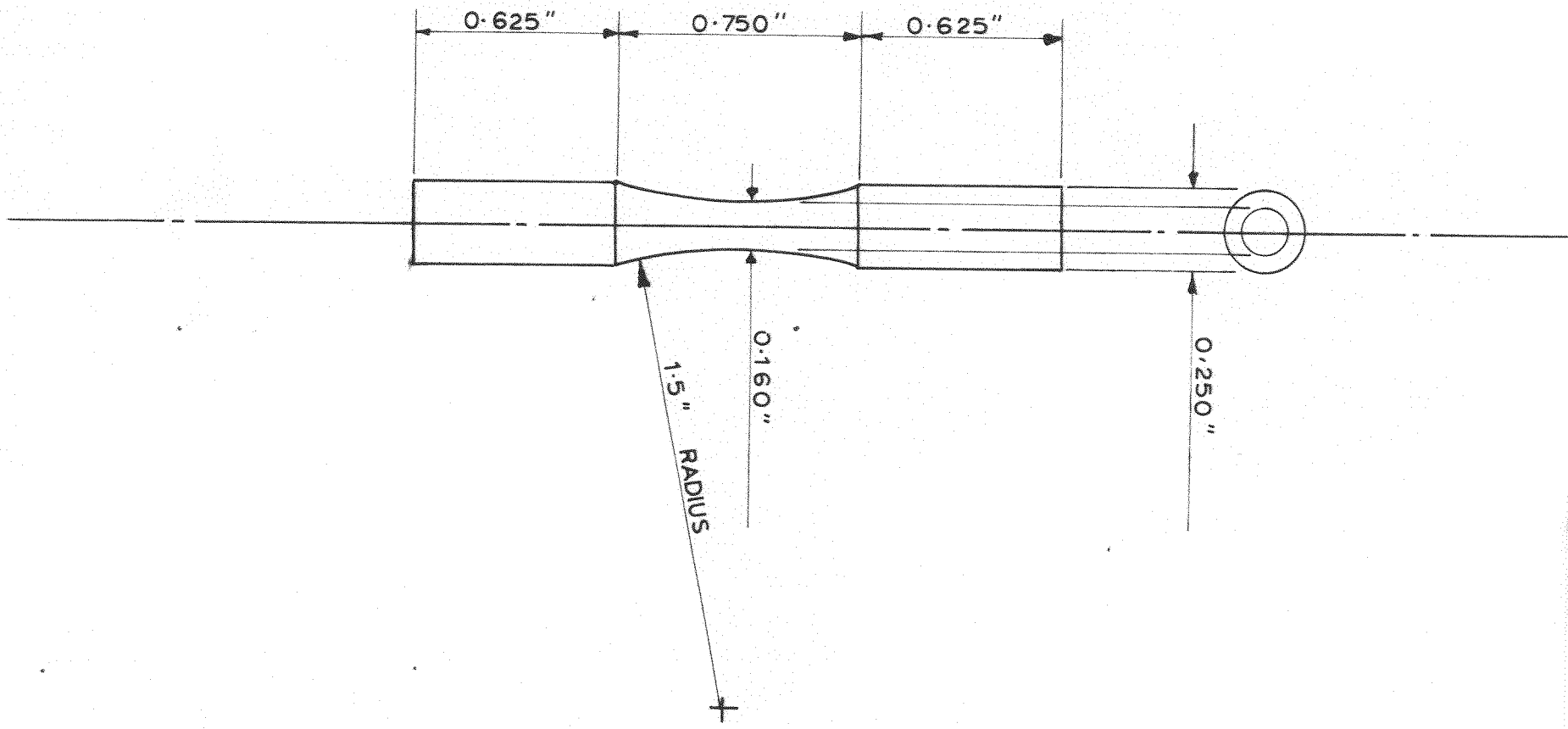

FIG. 26(a). ROLLS ROYCE PLAIN FATIGUE SPECIMEN

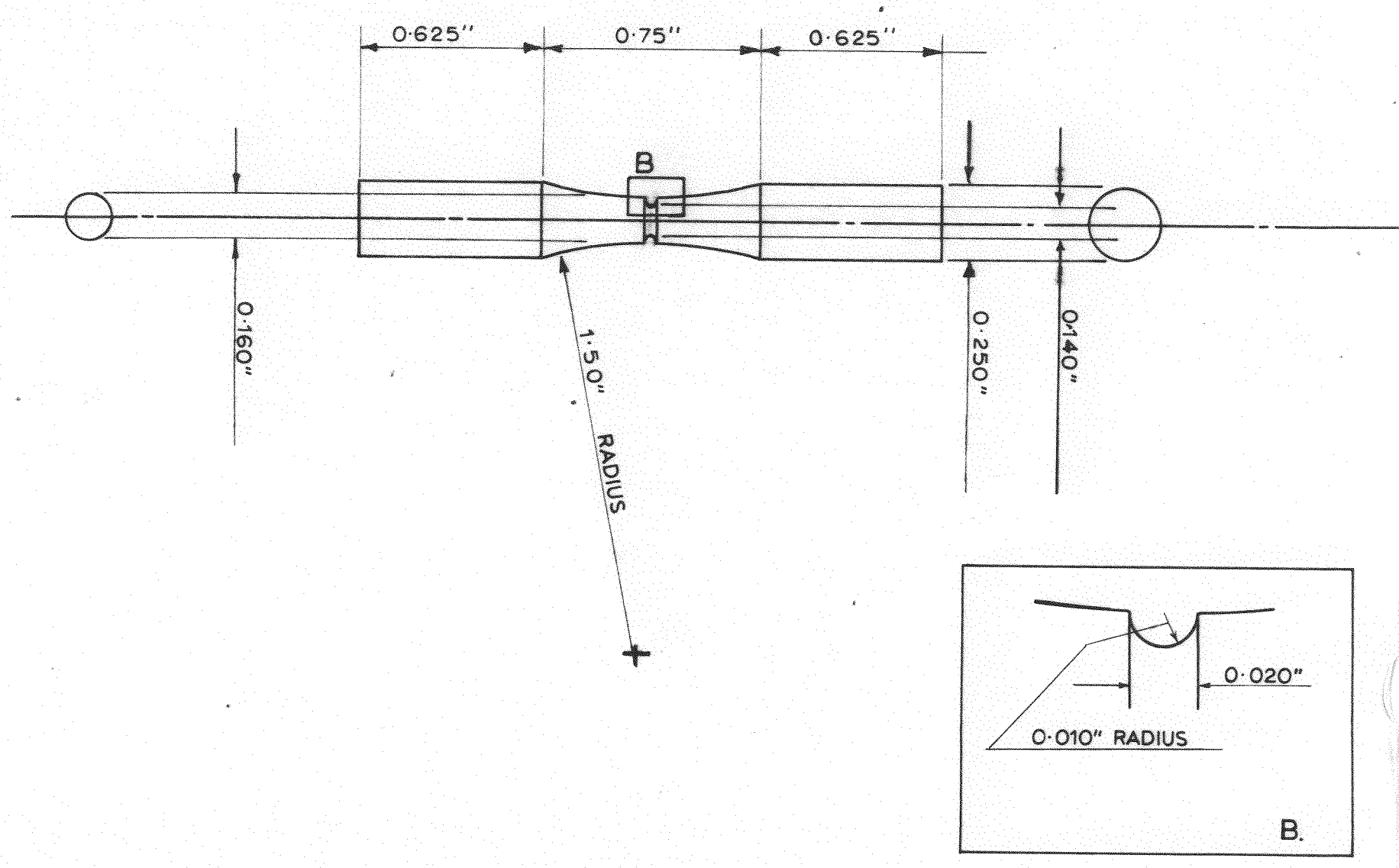

FIG. 26(b). ROLLS ROYCE NOTCED FATIGUE SPECIMEN $K_t = 2{\cdot}0$.

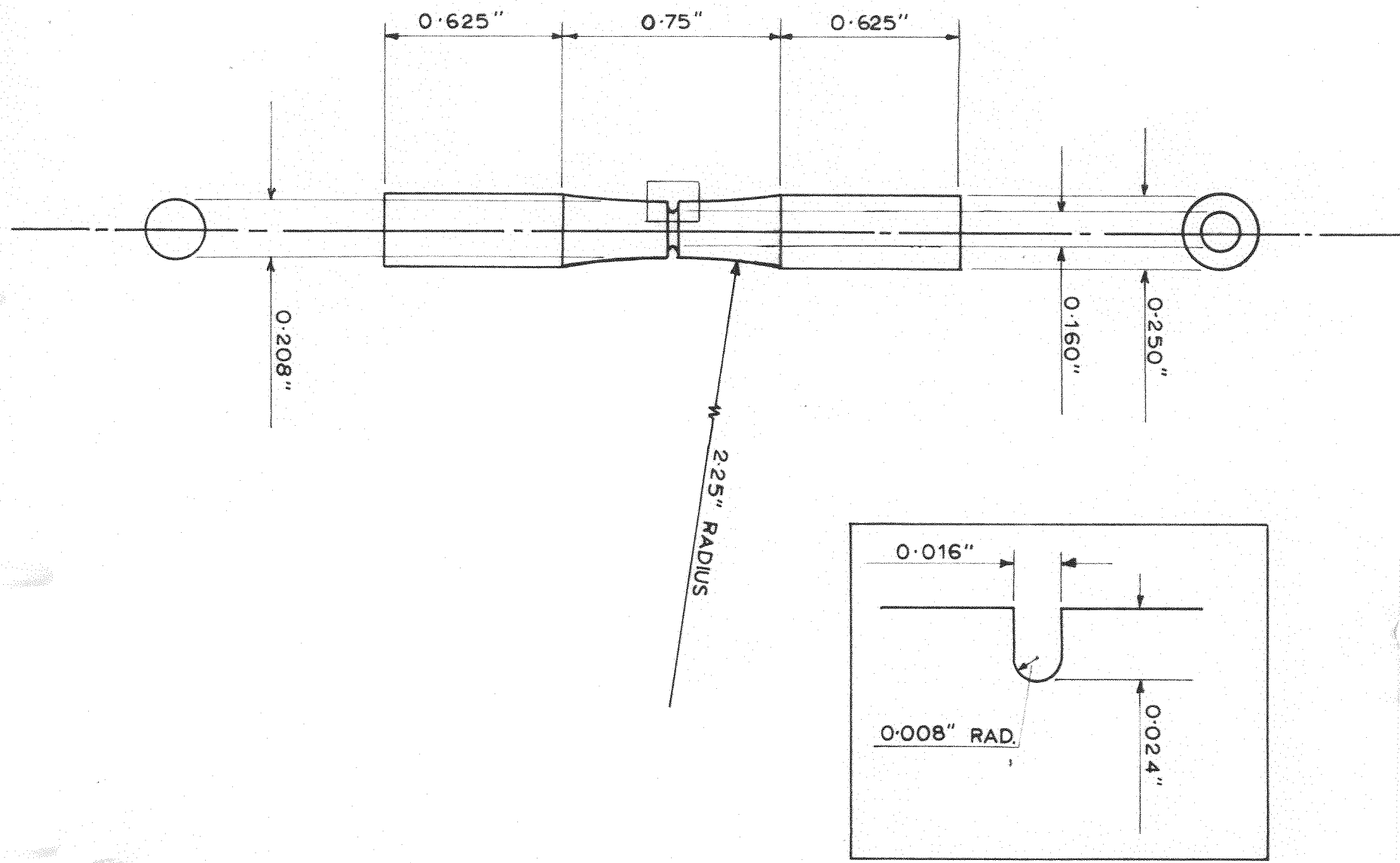

FIG. 26(c). ROLLS ROYCE NOTCHED FATIGUE SPECIMEN $K_t = 3.0$.

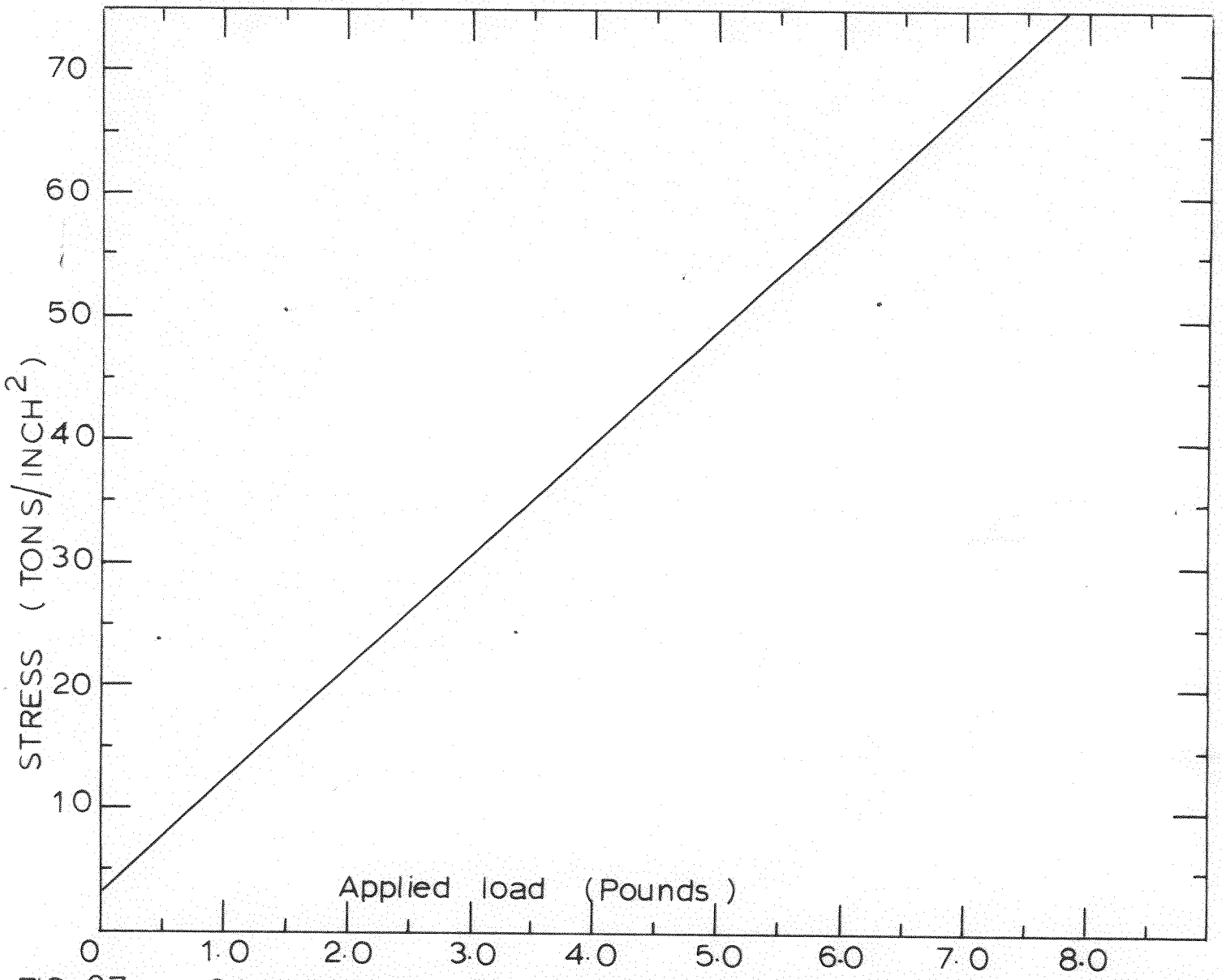

FIG. 27. CALIBRATION OF ROLLS ROYCE ROTATING CANTILEVER FATIGUE MACHINE FOR SPECIMENS SHOWN IN FIG. 26 (a).

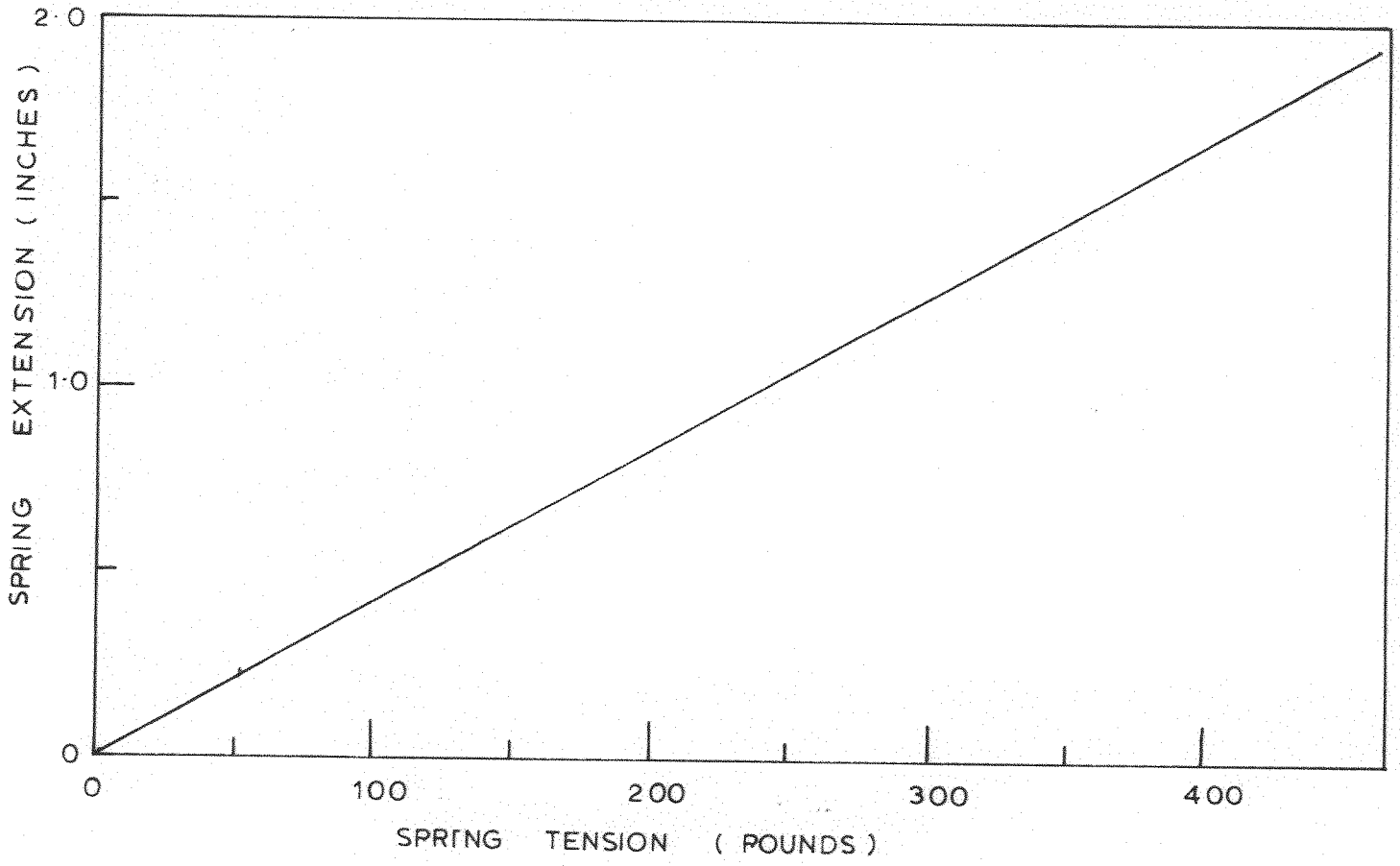

FIG. 28 CALIBRATION OF SPRING OF RESONANT BEAM FATIGUE MACHINE.

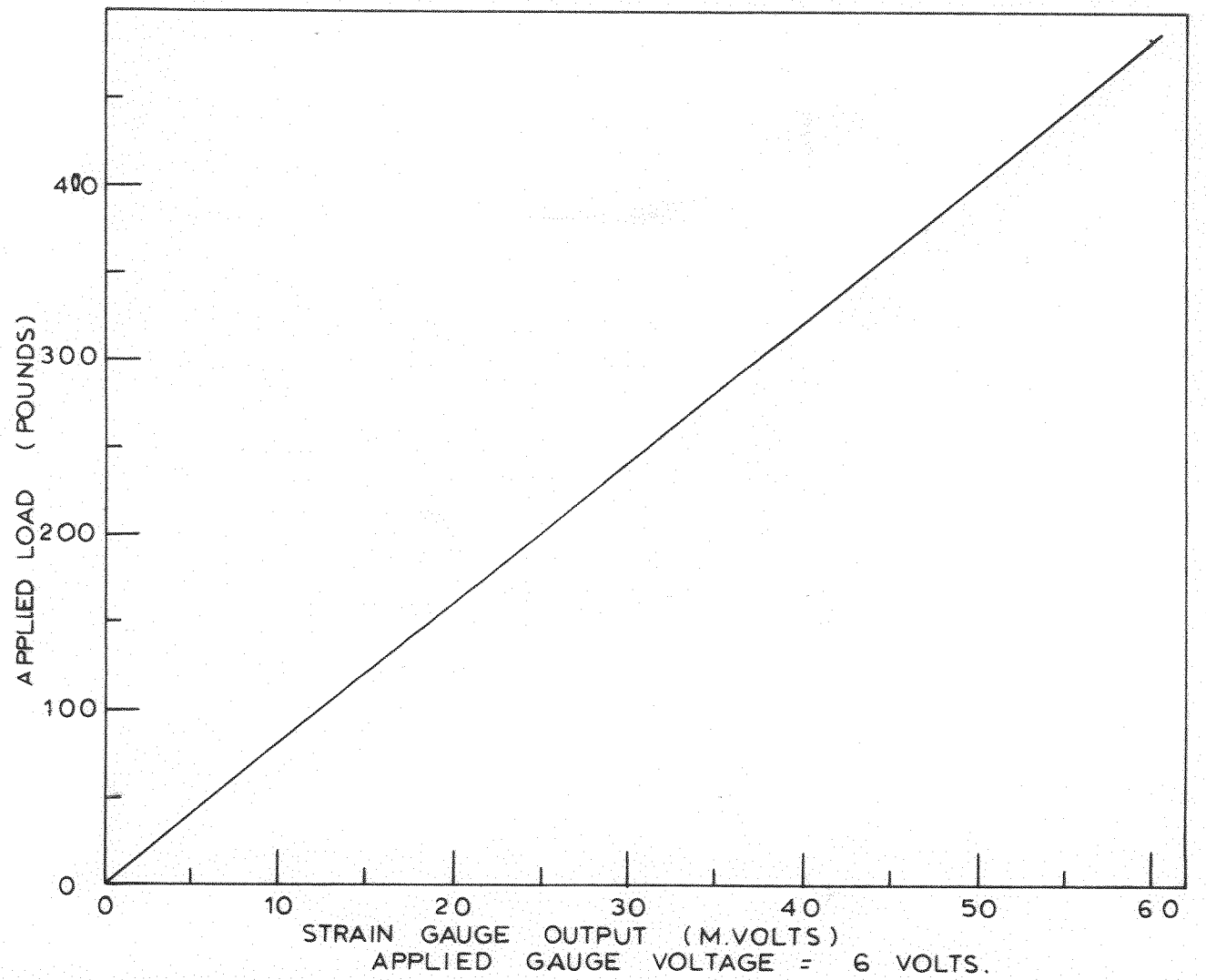

FIG. 29. CALIBRATION OF STRAIN GAUGES OF RESONANT BEAM FATIGUE MACHINE.

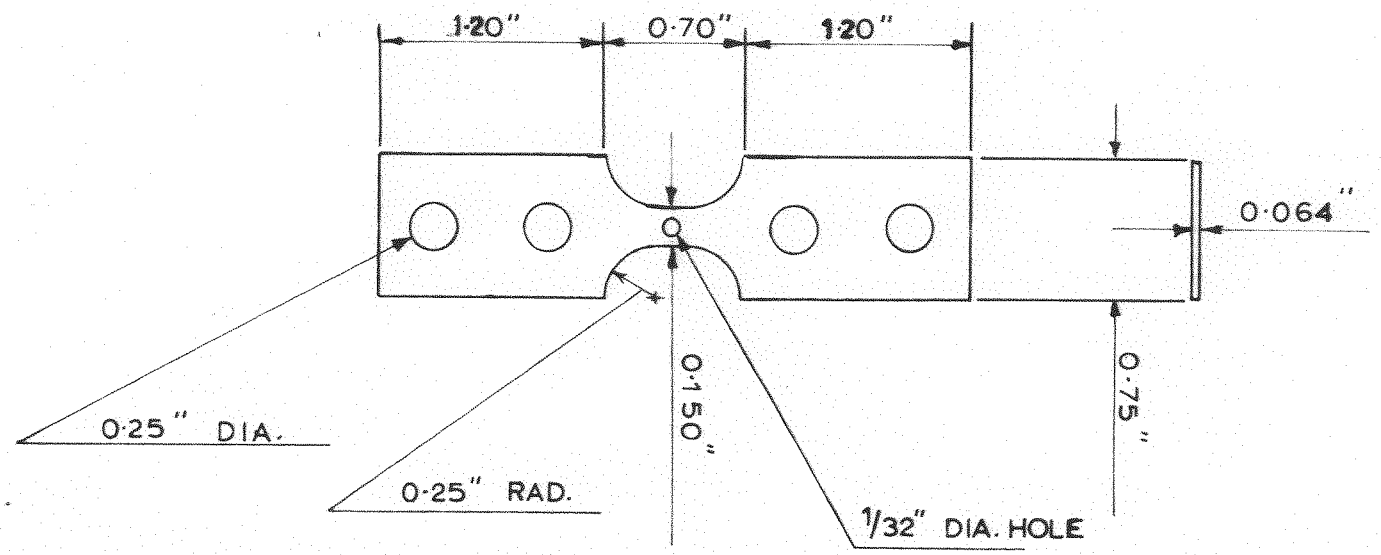

(a) $K_t = 2{\cdot}5$

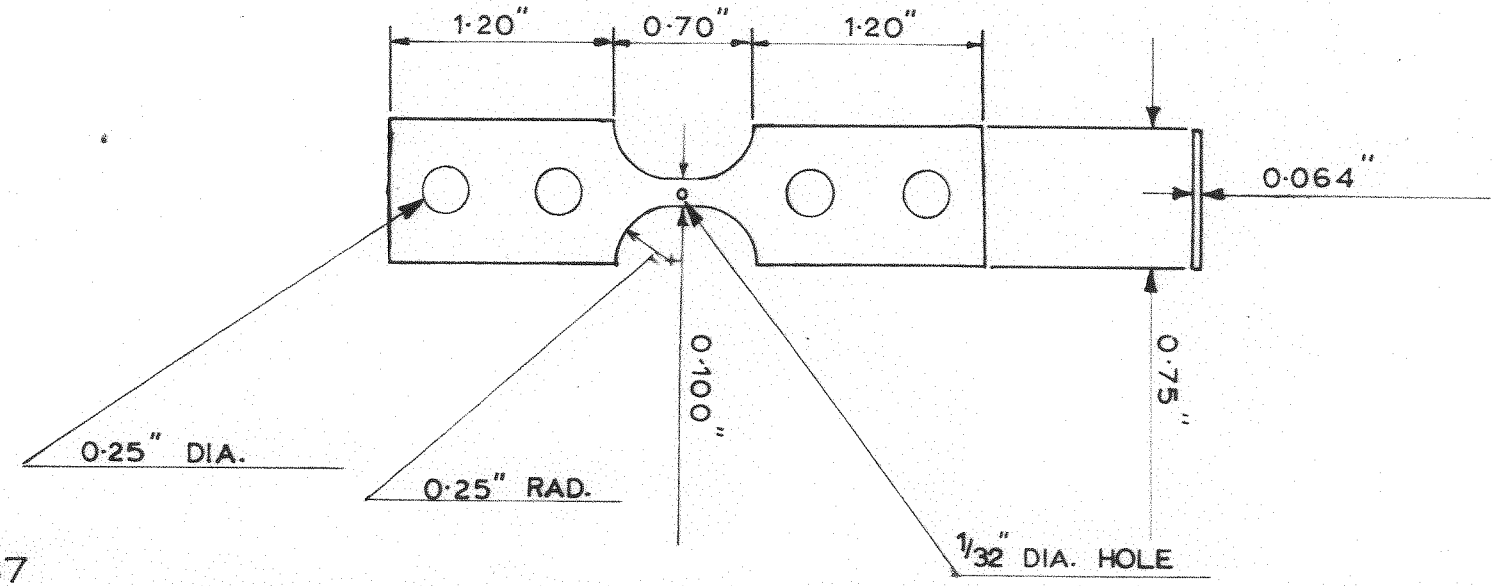

(b) $K_t = 2{\cdot}37$

FIG. 30. DIRECT STRESS SPECIMENS.

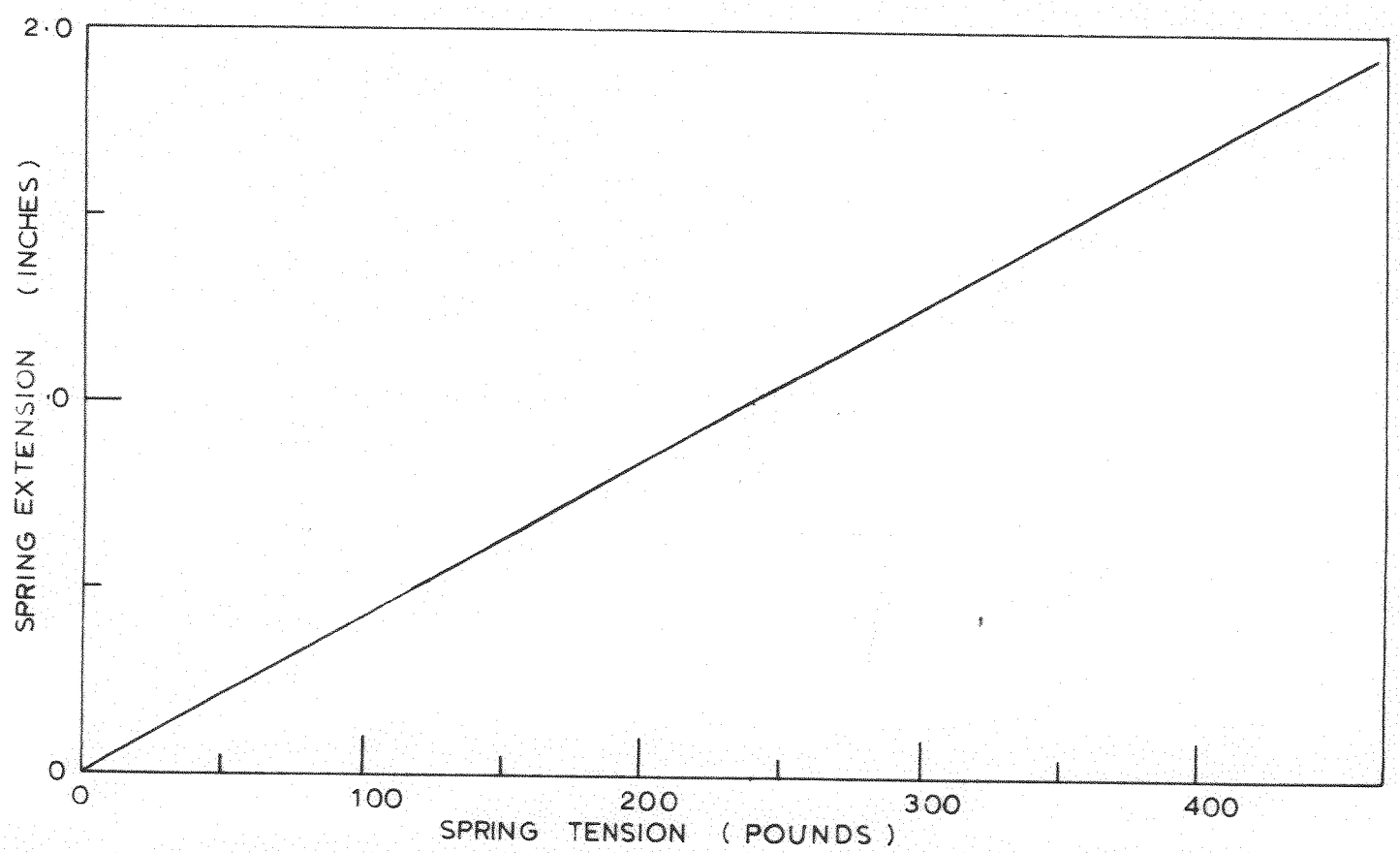

FIG. 31. CALIBRATION OF SPRING OF RANDOM LOADING FATIGUE MACHINE.

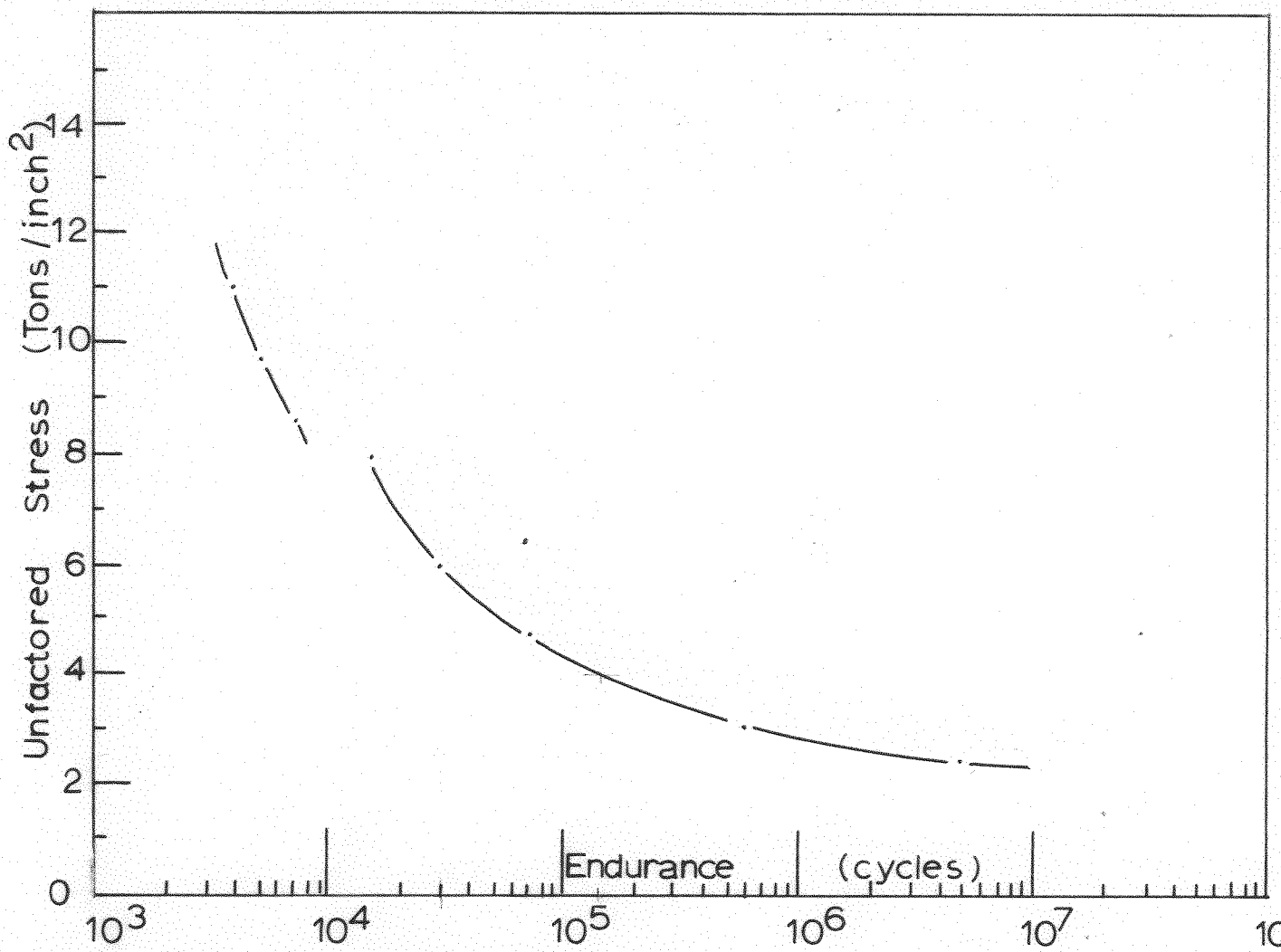

FIG. 32. S/N CURVE OF L73 ALUMINIUM ALLOY. DIRECT STRESS TESTING OF NOTCHED SPECIMENS $K_t = 2{\cdot}5$ FREQ. = 90 C.P.S.. FACTORED STATIC MEAN LOAD = 15 TONS/INCH^2

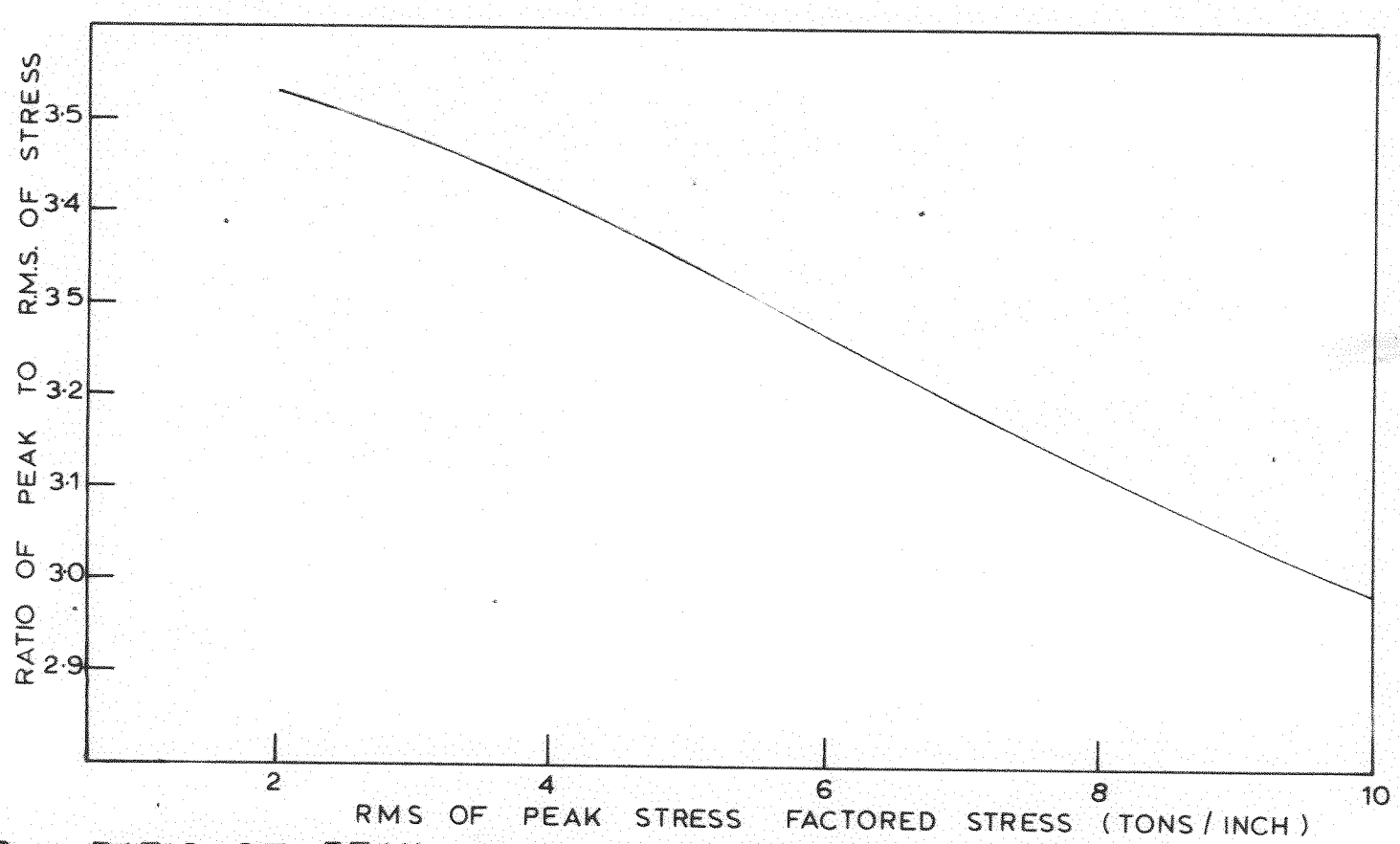

FIG. 33. RATIO OF PEAK TO R.M.S. OF STRESS AGAINST FACTORED R.M.S. OF PEAK STRESS.

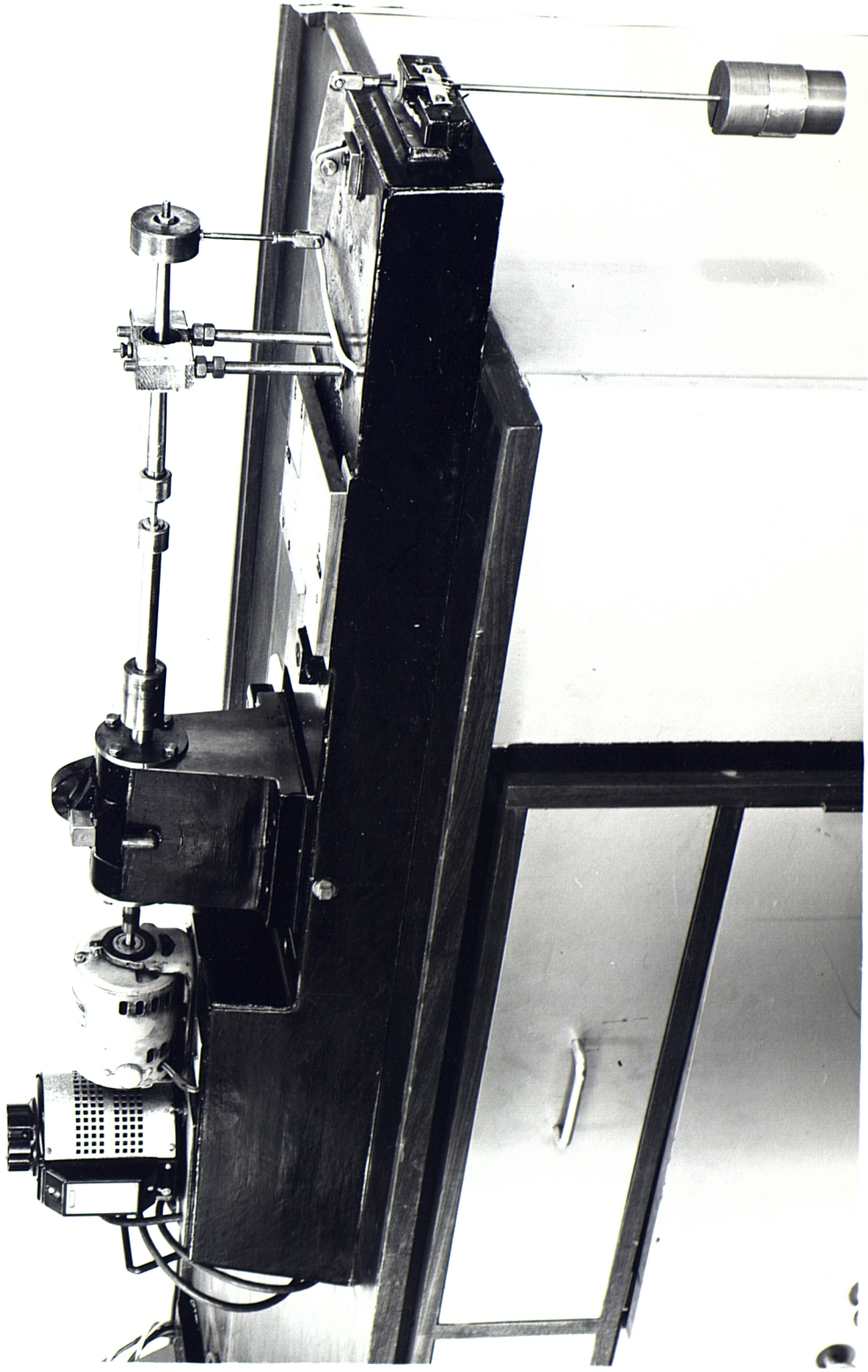

Plate I

Rolls Royce Rotating Cantilever Fatigue Machine.

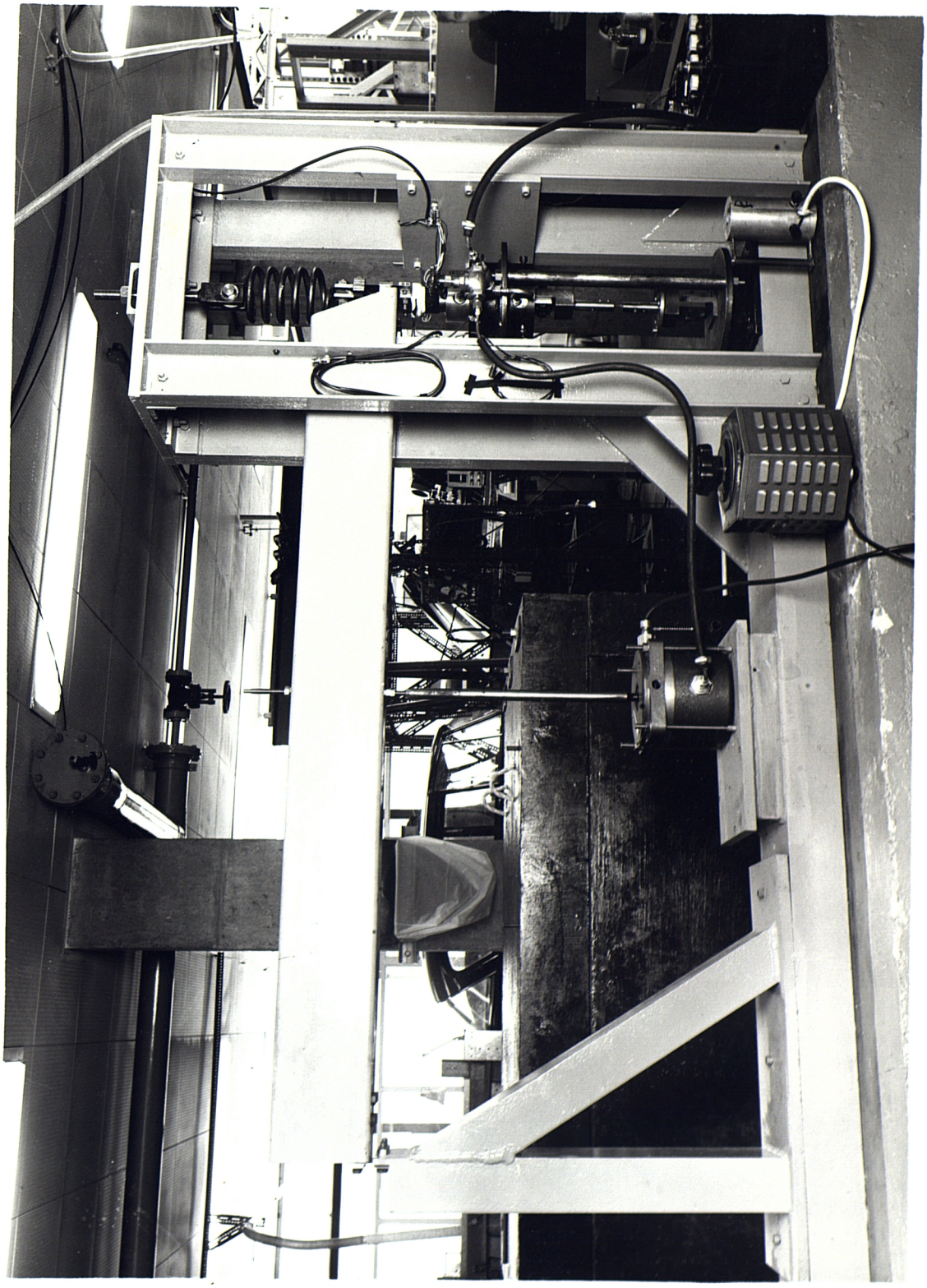

Plate II

Resonant Beam Fatigue Machine (120 c./sec.)

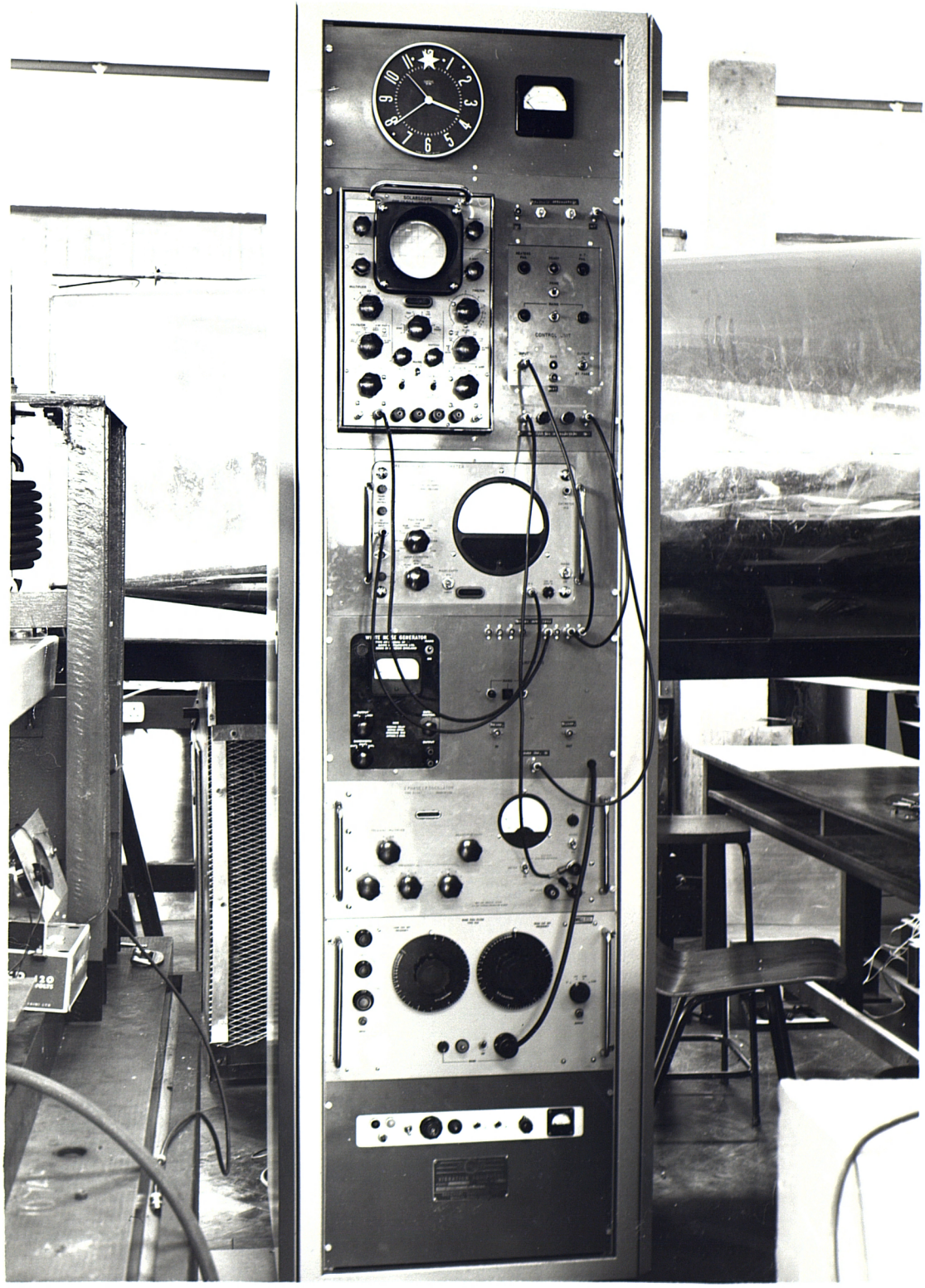

Plate III

Control Cabinet for Resonant Machine.

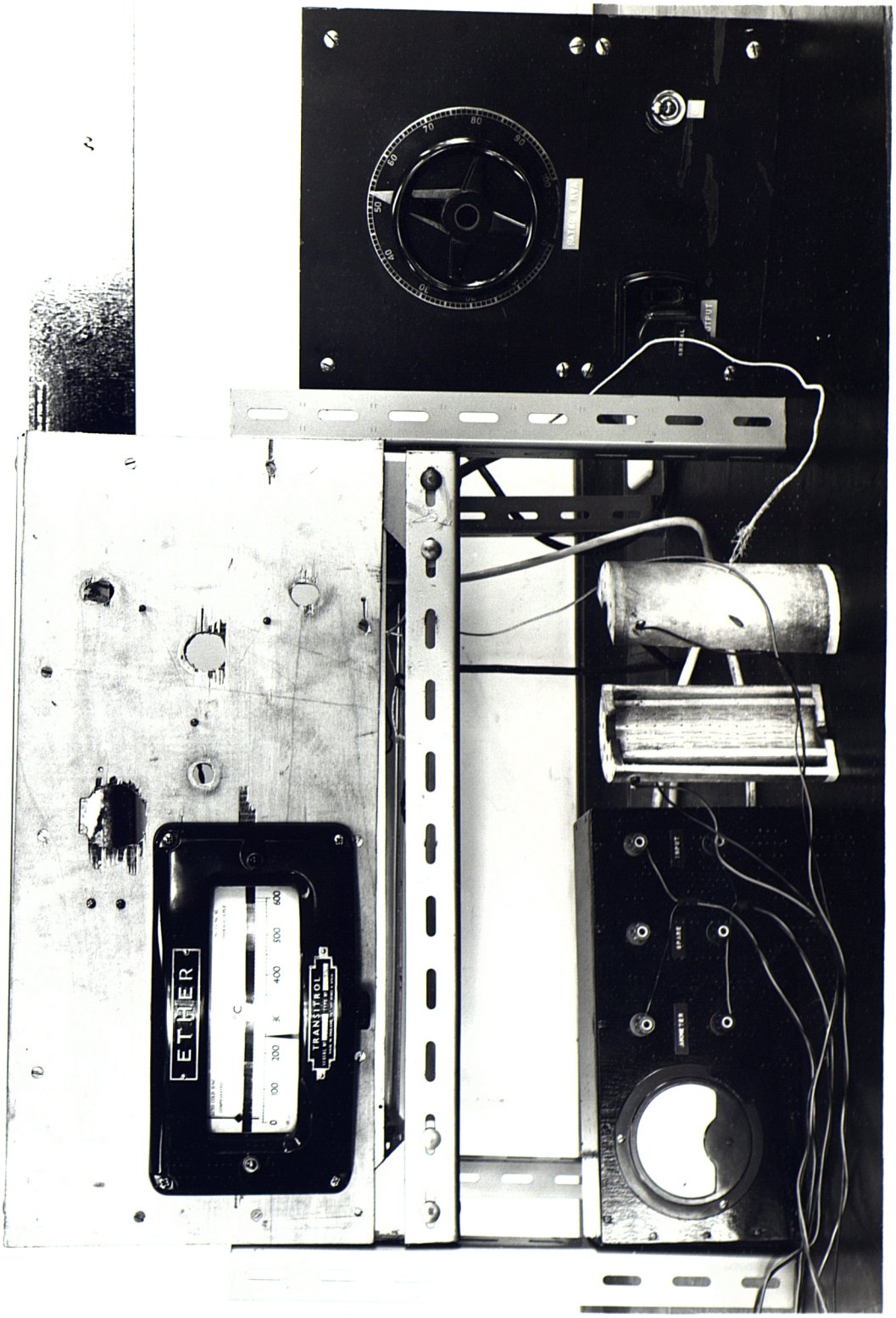

Plate IV

Electric Furnace and Controls.

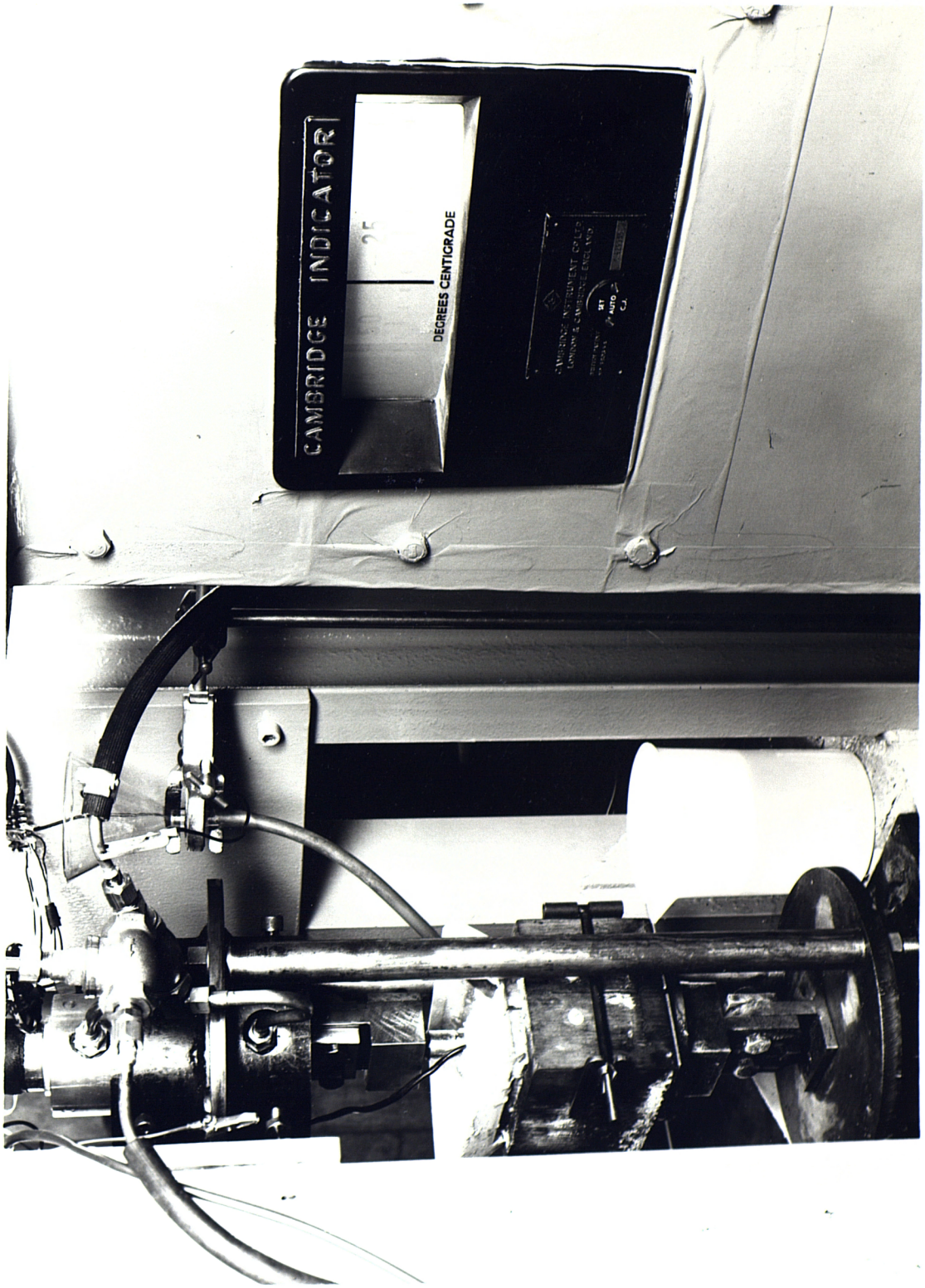

Plate V.

Ice Box.

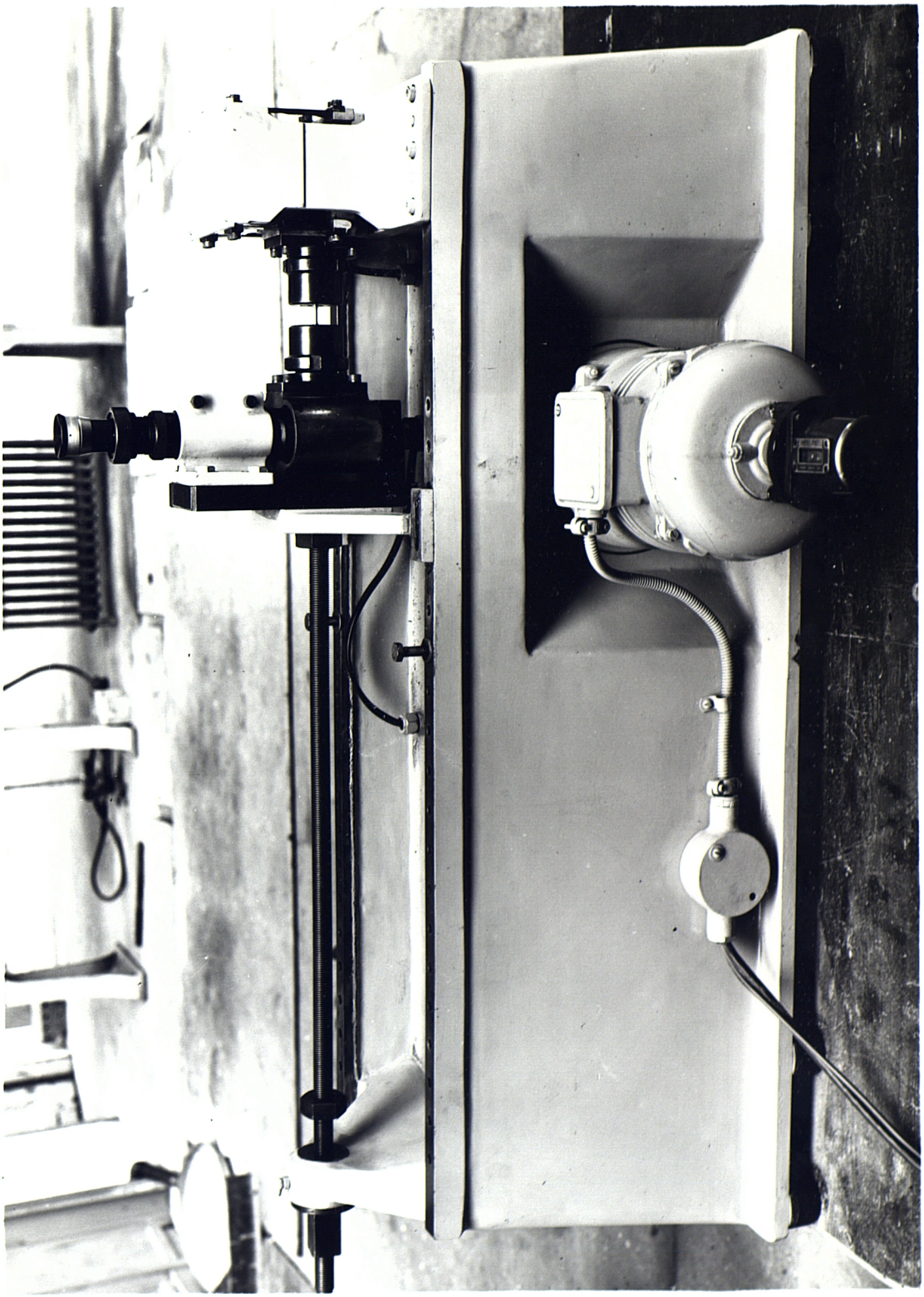

Plate VI

Avery Midget Pulsator.

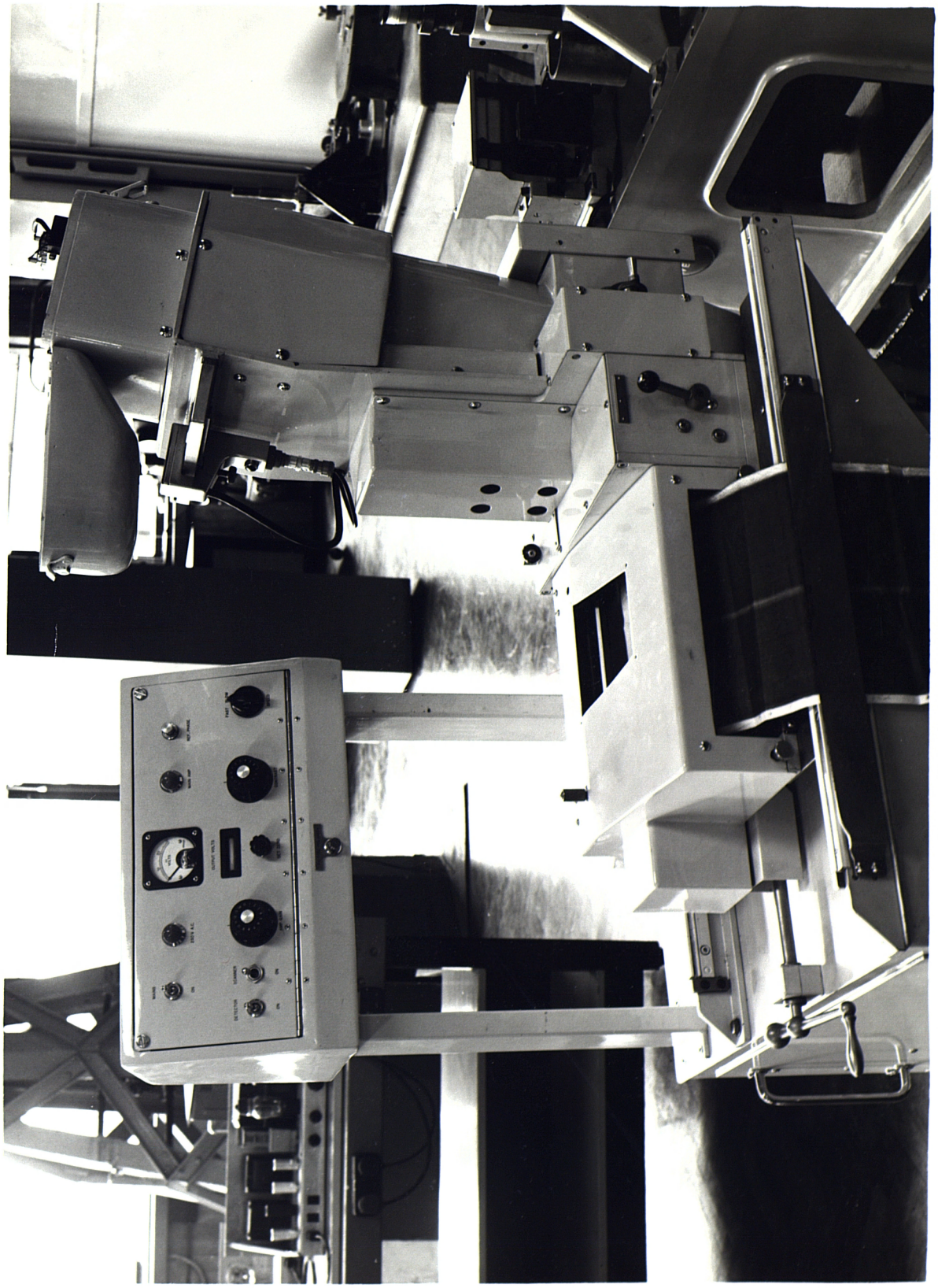

Plate VII

Infra Red Camera

Plate VIII

Infra Red Camera

Plate IX

Hounsfield Impact Test Specimens. -196°C (left), -50°C (middle), +100°C.

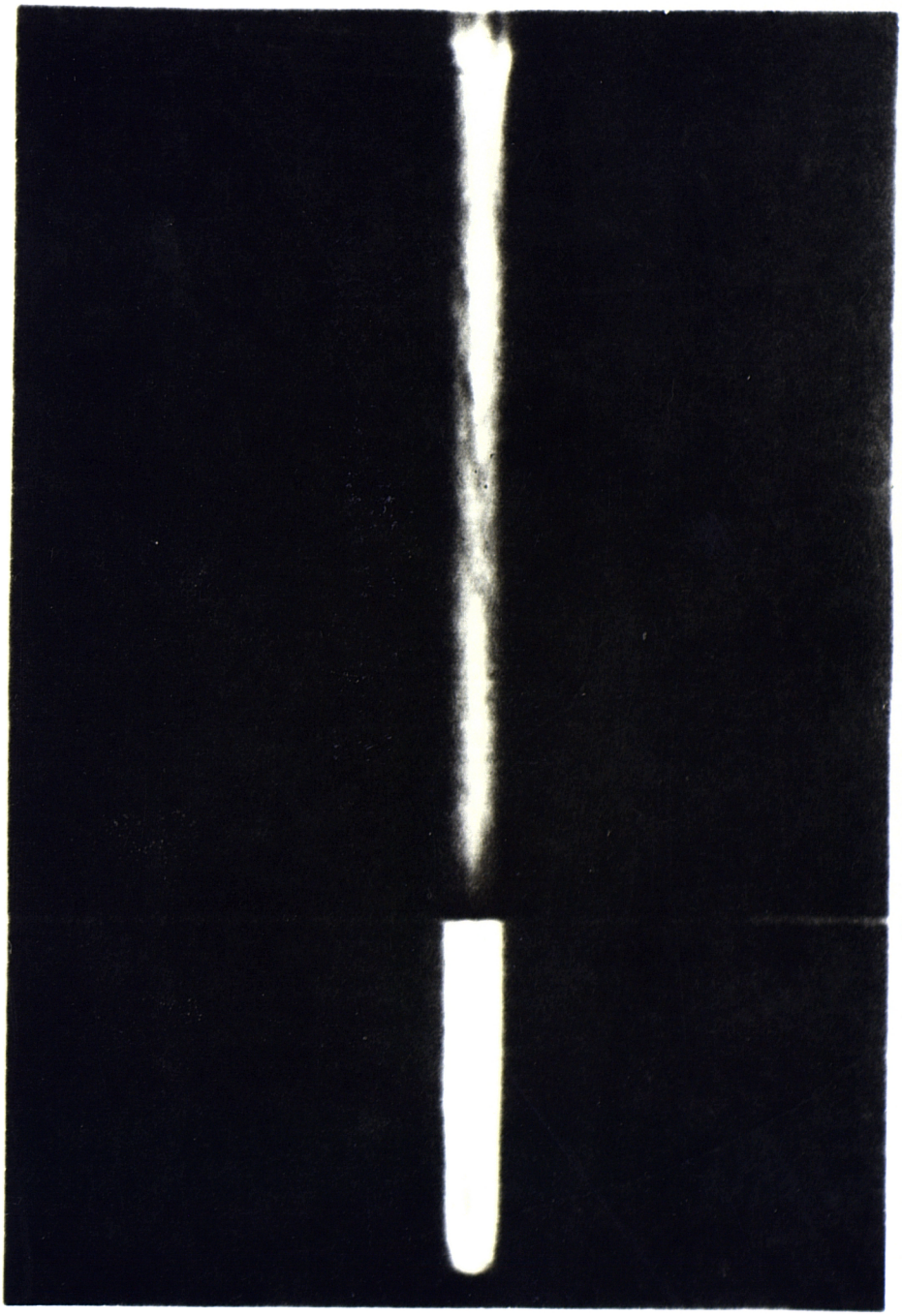

Plate X

High - Low Thermograph of 18/8 Stainless Steel.

A - onset of test; B - change of stress; C - failure.

Plate XI

Thermograph of Mild Steel.

A - onset of test; B - failure.

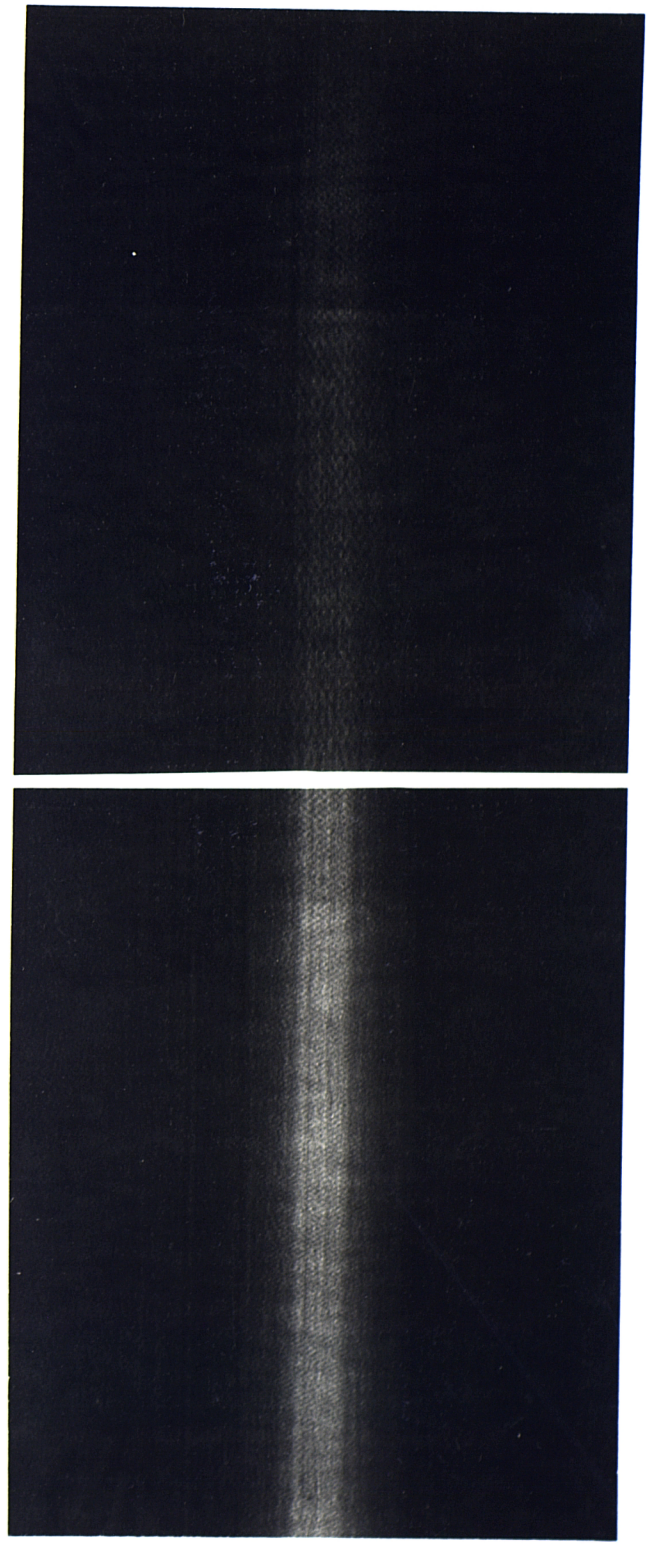

Plate XII

Thermographs of Mild Steel.

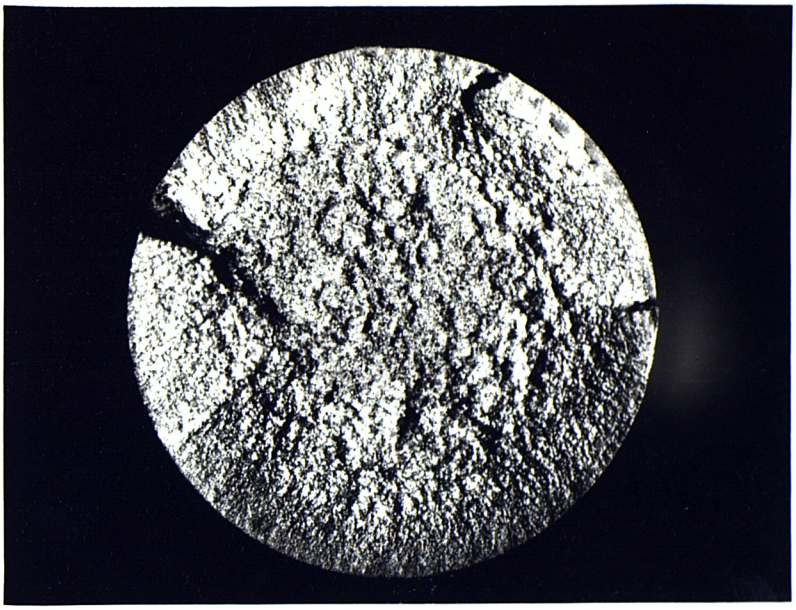

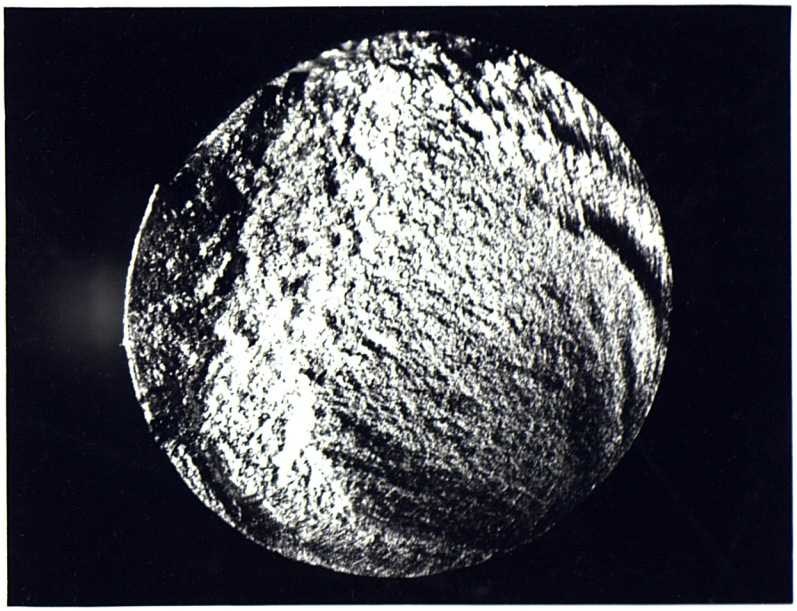

Plate XIII X15

Concentric (above) and Eccentric (below) Propagation Paths in Plain Specimens of Stretched 70/30 brass.

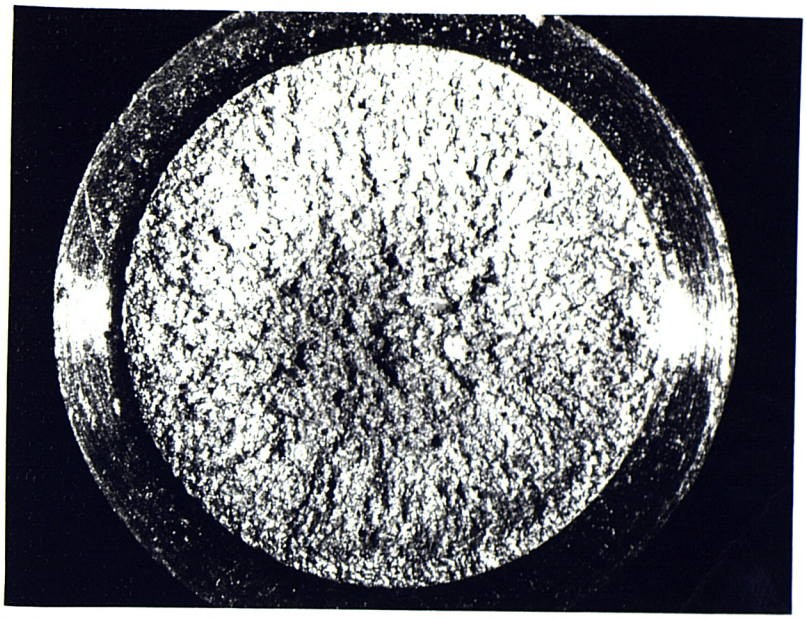

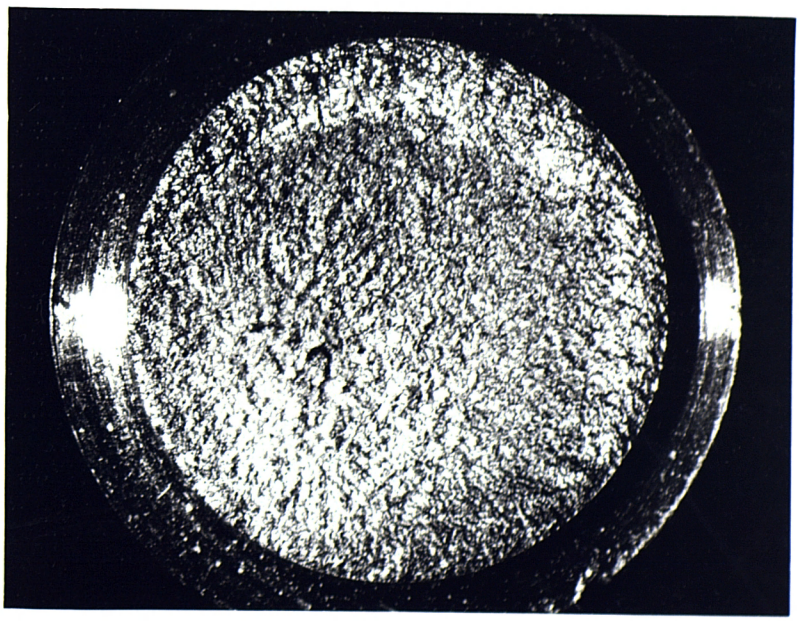

Plate XIV

X15

Concentric (above) and Eccentric (below) Propagation Paths in Notched Specimens of Stretched 70/30 Brass.

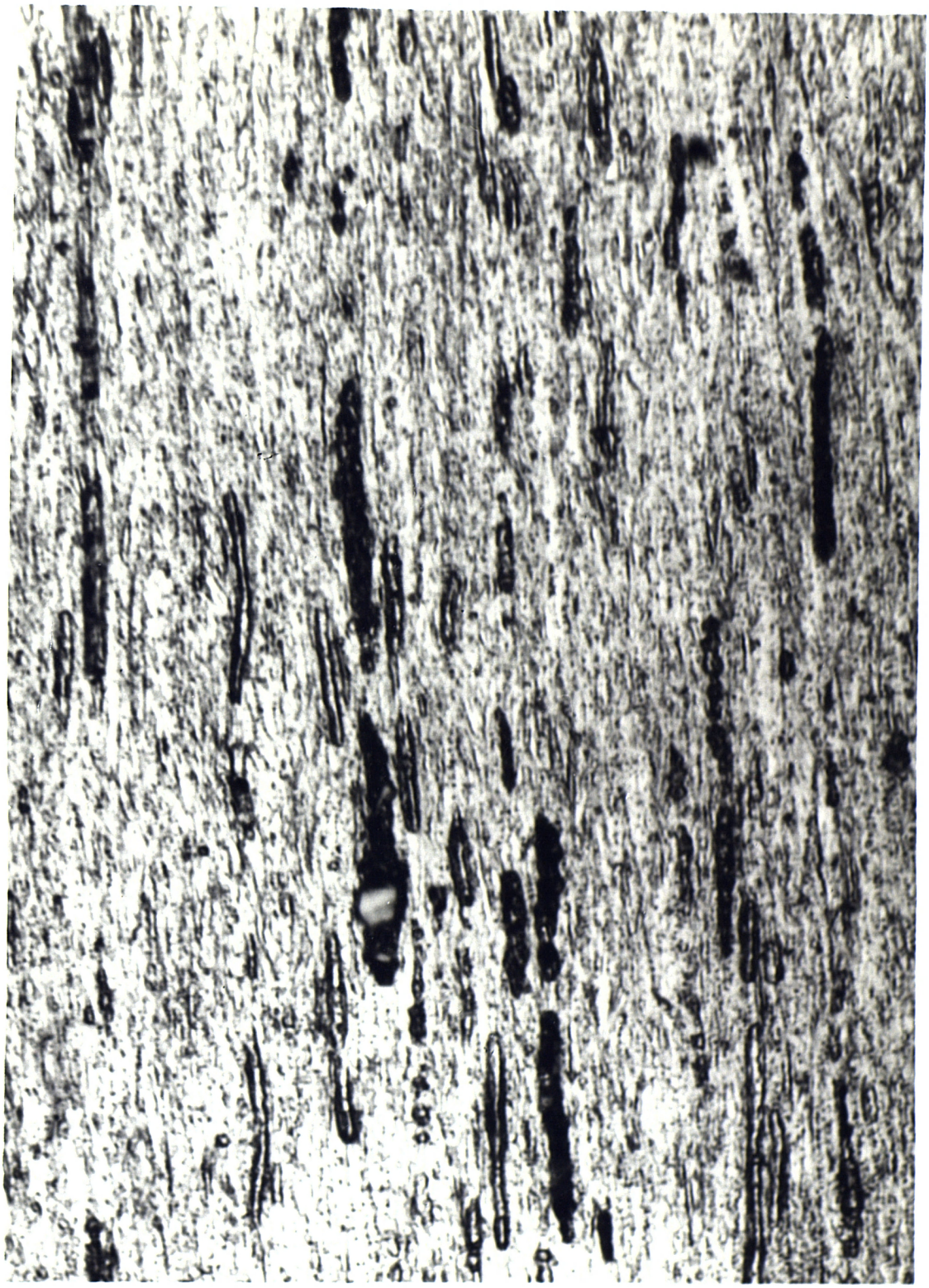

Plate XV

X3000

Martensite in 18/8 Stainless Steel Cold Rolled to give a Reduction in Area of 65%.

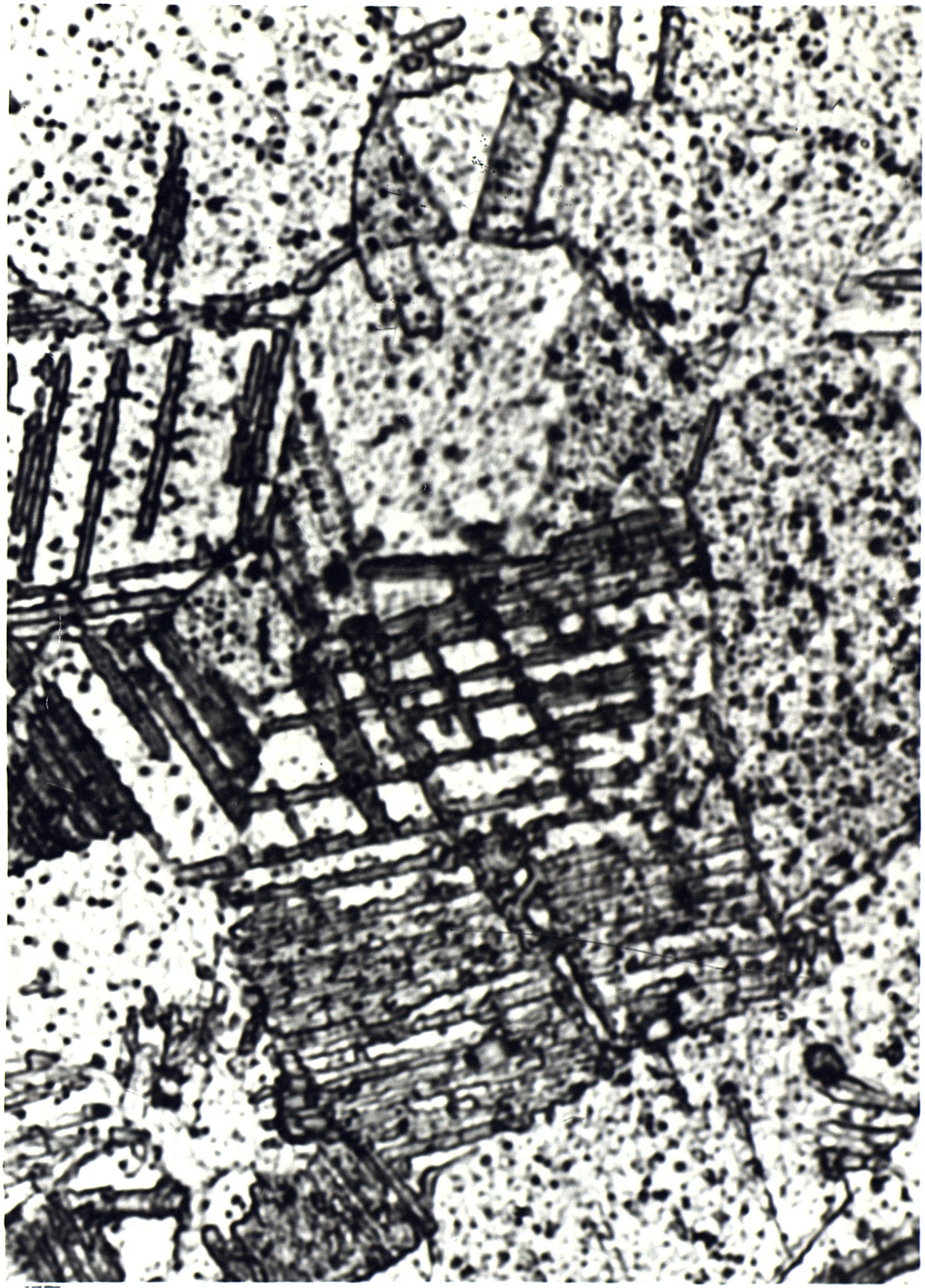

Plate XVI X2800

Martensite Formed in 18/8 Stainless Steel During Fatigue Testing at -80°C.

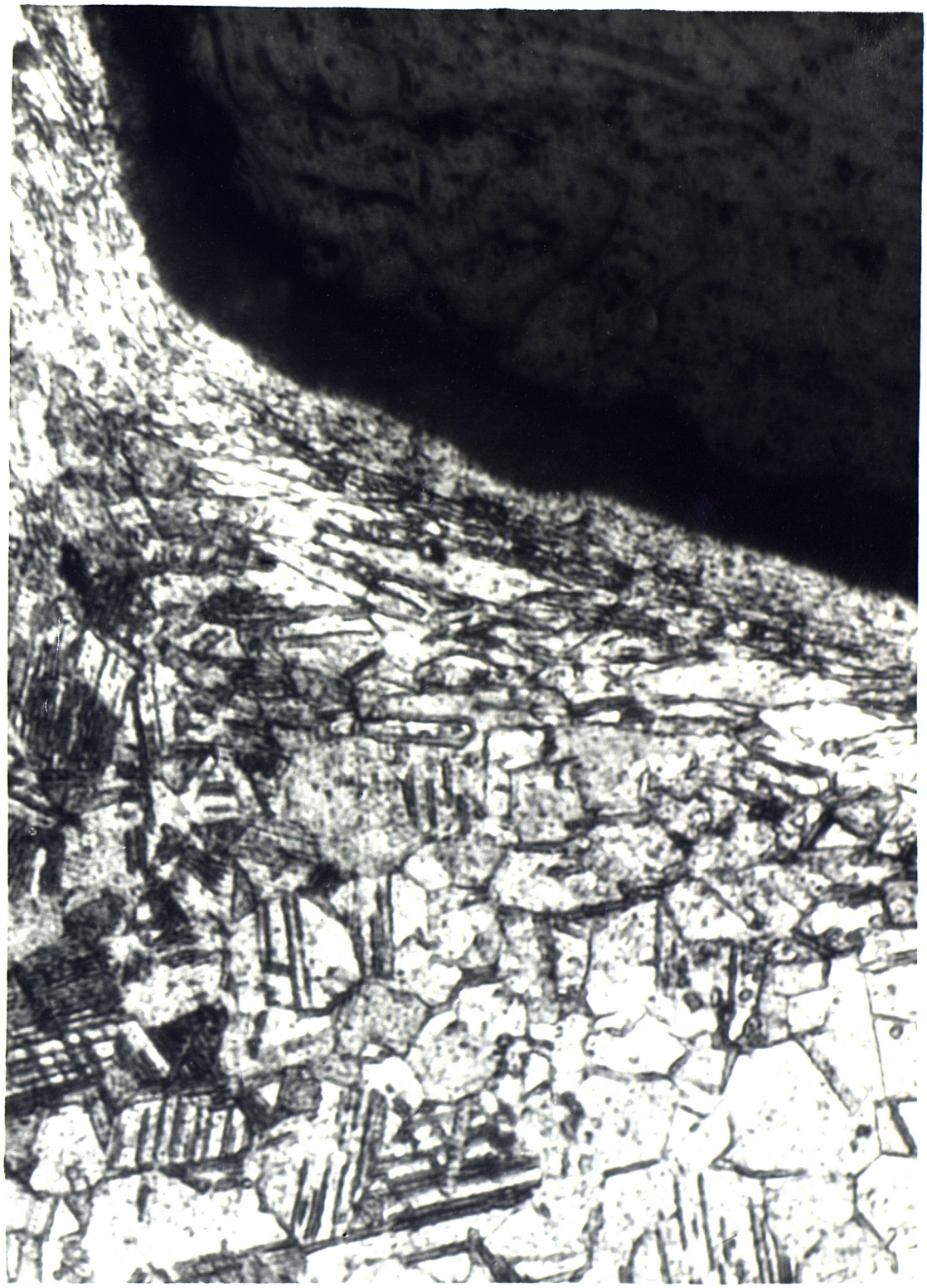

Plate XVII X600

Deformation of 18/8 Stainless Steel Caused by Machining.

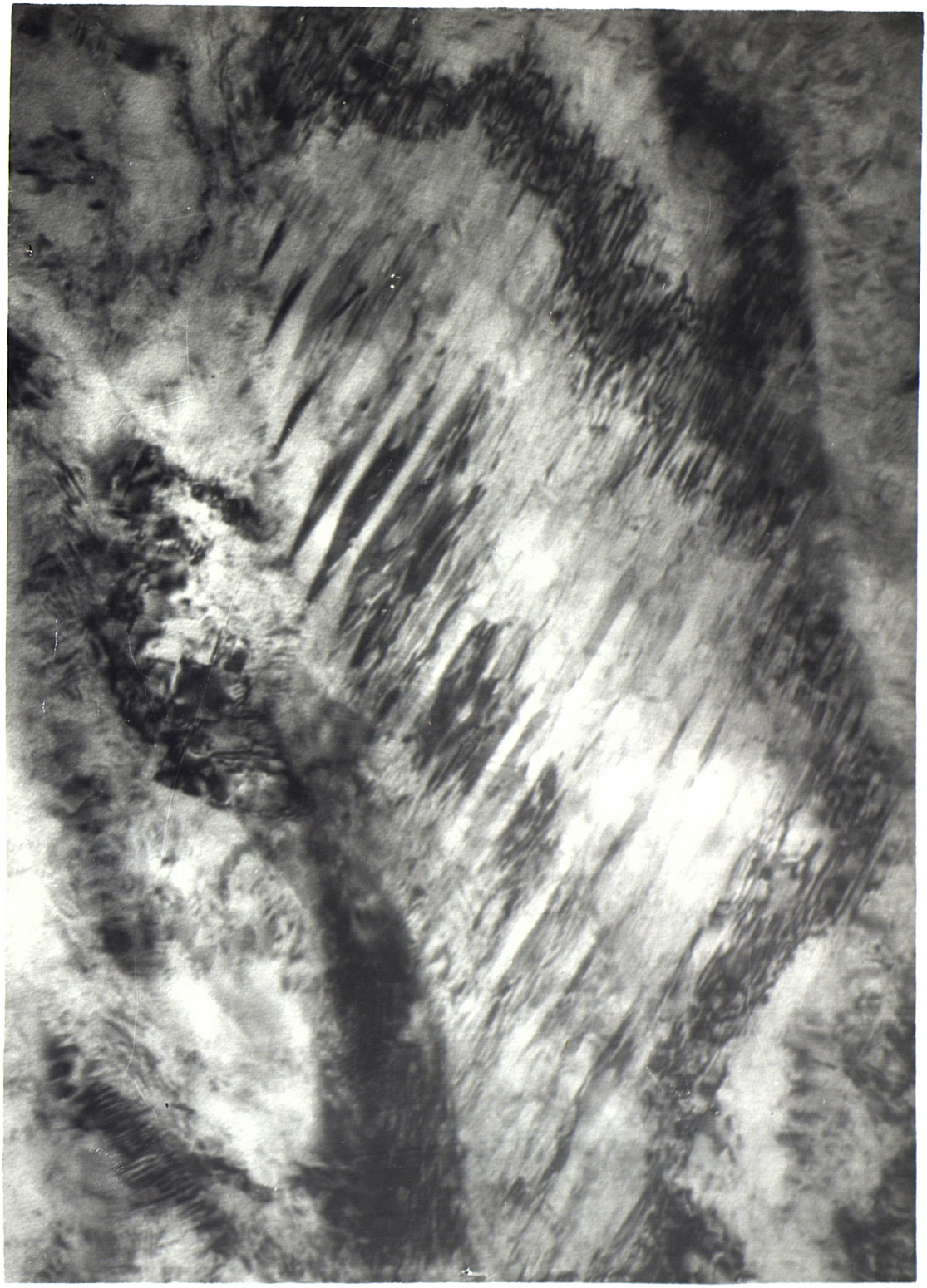

Plate XIX

0·2 μ

Acicular Martensite in 18/8 Stainless Steel with a Raised Nitrogen Content. Cold Rolled to give a Reduction in area of 60%.

PLATE XX Slip lines in 18/8 stainless steel fatigue tested at 250°C. x 3000

PLATE XXI Surface replica of slip in 18/8 stainless steel fatigue tested at 250°C. x 18000

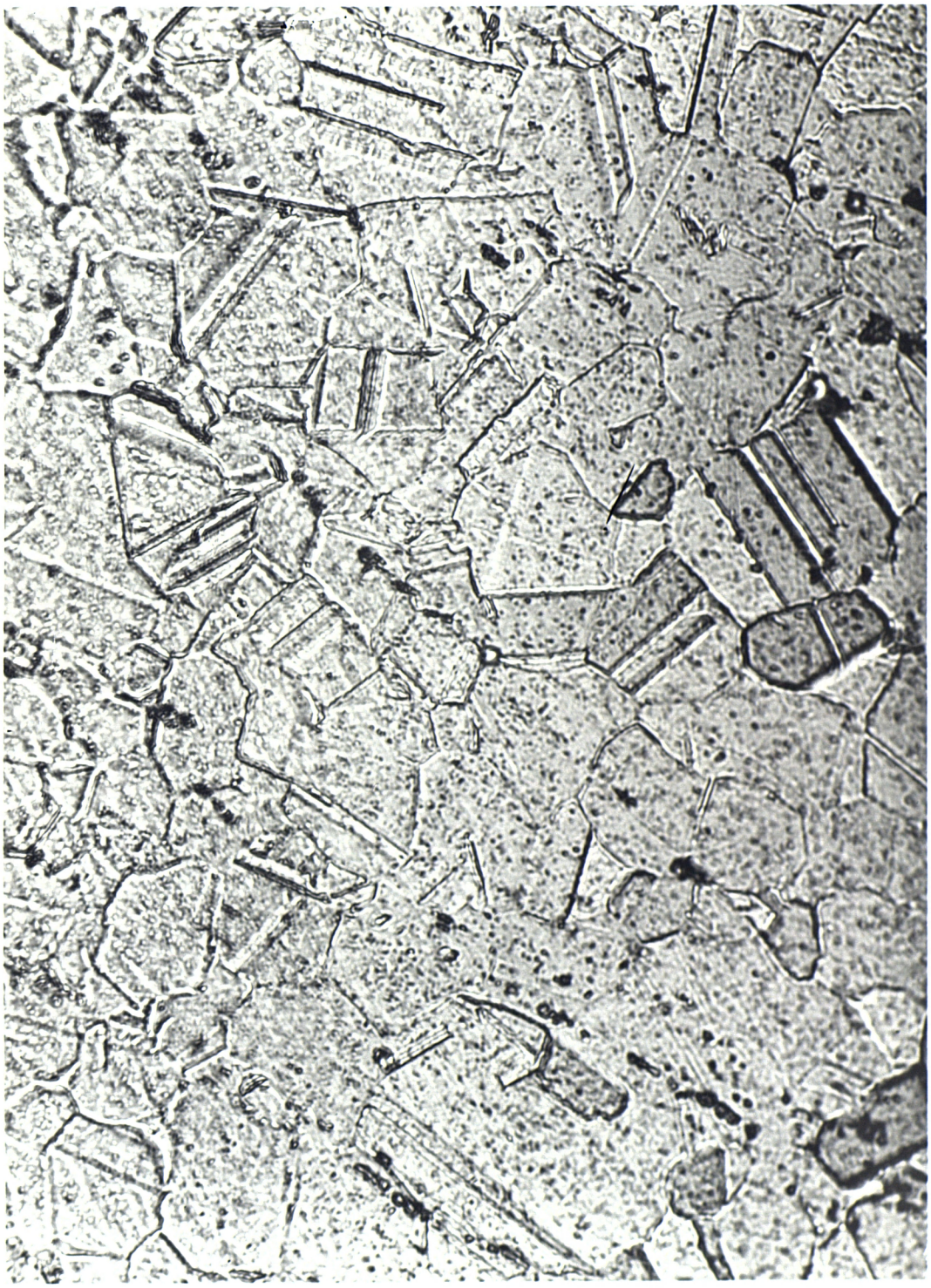

PLATE XXII Stainless steel fatigue tested at 350°C. x 2400